NUMERICAL ANALYSIS FOR SHALLOW TUNNELS IN WEAK GROUND SUPPORTED BY UMBRELLA ARCH METHOD

TAN WOOI LEONG

SCHOOL OF CIVIL AND ENVIRONMENTAL ENGINEERING
NANYANG TECHNOLOGICAL UNIVERSITY

2005

NUMERICAL ANALYSIS FOR SHALLOW TUNNELS IN WEAK GROUND SUPPORTED BY UMBRELLA ARCH METHOD

TAN WOOI LEONG

SCHOOL OF CIVIL AND ENVIRONMENTAL ENGINEERING

A thesis submitted to the Nanyang Technological University in fulfilment of the requirement for the degree of Master of Engineering

2005

ACKNOWLEGDEMENTS

The author gratefully acknowledges the assistance and guidance of his supervisor, A/P A.M. Hefny, who offered him invaluable advice and assistance in his preparation of this thesis. Thanks are also due to A/P P.G. Ranjith and all laboratory staff, especially Eugene and Mr. Koh Poh Seng. Most importantly, the author would like to express his gratitude to Nanyang Technological University for providing him with the Postgraduate Research Scholarship, which enabled him to complete his thesis.

TABLE OF CONTENTS

SUMMARY

The use of the Pipe Umbrella Arch method for tunnel face pre-support in weak ground is increasingly becoming more and more popular. The design of the Umbrella Arch is mainly based on experience and when numerical methods are used, crude approximations are adopted. Most of the approximations are based on the theory of "equivalent material" in which the ground reinforced zone is replaced with a new material of parameter derived from the weighted averages of the properties of the individual components in this zone. These approximations ignore many of the basic characteristics of the Umbrella Arch especially the overlapping length between consecutive arches in the longitudinal direction.

In this work, 2D and 3D numerical studies are performed to evaluate the differences in the estimated ground displacements when different modelling approximations are used for the Pipe Umbrella Arch. The studies are based on the analyses of three well-documented case histories in which Pipe Umbrella Arch was used during construction to limit the ground displacement. These three case histories are selected from fifty-six case histories compiled and presented in tabular form in this thesis. One of the case histories is in the use of the Pipe Umbrella Arch in fractured rocks and the other two are for cases of Pipe Umbrella Arch in soft soils. 3-D numerical analyses for the two cases in soils generated ground surface displacements which are found to be in excellent agreement with the field results both in value and distribution trend. The effect of different tunnel reinforcement on the ground surface displacements during tunnel excavation was also evaluated for one case history. Parametric studies carried out for two case histories in soils to investigate the effect of various pipe parameters and pipe arrangement showed that pipe parameters and pipe arrangement play an important role in controlling the ground surface settlement during tunnel excavation regardless of the soil condition.

LIST OF TABLES

LIST OF FIGURES

CHAPTER 1 - INTRODUCTION

1.1 Background

Tunnel excavations in shallow ground usually occur in urban or developed areas. Services (e.g. pipelines, cables, sewage etc.) and transportation systems such as roadways and railways (e.g. Mass Rapid Transit in Singapore) are constructed in underground tunnels in places where land is valuable and conservation of this resource will yield tremendous development potential. Soft and weak ground is usually encountered when tunnelling at shallow depths. Hence excavating a tunnel under weak and shallow ground conditions will pose many problems for the design engineers and create possible hazards to above ground structures and human lives. A major concern is to restrict the large deformations on the ground surface that occurs concurrent with excavations, and also curb the convergence that occurs at and behind the tunnel face.

The completely mechanized tunnel boring machines (TBMs) and the conventional excavation techniques with ground improvement are two types of tunnel excavation techniques that are frequently used for shallow grounds (Grasso et al, 1993). Slurry, mud and Earth Pressure Balance (EPB) shields are efficient but they are costly, and the high-pressured work environment might create worker health and safety issues. These machines are limited when large diameter tunnels are constructed and thus when such tunnels are constructed, excavation by roadheaders, backhoes and a combination of ground reinforcement and improvement techniques will be a more economical and amicable solution.

Soil stabilization at the tunnel face prior to excavation is essential since the tunnel face fails very fast, especially for weak soil condition, which will consequently lead to tunnel collapse. Tunnel face failure and convergence as a result of tunnel excavations can be greatly reduced if tunnel-reinforcing techniques are implemented. It will be natural to foresee that reinforcement had to be installed prior to any tunnel excavation activities in order to minimize or reduce the effect of soil deformation during excavation because many studies of ground surface

deformations due to weak and soft ground tunnelling have indicated that a large amount of total soil deformation occurs during the construction phase of a tunnel even before concrete lining are installed. The magnitude of soil deformation that occurs during this phase is greater than the long term deformation after completion of the lining. Pipe Umbrella Arch method is one such type of pre-reinforcement methods that creates a reinforced arch around the tunnel crown which reduces the instability of the soil due to convergence around the tunnel face ahead of the excavation. A few other types of tunnel reinforcing techniques has also been developed and studied in the past years, such as jet grouting arch, spiling method and mechanical pre-cutting (Pelizza and Peila, 1992).

Of all the pre-reinforcement techniques discussed herein, the steel pipe Umbrella Arch method has the highest flexibility, feasibility and efficiency. It is also easy to execute, and is suitable for various types of ground. The Pipe Umbrella simply functions as a reinforced arch that transfers the load of the ground above the tunnel to the support (shotcrete or steel ribs). Steel pipes are placed in pre-drilled holes or installed using pipe jacking or micro tunnelling techniques to form an arch or gate type arrangement around the tunnel crown. Hence, the tunnel face area is stabilized in both the transverse and longitudinal directions. Such pre-reinforcement technique improves ground conditions and contributes to the permanent stabilization of the opening by restricting deformations.

Although pre-lining techniques such as the Pipe Umbrella Arch can greatly improve the overall stability of the cavity and consequently contribute to the progress of tunnelling projects, there are very few studies that can provide a reliable and accurate design method that will account for all important aspects of the Pipe Umbrella mechanism, such as the overlapping length of the pipes and the interaction between the pipes and the ground etc. In most studies that were conducted so far, the Pipe Umbrella Arch is modelled as a composite strip of an equivalent strength that is derived using the method of weighted averages for the strength of the soil/rock, steel pipe and grout. Such a method usually produces crude approximations as pointed out by Hoek (2000) and are not suitable for design

purposes. As such, most tunnel engineers usually base their design of the Umbrella Arch on field experiences or on very conservative designs.

1.2 Objective and Scope of Study

The objective of this study is to investigate numerically the reinforcing capability of Pipe Umbrella Arch method in reducing ground surface settlement during tunnel excavations in weak grounds.

The research work includes the following main aspects:

1. Reviewing and collecting past case histories of Pipe Umbrella Arch.
2. Conducting 2-D numerical analysis on a well documented case history for the use of Pipe Umbrella Arch method in fractured rocks to investigate the effect of different approximations on the tunnel closure and induced ground surface settlement.
3. Conducting 3-D finite element analyses on well documented case histories for the use of Pipe Umbrella Arch in soils to investigate the effectiveness of such analyses on simulating the reinforcing capability of Pipe Umbrella Arch.
4. Using the calibrated 3-D models for the case histories studied to investigate the effect of various tunnel reinforcements on the induced ground surface settlement above the tunnel.
5. Conducting a parametric study to investigate the impact of different pipe parameters and pipe arrangements on the reinforcing effect of the Pipe Umbrella Arch during excavation.
6. Investigating the effectiveness of using 2-D finite element analyses to simulate the reinforcing effect of the Pipe Umbrella Arch that is 3-D in nature, through comparison between results obtained from the 2-D analyses and 3-D analyses.

1.3 Organization of Study

Chapter One presents an introduction of the history of tunnelling and technological advances in tunnelling techniques. This is followed by the objective of the study and a brief outline of the structure of the report. Chapter Two reviews literature relating to the pre-lining method of reinforcement using forepoling techniques with special focus on the Umbrella Arch method. Chapter Two also identifies other types of reinforcement for tunnelling stability. Chapter Three describes the construction process and lists comprehensive case histories of the Umbrella Arch method, and this is followed by Chapter Four, which identifies and evaluates different design methods for the Pipe Umbrella Arch. Chapter Four also compares the generated ground displacements from the different methods used. Two and three-dimensional finite element analyses are conducted to calibrate two case studies from the Maiko Tunnel in Chapter Five. In addition, parametric studies of the Pipe Umbrella Arch and the optimum design for the studied cases are discussed in Chapter Six. Chapter Seven discusses the derivation of a methodology that can accurately represent the 3-D Pipe Umbrella Arch using 2-D finite element analysis. Chapter Eight concludes the major findings of the study and make recommendations for future works.

CHAPTER 2 – LITERATURE REVIEW

2.1 Tunnelling in weak ground at shallow depth

Numerous tunnelling operations encounter soft or weak ground conditions during excavation at shallow depth, and hence tunnelling method, ground improvement and reinforcement support had to be meticulously selected. Many analytical and field studies had attempted to provide a basis for decision, but ambiguous site conditions and the lack of comprehensive site investigation usually make decision making critical and difficult. The economic value of the method used will be a major determinant for selection process although minimising the disturbance to surface structures and activities also plays a significant role.

Tunnelling in soft ground is influenced by ground variability, which would influence the efficiency of the tunnelling operations, and the excessive groundwater which might cause soil weakening that leads to tunnel collapse and also upheaval of the ground and seepages into the tunnel. Pake (1976) describes the problems related to soft ground tunnelling citing the example from the Edinburgh sewage disposal facility. Heuer (1974) modified Terzaghi's (1950) classification of the types of ground encountered in soft ground tunnelling as shown in Table 2-1. According to Whittaker et al (1990), Terzaghi (1950) observed that water seepage in and around the periphery of the tunnel would pose the most serious problem in soft ground tunnelling. The ground classification is based primarily on the stand up time of the ground, and the cohesion of the ground is its major determinant. When the circumferential stress acting on the tunnel is greater than the ground's unconfined compression strength, then the ground will fail immediately upon exposure, thus the stand up time is shorter and the ground will run, flow and squeeze instantaneously (Heuer, 1990). Tunnelling operations in soft ground generally uses a shield to protect the workers executing the excavation works and a shield also ensures an efficient and effective operations especially tunnelling under water tables. The shield is usually coupled with a layer of concrete or cast iron linings, and depending on different ground conditions, other ground supports in the form of face pre-

reinforcement or post reinforcement are employed to further enhance the tunnel stability.

Ground loss and settlement are the basic considerations for a tunnel designer when dealing with soft ground tunnelling. The effects on surface settlement due to different soft ground conditions, ranging from granular soils with no cohesion to hard clays, encountered in tunnelling have been explored by Peck (1969). A good knowledge of the ground conditions whereby tunnel excavation is to be executed is essential because it will affect the method of excavation and type of tunnel supports best suited to enhance tunnel stability.

2.2 Tunnel Face Stability

The stability of the tunnel face during construction, the tunnelling-induced ground settlement particularly in shallow underground works and the design of the tunnel liner system that will be constructed to ensure the stability of the cavity are three main aspects involved in the design of soft ground tunnelling as specified by Peck (1969).

Tunnel face stability was investigated by Broms and Bennermark (1967), who had proposed using a face stability index, N, which is the ratio between the difference of the natural pressure and the pressure applied to the tunnel face, and the undrained shear strength, to analyse tunnel face stability. The stability index is devised based on cohesive ground (clay) and it was found that the tunnel face would be stable when the index is less than six.

$$N = (\sigma_S + \gamma H - \sigma_T) / S_U \qquad (1)$$

where, γ = unit weight of soil

H = depth of tunnel axis

σ_S = surface surcharge

σ_T = tunnel support pressure

S_U = undrained shear strength at tunnel axis

The claims made by Broms and Bennermark (1967) of N<6 for stability of tunnel face were substantiated by Mair (1979), Schofield (1980) and Davis et al. (1980) who concluded that the stability index depends on the depth of cover to diameter ratio and that stability index, N is equal to between five and seven for depth of cover to diameter ratio of 1.5. A larger range of N for tunnel face stability was given by Kimura and Mair (1981) who carried out centrifuge tests on reconsolidated clay and verified that the stability of the tunnel face can be confirmed for values of N between five and ten depending on the depth.

However, Romo and Diaz (1981) felt that the stability index does not explicitly reflect the actual stability of the tunnel face and so they devised a safety factor (which is defined as the ratio between shear strength of the soil and maximum shear stress) for the stability index. A series of plots of contours and critical surfaces corresponding to a number of stability ratios and tunnel depth to diameter ratios were devised and the relationship between the safety factor and stability ratio was obtained. Results correlated well with the reported case histories from Peck (1969) whereby tunnel face failure occurs for stability index in the range between six and seven. The reported stability index at safety factor of one is approximately 6.5. Although their results showed good correlation with case histories by Peck (1969), it should be noted that they had assumed that the soil behaved as a non linear elastic material having a hyperbolic stress strain curve and that no slippage would occur at the shield-soil interface during the tunnel face excavation.

Table 2-1: Ground Classification (modified from Terzaghi (1950) by Heuer (1974))

Classification	Behaviour	Typical Soil Types
Firm	Heading can be advanced without initial support and final lining can be constructed before ground starts to move.	Loess above water table; hard clay, marl, cemented sand and gravel when not highly overstressed.
Ravelling (Slow or Fast)	Chunks or flakes of material begin to drop out of the arch or walls sometime after the ground has been exposed, due to loosening or to overstress and "brittle" fracture (ground surfaces, opposed to squeezing ground). In fast ravelling, the process starts within a few minute, otherwise the ground is slow ravelling.	Residual soils or sand with small amounts of binder may be fast ravelling below the water table, slow ravelling above. Stiff fissured clays may be slow or fast ravelling depending upon degree of overstress.
Squeezing	Ground squeezes or extrudes plastically into tunnel, without visible fracturing or loss of continuity, and without perceptible increase in water content. Ductile, plastic yield and flow due to overstress.	Ground with low frictional strength. Rate of squeeze depends on degree of overstress. Occurs at shallow to medium depth in clay of very soft to medium consistency. Stiff to hard clay under high cover may move in combination of ravelling at execution surface and squeezing at depth behind surface
Running	Granular materials without cohesion are unstable at a slope greater than their angle of repose (± 30°-35°). When exposed at steeper slopes they run like granulated sugar or dune sand until the slope flattens to the angle of repose.	Clean, dry granular materials. Apparent cohesion in moist sand, or weak cementation in any granular soil, may allow the material to stand for a brief period of ravelling before it breaks down and runs. Such behaviour is cohesive-running.
Flowing	A mixture of soils and water flows into the tunnel like viscous fluid. The material can enter the tunnel from the invert as well as from the face, crown, and walls, and can flow for great distances, completely filling the tunnel in some cases.	Below the water table in silt, sand, or gravel without enough clay content to give significant cohesion and plasticity. May also occur in highly sensitive clay when such material is disturbed.
Swelling	Ground absorbs water, increases in volume, and expands slowly into tunnel.	Highly pre-consolidated clay with plasticity index in excess of about 30, generally containing significant percentages of mont morillonite.

Tunnel face stability in sandy and pervious water bearing grounds was investigated by Leca and Dormieux (1990). They proposed a support pressure (σ_T) to be applied to the tunnel face using a three-dimensional failure mechanism as described in Leca and Dormieux (1990) involving the rigid body movement of 2 conical blocks. They had proposed a limiting face pressure (σ_T*) for dry cohesionless soils as shown in equation (2),

$$\sigma_T {}^* = (\alpha_S \sigma_S + \alpha_\gamma \gamma D) \qquad (2)$$

where α_S and α_γ are weighting factors dependent on friction angle and depth of cover to tunnel diameter ratio, H/D, and σ_S is the overburden pressure.

This approach was further investigated by Chambon and Corte (1994) who formed a relationship between the tunnel face axial deformation and the pressure applied to the tunnel face based on centrifuge tests of Fontainebleau sand as shown in Figure 2-1. They observed that the critical and collapse pressure (P_c) increases with the tunnel diameter.

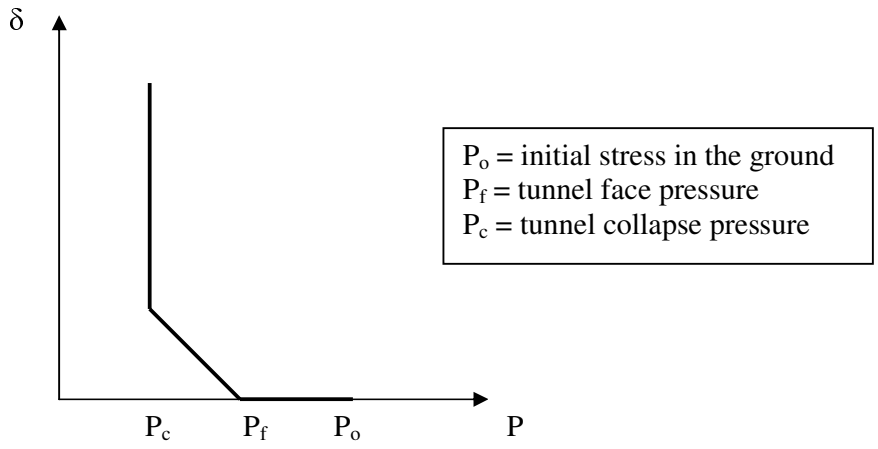

Figure 2-1. Schematic trend of the tunnel face axial displacement (δ) with reference to the applied pressure (P) (after Chambon and Corte, 1994).

Einsenstein and Ezzeldine (1994) also carried out a study to investigate ground behaviour with respect to stress reduction at the face of an excavation using a shield by means of two separate analyses involving an axisymmetrical and a three dimensional finite element analysis in an ideal elasto-plastic field. The results obtained were compared to the results obtained from Chambon and Corte (1994) and it was found that the face pressure (P_f) (Figure 2-1) was very close to the value of Rankine's active pressure.

In other studies for cohesionless soil, Mair et al. (1996) gave dimensionless results of the face pressure $\sigma_T/\gamma D$, where σ_T is the tunnel face pressure, γ is the unit weight of the soil and D is the tunnel depth, calculated from upper bound and lower bound solutions obtained from limit equilibrium approach and found that the value is 0.15 which is similar to the value from Atkinson and Potts (1977) who conducted a two dimensional numerical study. The value found from three-dimensional studies by Leca and Dormineux (1990) gave a value of 0.3 for lower bound solutions and about 0.08 to 0.15 for upper bound solutions.

In order to determine the criteria for implementation of tunnel face reinforcement in soft soils, Grasso et al. (1993) conducted numerical three-dimensional and axisymmetric finite element analysis using formulas from the arching theory devised by Cornejo (1989). A safety factor is devised from the arching theory as a ratio of the moments of the reaction forces derived from the shear strength of the material and the applied forces that resulted from gravity. If the safety factor falls below an acceptable value, the tunnel face requires reinforcement. Cornejo (1989) had tabulated safety factors for soils and soft rocks with cohesive-friction behaviour, granular soils without cohesion and clayey soils in 2 categories of ground conditions:

1) Isotropic, homogenous ground
2) Stratified ground and soft rock with strength properties varying according to the depth.

Besides problems of tunnel face stability in soft ground, tunnels in rock also experience tunnel face deformations. These deformations were investigated by Lunardi (2000) who categorised the deformations into the following types:

(1) Pre-convergence ahead of the tunnel face

(2) Convergence of the cavity and,

(3) Extrusion of the tunnel face

The three types of deformation are illustrated diagrammatically in Figure 2-2. From the studies conducted in the Frejus Motorway Tunnel and the Santo Stefano Tunnel in Italy, Lunardi (2000) concluded that there exists a close connection between the extrusion at the tunnel face and the pre convergence and convergence of the cavity. Furthermore, it was also observed that the failure of the tunnel face or advance core will attribute to the collapse of the cavity even if the cavity has been reinforced and hence he confirmed that the overall stability of the tunnel will depend on stability of the advance core. And as such, the advance core has to be reinforced prior to excavation so as to produce an arch effect ahead of the advance core, which will stabilise the tunnel cavity whilst the excavation has passed ahead of it.

The rigidity of the core will determine the stability of a tunnel since the deformation of the advanced core causes the extrusion of the face, pre convergence behind the face and the convergence of the cavity.

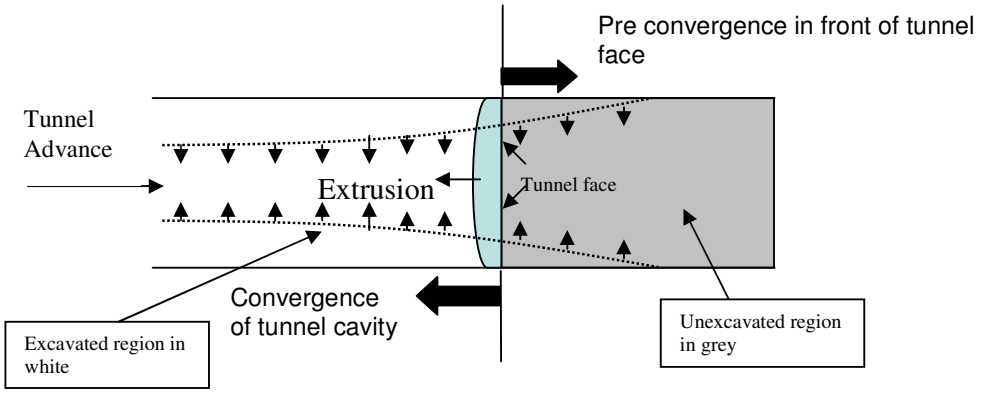

Figure 2-2. Types of deformation in tunnel excavation (longitudinal cross sectional view).

In order to control and considerably reduce the deformation of the cavity, the deformation properties and the rigidity of the advanced core has to be artificially regulated by means of appropriate stabilization techniques. A study was performed together with experimentation on the Vasto Tunnel in Italy and Lunardi (2000) concluded that if the medium of the advanced core is stressed in the elastic range, radial stabilization measures such as concrete lining or radial rock bolts would be sufficient.

If the medium is stressed in the elastic-plastic range;

1) Radial stabilization measures such as radial rock bolts would be sufficient only if the stress state is low.
2) Longitudinal stabilisation measures on the advance core are required e.g. longitudinal face reinforcement etc., and no radial measures are required i.e. no rock bolts required, if the stress state is high.

And, if the medium is stressed in the failure range;

1) It is a must to stiffen the advance core (Figure 2-2 grey portion) with pre-confinement action on the future cavity
2) A protective crown of improved ground can be created around the advance core. If this is insufficient, radial measures on the cavity can be further implemented.

2.3 Tunnel Support System

Tunnel construction has gone through major advancement in excavation techniques over the years with the use of hi-tech machineries, ground reinforcement or ground improvement to stabilise the tunnel face and prevent any tunnel collapse. The advance rate of tunnel excavation has consequently increased significantly with the introduction of the tunnel boring machines (TBM). Many studies and researches have been dedicated to many aspects of tunnel design and excavation to improve and enhance the efficiency and lower the cost of excavation works. However interestingly, there are limited studies that dedicate to the study of face

reinforcement and pre reinforcement, although they play an important role in determining the overall stability of the tunnel face and preventing convergence of the cavity. There exist many types of ground improvement and reinforcement methods to stabilise the cavity and every individual method will produce different action on the cavity or tunnel face to effect the necessary stabilisation. Lunardi (2000) categorised these methods into three different groups whereby each group would exert a different kind of effect on the cavity. Table 2-2 shows the categorisation of the different kinds of stabilisation instruments.

The use of ground reinforcement to maintain the stability of the tunnel face during excavation will usually reduce the problem of the weakening of the ground that may cause tunnel collapse and consequently, produce disturbance to existing surface structures. The problem of tunnel collapse will cause the land above the tunnel to subside especially when the excavation is carried out at shallow depth and in weak and soft soils. Many examples of tunnel construction using ground reinforcement on the face of the tunnel have been successfully carried out in Italy (e.g. Poggio Orlandi and Saint Vitale tunnel (Lunardi, 2000)) and France (e.g. Tartaiguille tunnel (Wong et al., 2000)) and in recent years in Japan (e.g. Mito tunnel (Itoh et al., 2001)). These projects have established the fact that face reinforcement is essential in maintaining tunnel stability and preventing tunnel collapse.

Table 2-2: Kinds of stabilisation instruments and the type of effect exerted (reproduced from Lunardi (2000))

Action on the cavity	Stabilisation instruments	
Pre-confinement	Ground improvement ahead of the face	• Traditional injections • Freezing • Sub-horizontal jet grouting • Mechanical pre-cutting • Drainage pipes • Tunnel face reinforced with horizontal fibre glass pipes
Confinement		• Spritz-Beton (sprayed concrete) • Mechanical pressure shield • Earth pressure balanced shield and hydroshield • Open face shield • Concrete invert
	Radial ground improvement	• Full length anchored roof bolts • End anchored roof bolts
Pre-support		• Forepoling

There are basically 2 different types of stabilisation as discussed by Lunardi (2000). The first type is that of conservation whereby the main effect is to contain the relaxation of the minor principal stress and the second type is improvement, whereby the main action is to increase the shear strength of the medium.

Mechanical Pre-cutting, a method of cutting a slot by means of an over-sized chain saw into the tunnel face to be excavated and shotcreting the slot (Walsum, 1992), coupled with reinforced shotcreting and reinforcing of the tunnel face with horizontal fibre glass pipes would constitute a conservation effect whereas truncated cone umbrellas of ground coupled with traditional injections and freezing or drainage would cause an improvement effect. The methods mentioned would produce a pre-confinement action on the cavity, which in other words referred to reinforcing the tunnel cavity prior to excavation. The excavated tunnel when lined with a layer of shotcrete will produce a confinement pressure similar to that of the earth pressure shield and open shield. The end anchored bolts, which are installed on the walls of tunnel, perform the role of containing the relaxation of the minor principal stresses by applying an active confinement pressure on the walls of the tunnel whereas the full length anchored bolts increase the shear strength of the ground. Forepoling technique is classified as a pre-support as it was deemed as incapable of producing an arch effect. However, this technique has proven to be very effective in shallow tunnel construction and has successfully been used for urban tunnel projects in Japan, Italy and the United States. Upon knowing the various support systems, the most critical problem is to determine which type of reinforcement is best suited for a tunnel since the response of the support system depends on the type of ground, tunnel requirements and site conditions.

Schematic diagrams for the Umbrella Arch method and face reinforcement are shown in Figures 2-3 and 2-4. Figure 2-3 shows the longitudinal section of a tunnel section with an umbrella arch and face reinforcement whereas Figure 2-4 depicts the cross sectional view.

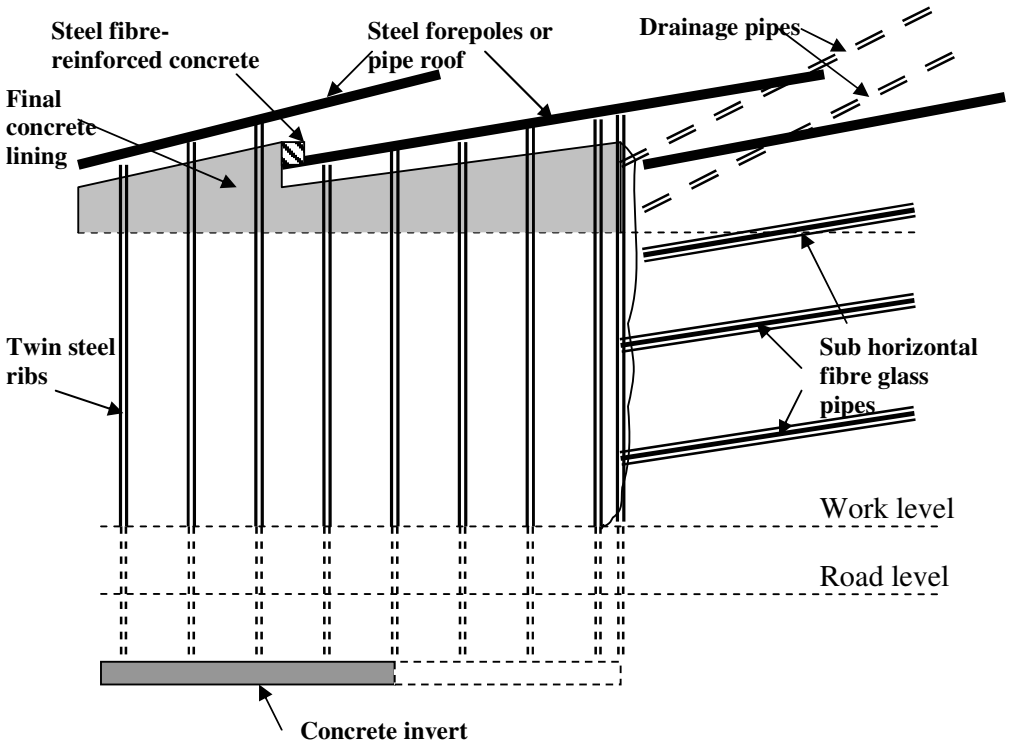

Figure 2-3. Longitudinal section of umbrella arch and other face reinforcement.

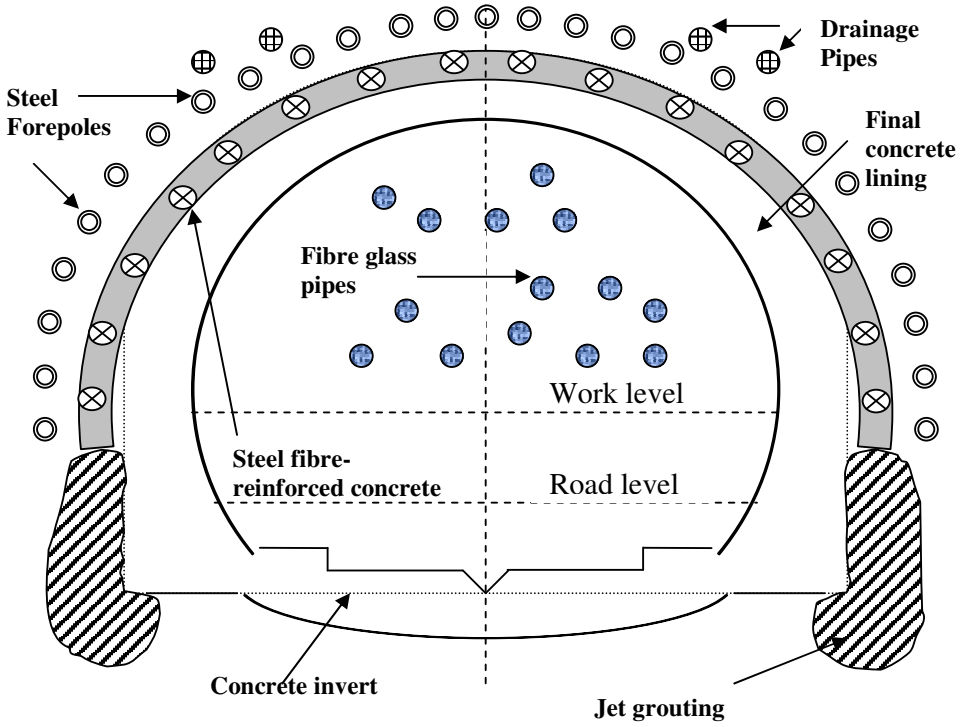

Figure 2-4. Cross-section showing an umbrella arch and face reinforcement.

It is not possible to implement all stabilisation measures depicted in Figures 2-3 and 2-4 due to operational costs. Thus a support system which can provide maximum stability with least operational costs and ease of implementation will be favoured but in practice, the tunnel engineer will know that a few support systems had to be used together to produce maximum stability for tunnel excavation.

2.3.1 Forepoling

A type of support system, which is gaining popularity for large-scale excavations in soft ground and rock are tunnel reinforcements by forepoling method. This method is essentially a technique whereby steel, fibreglass or concrete tubes are installed around the crown or face of a tunnel to act as pre-reinforcement prior to tunnel excavation. The pipes or tubes are installed around the tunnel crown by means of specially designed forepoling rigs. This technique of inserting steel pipes in advance of tunnel excavation has gained prominence due to its effectiveness and rather simple execution which in return produces the desired stability effect required to ensure tunnel stability and worker safety. Figure 2-5 shows the forepoling method and Figure 2-6 shows a forepoling rig at work.

Figure 2-5. Forepoling method used for tunnel excavation in Greece. (Zeccos, 2002)

2.3.1.1 Reasons for using Forepoling methods

In developed or urban areas, tunnels are usually designed at shallow depths and in weak ground, and in order to avoid making disturbance to structures on the surface, forepoling can be adopted as a form of support. Forepoling is usually coupled with additional support systems such as shotcreting, jet grouting and fibreglass tubes to enhance the tunnel stability. Steel pipes (see Figure 2-7) that are installed in the tunnel crown will form an umbrella arch of reinforced zone that will stabilise the tunnel face in both the transverse and longitudinal directions. Then, tunnel works can be carried out safely and effectively under this reinforced arch, which prevents the overburden above the excavated ground from collapsing. This method has proven to be simple, effective, flexible and highly feasible in various soil conditions from soft soil to hard rocks as described by Pelizza and Peila (1992). The economic value of the forepoling technique has not really been explored using mathematical or analytical studies although certain studies quoted a higher cost as compared to jet grouting arch, but its effectiveness in tunnel face stability cannot be fully ignored. More studies must be done to optimise its usage in relation to tunnel face stability so that this technique can reap higher economies of scale with optimum combination of pipe geometry, numbers and spacing.

Figure 2-6. Forepoling rig (Rotex OY)

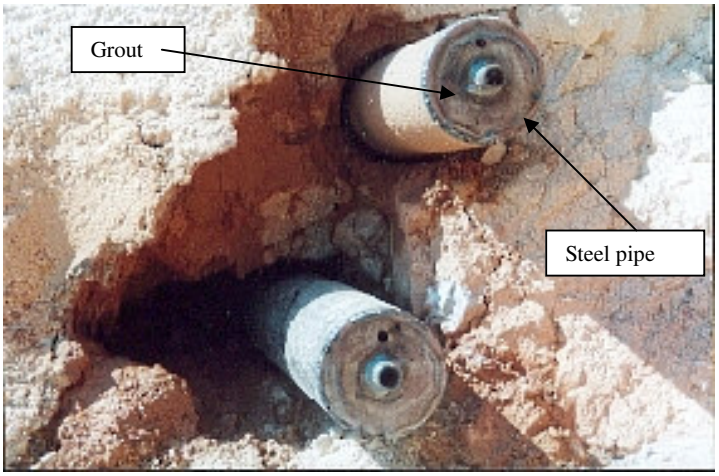

Figure 2-7. Close up view of steel fore piles.

2.3.1.2 Types of Forepoling methods

When weak and soft ground or weathered rocks are encountered in tunnelling at shallow depth usually in urban areas, forepoling methods are engaged to provide for stabilising the crown so as to prevent collapse during stand up time and curing of the concrete lining. Forepoling is usually used as an auxiliary method to ensure that minimum disturbance affects the ground surface structures. The popularity of using forepoling as an auxiliary method stems from the fact that it is easy to execute and minimum site disturbances or machine manoeuvre is required because only forepoling rigs are required. Large-scale tunnelling projects which involve NATM or where settlement and safety are main priorities can use forepoling methods to control crown settlement as well as to stabilise the tunnel face. There are three main categories of forepoling method:

(1) Non-grouting
(2) Grouting
(3) Injection

For non-grouting category, steel pipes are usually inserted into pre-drilled holes or the pipes are jacked into position around the tunnel crown. This forepoling method is commonly known as pipe roof method. These structural elements have

comparatively higher resistance and rigidity than the ground, thus making them effective ground reinforcement. Steel pipes with diameters ranging from 100mm to 1000mm are used and jacked using micro tunnelling techniques to form an arch or box shaped arrangement around the tunnel crown. Pipe jacking involved the transmission of horizontal pushing forces against a vertical backstop to propel concrete or steel pipes simultaneously with excavation within a shield (Whittaker et al., 1990). Pipes are installed in the direction that is parallel to the tunnel axis and usually there is no spacing between pipes. Pipe lengths differ depending on site requirements and ground conditions. Figure 2-8 shows the application of a pipe roof method.

The pipe roof method has been employed in projects with extremely shallow overburdens and weak ground most often in Japan and America, and has successfully controlled surface subsidence (Satoh et al., 1996; Rhodes and Kauschinger, 1996; Hoste, 1980; Mcfeat-Smith, 1997).

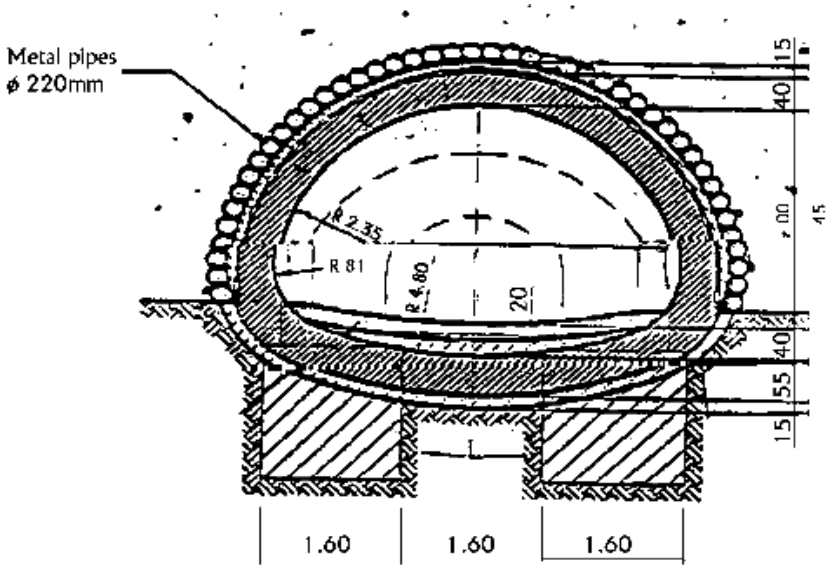

Figure 2-8. Schematic diagram of Pipe Roof method (Rotex OY).

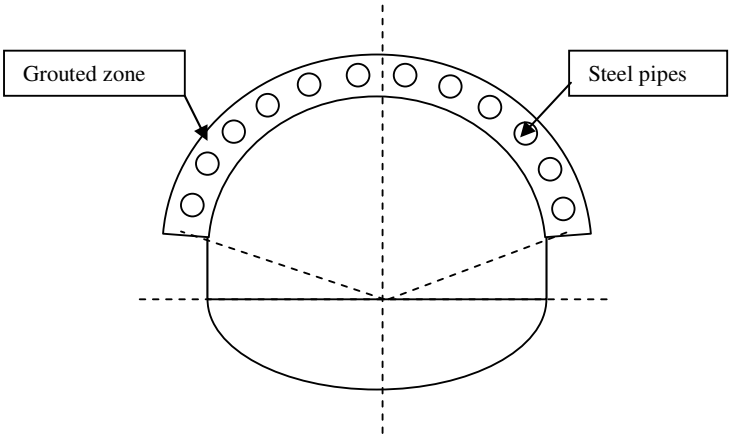

Figure 2-9. Schematic diagram of Pipe Umbrella Arch method.

In the grouting category, steel pipes or reinforcement are inserted into drilled holes and then mortar is poured into the holes and pipe shaft. This form of forepoling method is known as Umbrella Arch or Spiling method. Grouting enhances the stability of the tunnel crown by forming a reinforced arch that controls permeability and improves the cohesion and other geotechnical parameters of the reinforced soil mass. Grout flows through holes on the steel pipes onto the surrounding soil mass. The Umbrella Arch method is usually used in weak and weathered rocks and pipe diameters range from 100 to 200mm with pipe spacing between 200 to 600mm. Typically, 30-40 pipes of lengths between 12-14 m are used depending on the tunnel diameter. In the longitudinal direction, the pipes are usually installed at an angle of 5 degrees to the horizontal and at 8m intervals providing 4m of overlap. Figure 2-9 shows a section of the Umbrella Arch method.

The Umbrella Arch method is used most often at the portal or at fractured zones in especially poor ground conditions over a long work section or where surface settlement is restricted but is also executable in other soil condition from moraine to sand. It is commonly employed as an auxiliary reinforcing method in large diameter NATM tunnels in Italy. The method is flexible, easily carried out and controlled, and can be easily alternated with excavation. Generally, Barisone et al (1982) stated in the design of steel elements for the Umbrella Arch method in rocks that the pipes are designed as horizontal, fixed end beams, and only the resisting section of the

steel pipes are taken into account when calculating the bending and shear stresses in the pipes from the load acting on the tunnel. They also claimed that the pipe spacing does not influence the stresses in the tunnel in rock as significantly as the type of end constraints of the beams. Hence the emphasis is placed on the grout injection through the perforated pipes and an effective support-rock coupling. A more comprehensive description of the construction procedure of the Umbrella Arch method will be given in Chapter 3.

In the injection category, quick hardening cement or urethane is injected with different layouts into drilled holes at high pressure depending on the degree of instability of the ground. This method is commonly known as horizontal jet grouting and is used typically in sandy gravel soil with thin overburden. Sub-horizontal holes are drilled similar to the Umbrella Arch method using the forepoling rigs but instead of steel pipes, grout is pumped into the holes at high pressure to form concrete tubes. The jet grouted zones functions as a beam similar to the pipe roof but unlike the Spiling method which functions as a reinforced arch. Figure 2-10 below shows the horizontal jet grouting method.

The jet grouting method has high durability and might not be easily carried out while feasibility depends on the ground condition. It is unsuitable for grounds with high percentage of clay and boulders and it is also difficult to control. Case histories of horizontal jet grouting were discussed by Naito (1992), Higo et al. (1996) and Hara et al. (1996).

The forepoling methods are usually used in combination with other reinforcing methods such as shotcrete, steel arches (Figure 2-11), micropiles, rock bolts, face reinforcement etc.

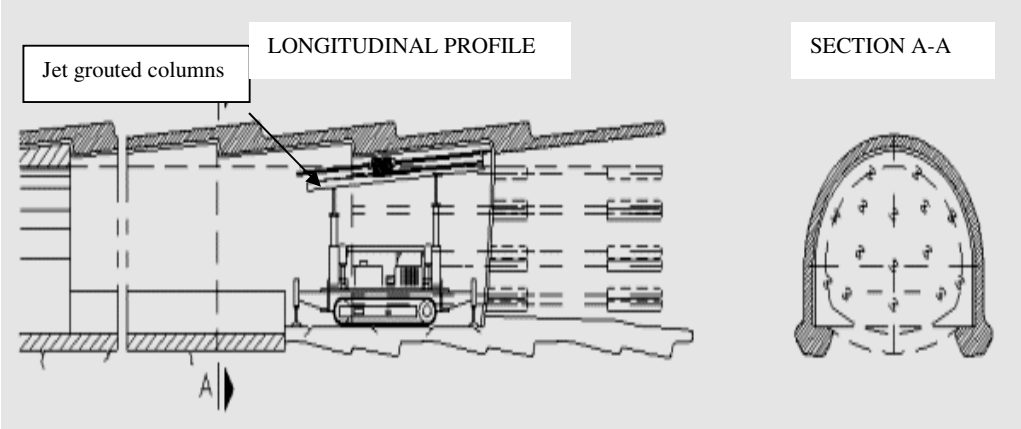

Figure 2-10. Schematic diagram of Horizontal Jet Grouting (Rocksoil S.p.A).

Figure 2-11. Forepoling works in a tunnel in Switzerland (steel ribs are used as additional support).

2.3.1.3 Case Histories of tunnels using Forepoling method

(1) Umbrella Arch Method

An extensive and well-documented case study of the 3.3 km Maiko Tunnel in Kobe City, Japan was presented by Murata et al. (1996) whereby the Umbrella Arch method was used as an auxiliary support. The Maiko Tunnel is a twin highway tunnel with each horseshoe shaped tunnel having a width of 16.6 m and a height of 10.9 m. The shallow overburden range from 7 to 35 m and the tunnel was dug mainly in overlapping layers of sand and gravel over a span of 350 m. The sand and gravel formation, which has strength of 0.28 MPa was underlain by clay with peak

strength of 0.16 MPa. The twin tunnels are separated only up to a maximum distance of 1.1 m at a certain stage of excavation and hence the two tunnels encountered the problem of convergence to each other. Controlling the surface settlement to minimise disturbance to surface structures was the main priority and objective of the project. Due to the large size of the tunnel cross-section, the top heading and bottom benching method was adopted for excavation. The Umbrella Arch method was used as an auxiliary method together with lining concrete, shotcrete, steel ribs, side piles and urethane injection to enhance the stability of the tunnel. Forepoling process utilised 45 nos. of steel forepoles of 114.3 mm outer diameter, 6.0 mm thickness and length 12 m. The forepoles are installed at 8 to 9 m intervals. Field observations and measurements showed that the ground subsidence was controlled within the allowable settlement of 20 mm.

In the construction of the Kokubu River Diversion Channel in Matsudo City, Chiba Prefecture, Japan, the Umbrella Arch was also utilised for 1230 metres of the tunnel and documented by Matsuo et al. (1996). The flood control tunnel is 8.8 m in diameter and is constructed by the ringcut, short bench NATM method. The tunnel runs through mainly fine sand strata in the upstream stretch and some clay formation at the downstream stretch. Umbrella Arch method was employed for most of the downstream stretch of the tunnel, which included fine sand (friction angle = 35˚) and clay (cohesion = 0.25 MPa). The tunnel was dug below ground water table. Auxiliary methods of support included column jet grouting, chemical grouting, steel sheet pile forepoling and Advanced Bit forepoling method. 20 to 28 forepoles were used and they are 30 cm in diameter, 2.8m long, spaced at 35 cm interval and inserted at an angle of 18˚ to the horizontal. The forepoles were placed at every 1.0 m interval. The advanced bit forepoling method applied in this tunnel is characterised by the use of short length forepoles. The authors conducted two dimensional finite element analyses whereby the forepoles were modelled as a single zone and the effective strength of the shotcrete was taken into consideration. Analyses were carried out for combinations of forepoles with and without column jet grouting or chemical grouting. Results showed that the surface settlement was contained within acceptable limits of 20 mm and they concluded the method was

effective in stabilising the tunnel face as the reinforced region formed a contiguous conical shell which aided the formation of a ground arch and contributed to overall ground stability.

Haruyama et al. (2001) had presented a case study involving the construction of the Ohme Tunnel along the Metropolitan Inter-City Expressway in Tokyo, Japan. Grouted steel forepoling and horizontal jet grouting were used as auxiliary methods for controlling subsidence. The tunnel has a cross section of 260 m^2 and overburden of 7-8 m. The tunnel is driven through loam (cohesion = 0.3MPa) and loam and gravel (cohesion = 0.06MPa) formation. Numerical and field settlement measurement were taken and compared favourably. The numerical results were obtained from a 2-D finite element analysis that modelled the forepoles as a region of reinforced zone above the tunnel crown. The forepole zone was assumed to have modulus of elasticity of 1000 MPa and Poisson's ratio of 0.25. It was implied from the analyses that a combination of forepoling, jet grouting, footpile, shotcrete and steel support had worked to control the subsidence.

The diversity of the forepoling method is presented in the construction of a tunnel under a riverbed (Yang et al., 2001). The 90 m tunnel runs under the Han River in Seoul, Korea. The overburden is approximated at 15.6 to 37m and weathered and soft rocks of cohesion of 25 kPa were encountered. Steel forepoles are of length 15 m with overlap length of 7 m and a total of 26 pipes were used in cross section. Single layer of pipes spaced at 300mm are constructed over 120˚ of the tunnel crown. Labiles Wasserglass (L.W.) grouting, shotcrete of 25 cm thickness and steel lib with H-125x125 were used concurrently with the forepoling method to stabilise the tunnel. Crown settlement measured shows that 17.8 mm (weathered rocks) and 6.7 mm (soft rock) were recorded.

Pipe Umbrella Arch method had conventionally been installed as a single layer over the tunnel crown in most case studies. However, Miwa and Ogasawara (2001) described the construction of a double layer of forepoles that covered a 150˚ span of the tunnel crown. Construction of the Itsukachi Tunnel along the Tohoku

Shinkansen utilised the NATM method in combination with the Umbrella Arch method. The tunnel has a cross sectional area of approximately 80 m^2 and spans 1.175 km with shallow overburden ranging from 2-5 m. The tunnel has to run through fine silty sand mixed with cobbles (N = 6-8) and tuff breccia (N= >50). The forepoles has a diameter of 114.3 mm, thickness of 6.0 mm, length of 12.65 m and lap length of 6.65 m. Pipes are spaced at 450 mm intervals between each other and the reinforcement is used for 72.5 m stretch of the tunnel. After installation the pipes are grouted. In order to disperse the load acting on the umbrella arch, additional steel support is used. The bearing capacity of the leg portion was enhanced using 3.0 m long reinforcement bolts and urethane injection. However, the surface settlement measured and that obtained from finite element analyses was 45 mm, which is way off the criteria set. The authors credit the large displacement of the surface to the variations of the nature of the soil in the top heading and insufficient reinforcement to provide for the bearing capacity at the leg portion of the tunnel.

A combination of side drift excavation, pipe roof reinforcement method and Umbrella Arch method were used to great effect in minimising tunnel crown settlement for the construction of the Takatoriyama tunnels for the Kobe Expressway, Japan (Sekimoto et al., 2001). The site is underlain by weathered granite (uniaxial compression strength = 0.1MPa) in the north side and saturated sand and clay of the Osaka layer group (E = 100MPa) in the south. Extensive records detailing the type of reinforcement and construction method for 5 sides of the tunnels are listed in Table 3.1 of Chapter 3. Tunnel crown settlement was effectively controlled at 14 mm for the weathered granite section of the tunnel and within 18 mm for the Osaka layer section.

(2) Spiling Method

Korbin and Brekke (1977) showed in a field study that deformation induced tension was the major mechanism by which rock spiles or bolts displays its effectiveness, while bending was of minor significance. Results taken from the Bonneville and

Eisenhower tunnels revealed that the reinforced arch thickness was strongly dependent on ground type while the arch capacity was dependent on the opening size, shape and depth. The Eisenhower tunnel was reinforced with spiling, steel sets and a two stage concrete liner. Through comparisons of measured and anticipated results, it was revealed that the rock mass-reinforcement system had a major role in providing permanent stabilization of the tunnel opening, while the internal support system performed a secondary role.

Spiling method was also used in the construction of Section F-6 of the Branch Avenue Route in Washington D.C, United States as described by Gall et al (1998). However, in their study, they noted that the actual length of grouted pipe spiling was dictated by the material behaviour and the effective thickness of the clay layer in the ground where the pipes were installed.

(3) Pipe Roof Method

Larger diameter steel pipes are used in the pipe roof method of tunnel support for construction of the horseshoe shaped Shin-Minatogawa tunnel (Sasaki et al., 2001) with a diameter of 14 m. The overburden is 13 m and 85 m of the stretch used pipe roof reinforcement for tunnel stabilisation. Clay (E = 80MPa) and sand and gravel (E = 130MPa) were encountered. 5 steel forepoles of 2 m length were used for the construction of the side drift. Slight deformation of the ground was recorded during installation. In the construction of the tunnel core, the diameter of the steel pipes for the pipe roof was 812.8 mm outer and 787.4 mm inner with no spacing between pipes. Seventeen pipes of 85 m length were installed over approximately 120˚ span of the tunnel crown. The installation of the steel pipes created a subsidence of 12 mm as the pipes are placed from crown to shoulder. According to the authors, this could be due to the excavation of the hole housing the pipe which created holes 40 mm larger than the pipe diameter. During excavation of the upper section of the tunnel, a surface settlement of 15 mm was recorded.

Figure 2-12 and 2-13. Large diameter pipe roofs arranged in an arch shaped umbrella. (Mcfeat-Smith, 1997)

In the construction of large cross section tunnels, large diameter pipes or casing are used as the pipe roof (Figure 2-12, 2-13 and 2-15). The pipes are usually interlocked with T joints (see Figure 2-14) attached to the outside diameter of the pipe and inserted into a receiver slot contained within the inside diameter. The interlocking effect formed will reduce the subsidence and minimise any subsequent surface settlement. Grout will fill the interior of the pipe after welding of the pipe joints from the interior of the pipe. The reinforced pipe arch is then further supported with steel arch ribs or earth retaining struts and piles. The pipe roof method has been used extensively in Japan, Europe and the United States and it has been in used since the 1970s.

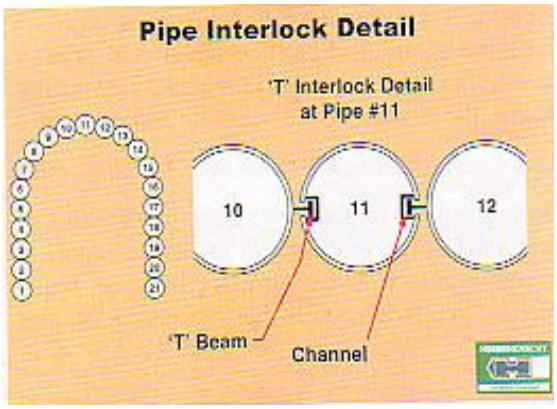

Figure 2-14. 'T' interlock joints (Mcfeat-Smith Ian, 1997)

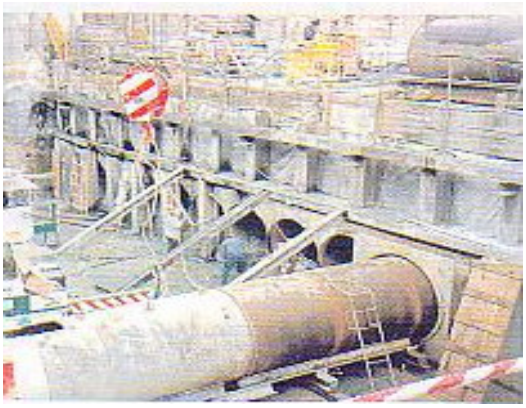

Figure 2-15. Pipe roof project.

The pipe roof method has also been employed under difficult conditions and in rocks since the 1970s. Large motorway tunnels in Italy had employed the method but the steel pipes were not drilled into the rocks, which seemed impossible. However they were inserted into pre drilled holes and grouted afterwards. The Alpe tunnel in Italy (Gentili and Pigorini, 1976) had successfully used thick steel pipes, which were injected with cement mortar and sand to form a protective roof over the tunnel crown to support the loose material above and to protect the workers beneath.

Metro works in Antwerp, Belgium in the early 1970s utilised pipe-jacking for roof slab of shallow stations in clayey soils whereby longitudinal steel pipes of one hundred and twenty and one hundred and eighty centimetres in diameter are driven (Hoste, 1980). Spacing between pipes was injected with asbestos cement and steel frames are mounted to support the tubes. This method gave complete satisfaction to the construction works in terms of the control of settlement.

The major supporting system in the construction of the Indian Creek tunnel (see Figure 2-16) in Atlanta, the United States, was provided by drilling approximately seventy-six centimetres diameter steel pipes into the crown of the tunnel to form an arch using the micro tunnelling technique (Rhodes and Kauschinger, 1996). The relatively short (sixty meters) tunnel is characterised by a busy interstate highway above the tunnel and its extreme shallow cover, which limited the soil arching effect.

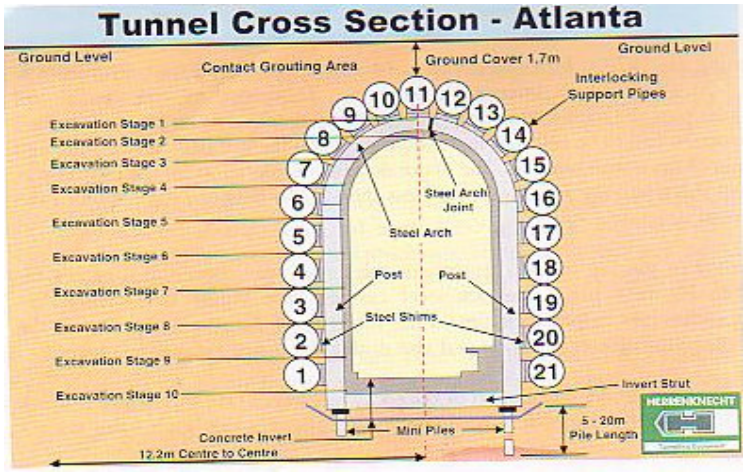

Figure 2-16. Tunnel cross section of the Indian Creek Tunnel (Mcfeat-Smith Ian, 1997).

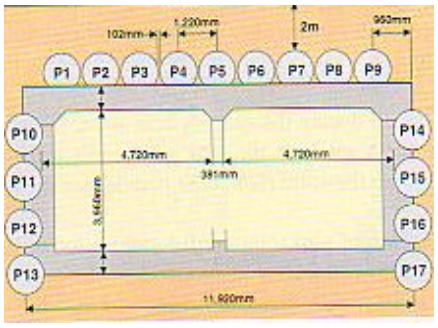

Figure 2-17. Example of a box shaped layout of the pipe roof method (Mcfeat-Smith Ian, 1997).

A similar project in Japan utilised the pipe-roof method to construct part of the Senseki Line in Sendai consisting mainly of organic clay and silt (Satoh et al., 1996). The roof pipes are one metre in diameter and installed over a total length of seventy-two metres of the tunnel with the pipes arranged in a gate type formation. The pipe roof method was selected to limit disturbance to the existing fifteen railway lines in the Sendai station yard. This non-open cut method provided safe train operations and minimized night work. The gate type layout is similar to the box shaped layout as shown in Figure 2-17.

Similarly, Itoh et al. (2001) and Matsumoto et al. (2001) also described the use of pipe roof method in the tunnelling process in soft ground. However they noted that the pipe roof method had to be coupled with auxiliary methods such as chemical

grouting at the foot level of the support in order to effectively control the crown settlement and surface settlement. Itoh et al. (2001) described the Mito Tunnel in Japan, which is underlain with an upper gravel layer and a lower clay layer. Measure to control excessive ground movement such as Pipe roof method was used to stabilise the tunnel crown and shotcrete was used to stabilise cutting face. Groundwater was controlled using horizontal drainage pipes driven from inside of the tunnel. The authors verified through finite element analysis and field measurements that the pipe roof method coupled with the drainage system were very effective in restricting settlement and groundwater control especially in urban tunnels with shallow overburden. In addition, Matsumoto et al. (2001) described the Satsuma Tagami Tunnel in the city of Kagoshima, Japan, which was constructed in volcanic fill. They had suggested the use of pipe roof with chemical grouting to enhance the support footing. All studies have shown that the pipe roof method was effective in reducing ground surface settlement.

One hundred and eight metres diameter and a total of thirty metres long pipe roof had been successfully constructed in the buried Nan Ling Tunnel in China along a double tracked railway (Li, 1990). There are a total of twenty-eight pipes of length ten metres, forming an arch shaped around the tunnel crown and sides. The pipes have diameters of 108 mm and 158 mm and they were filled with cement mortar. Measurements by inclinometers showed that the pipe deflections were maintained at a satisfactory level.

Table 2-3 shows some recent tunnel construction that used the Pipe roof method as a form of pre reinforcement for tunnel excavations. In general, the pipe roof method provides greater stability of the tunnel face and better ground deformation control because of a thickened reinforced zone around the tunnel perimeter. The ground between the pipes is restricted from falling by the close proximity of the driven pipes and hence this reinforced shell will control the ground deformation. Tunnel stability is reinforced by the reduction of the tunnel cross section.

The numerous case studies showed that the forepoling method is indeed popularly used throughout the world especially in large-scale excavations in weak ground. This method can be applied in various types of ground conditions as exemplified by the cases discussed in this section and more field cases are recorded in Chapter Three of this study.

2.3.1.4 Numerical Analysis for Forepoling methods

The usual assumption of rock as a linear elastic material was used to solve for simple situations using analytical or closed form solutions. As a result of this simplification, numerical methods were preferred to solve for rock mechanics problems. As shown in the case histories, many tunnel designers had relied on numerical analyses to design for tunnel support requirements prior to excavation (Sekimoto et al., 2001 and Murata et al., 1996). However, simulations of the support systems were often difficult, as numerical programmes did not specifically include the required support elements. Hence, most often the support system were collectively approximated as a composite material or material with an equivalent strength and represented as beam or shell elements in numerical analyses. Thus, such analyses would produce crude approximations, which may not represent the actual behaviour of the support system in field conditions. Numerous numerical analyses using approximations of a composite material to collectively represent tunnel support system are described in this section.

(1) Umbrella Arch method

Guilloux et al. (1996) conducted an axisymmetrical finite element study for the effects of pre-lining methods (jet grouting arch, umbrella arch method or mechanical pre-cutting) on the convergence of a tunnel. They proposed that the structure (ground and pre lining) would behave like a homogenized cylinder with equivalent characteristics so as to avoid a complicated model that incorporates the exact geometry of all the elements (ground, steel pipes, grout, etc). Using the above assumption, a dimensionless parameter K_s, which was a ratio between the rigidity of

the pre-lining material and the Young modulus of the ground, was used to represent the behaviour of the pre lining. By generalising the entire pre-lining method, the actual behaviour of the individual components in the method was ignored and hence crude approximation would occur. Generalization of all components into a homogenized cylinder would lead to crude approximations. The geometry of the components was neglected in this analysis but they might affect the overall reinforcing ability of the pre-lining arch, for example, the thickness of the grout zone and steel pipes would enhance the reinforcing ability of the arch and the length of the steel pipes would also affect the longitudinal support of the arch as illustrated by Sato and Ito (1993).

The umbrella arch method was used widely in Japan in the 1990s but there was no accurate method to simulate the actual behaviour of the steel pipes and grout material components in numerical analyses except to generalise the components as a single composite material possessing an equivalent strength derived from the method of weighted averages as described by Hoek (2000).

Nishimaki et al. (1995) used the beam on elastic floor method to analyse the ground stability by means of increasing the material properties in the reinforced zone with an improvement ratio that was determined from a three dimensional finite element analysis. Subsequently, a two dimensional finite element method was conducted by improving the material properties of the ground. The stability of the pipes was modelled based on the assumption of linear load distribution on the longitudinal beam element (steel pipes) with non variable spring constants over the shotcreted zone and over the in situ ground respectively. The load and spring constants were then varied to obtain the moment nearest to the value determined by the FEM analysis. They verified through field studies that the umbrella arch method reduced settlement at the crown and that tunnel face collapse was not evident when the method was implemented. Finite Element Method (FEM) was used to verify that the distribution of moment of the beam element (modelled as longitudinal steel pipes parallel to the tunnel advance) is similar to measurements taken from field studies. Results from the study also showed that the pipe spacing, which was

obtained based on Japanese standard of admissible pipe stress of 2100 kilograms per square centimetres and the elastic modulus of the ground, was limited to a range of thirty to sixty centimetres. By improving the material properties, the authors had generalised the support as a composite material with equivalent strength. Hence this will result in crude approximations. Furthermore, the improvement ratio was derived numerically and thus might not correlate well with actual field conditions. The model had assumed linear load distribution, which might not be suitable for field application since load distribution on the field is usually non-linear.

In Japan, the All Ground Forepoling (AGF), the Multi Ground Forepoling Method (MGF), the Reinforced Protective Umbrella Method (RPUM) and the Rodin Jet Fore Pile Method (RJFP) utilise the forepoling method together with jet grouting to form a reinforced zone of umbrella arch. All the methods were similar to the Umbrella Arch method except that they were addressed as different names by different authors. Their construction and functionality were exactly similar to the Umbrella Arch method.

Ohtsu et al (1995) described the Reinforced Protective Umbrella Method (RPUM), which is a combination of long length forepilings and grouting, and studied the behaviour of the ground due to tunnel excavation using a three-dimensional finite element analysis. They stated that the RPUM method was used to stabilise the tunnel face prior to excavation and the surrounding ground. The model was designed with shallow overburden and considered the long length forepiles and face progress. Ohtsu et al (1995) realised that a three dimensional analysis were necessary to predict the actual ground behaviour due to the forepilings and in their analysis, it was assumed that the pre lining arch (forepilings and shotcrete) acted as a combined shell element. The results derived from the three dimensional finite element analysis conducted for a horseshoe shaped urban tunnel (diameter=13m) excavated in soft ground (elastic modulus = 49MPa) and tertiary mudstone (elastic modulus = 490MPa) at a shallow overburden of 3-5m showed that ground surface settlement directly above the tunnel crown are similar to the settlement at the crown of tunnel and they attributed this phenomenon to the fact that the shallow

overburden acted as a beam and any deformations at the tunnel crown is directly translated to the ground surface. It was also found that relatively large settlement occurred at both the ground surface and crown of the tunnel before the arrival of the tunnel face because of the load transmission due to the excavation through long length forepiles. The settlement at the foot portion of the steel ribs was also determined to have greatly influenced the large settlement that had occurred at the ground surface and tunnel crown. The authors had also crudely approximated the pre-lining arch as a single shell element and hence they did not account for geometry of individual components.

Sato and Ito (1993) also used a three-dimensional finite element method to analyse the effect of the Rodin Jet Fore Pile method, which was similar to the other umbrella methods, on tunnel face stability. It was found that the numerical method was effective in simulating the actual ground deformation when the umbrella method was implemented after comparison with actual field results from the Shoryo Tunnel in Japan. The implementation of the method had reduced the deformation ahead of the tunnel face and successfully controlled the convergence of the sidewalls of the tunnel as verified by the authors. Settlement at the tunnel crown was also found to have reduced substantially when the method was implemented. Most importantly, they also found that the length of the umbrella made a significant difference in the deformation in the non-linear elastic analysis as compared to a linear one. This meant that the geometry of the individual components might be an important determinant of the overall reinforcing effect of the umbrella arch. Thus, generalization of the umbrella arch as a single composite material might be a simple approach but it might not yield an accurate result unless the geometry and strength of all individual reinforcing components are taken into account during the numerical analysis.

The length of the steel pipes and thickness of the grouted zone were important factors when analysing the Umbrella Arch method as shown by Kitamoto et al (2001) who used steel pipes that were almost half the length of conventional ones used in Umbrella Arch method to reinforce the tunnel crown. They named this pre

support method as Multi-Ground Forepiling (MGF) method. The forepole length was about 5.5m with pipe diameter of 76.3mm. The method used 38 grouted steel pipes per section with 300mm inter-pipe spacing and 3 sections were arranged in layers above one another with a total thickness of 1200 mm above the tunnel crown. Thus a thicker layer of pre-support as compared to conventional umbrella arch method was formed. They conducted a centrifuge test on the MGF method as compared to the conventional umbrella arch method. The pipe sections were again modelled as shell elements instead of singularly modelled elements. The centrifuge test had used sandy soil with little cohesion in the model. From the test results, it was shown that the MGF method could control the settlement effect much better than the conventional umbrella arch method and that this could be attributed to the close driving of the steel pipes thus creating a shell, and to driving the pipes at greater inclination which produced a thicker layer pre support above the tunnel crown. The test results also reviewed that the cylindrical theory can be used to effectively represent the effect of pre support thickness on surface settlement and explain the characteristics of surface settlement. In a comparison of maximum surface settlement and maximum pipe diametrical deformation, the authors showed that the results made from the cylindrical shell theory correlated well with test results. The theory was made on the basis of the fact that the crown settlement and surface settlement after the face has passed have a similar tendency and are equal in magnitude provided that tunnelling is executed in shallow and little cohesive grounds. Although the authors had similarly used combined shell elements to crudely approximate the whole support system, this analysis showed that geometry and thickness of individual components were important factors to consider when analysing the Umbrella Arch method numerically.

(2) Pipe Roof Method

Very few authors had numerically analysed the Pipe roof method but Matsumoto et al (2001) showed that the forepoling method is usually not implemented alone but with other auxiliary support systems to enhance overall tunnel stability. They conducted a two dimensional finite element analysis to predict the surface

settlement and angle of depression in volcanic fill, called Shirasu, when thirteen steel pipes of one metre diameter were placed in an arch shaped around the tunnel crown prior to excavation. It was noted in the study that the pipe roof was able to provide both cross sectional and longitudinal support effect provided that the ground at the support foot level is strong. Hence, chemical grout injection was implemented to enhance the support at the foot level. The authors noted that the pipe roof method was able to prevent collapse of the ground if the groundwater condition was limited to a manageable level. The chemical grout injection was thus recommended to curb the inflow of ground water through the space between the pipes and the ground after excavation.

2.3.2 Longitudinal face reinforcement

Besides the forepoling method, the face reinforcement method had gained popularity for its efficiency in controlling tunnel face stability. Both methods were also commonly used together in large-scale excavations to maximise tunnel stability during excavations. In order to minimise ground movement ahead of the tunnel face in soft ground or fault zones, sub-horizontal fibre glass pipes or bolts installed on the tunnel face have been used and is gaining popularity due to its cost effectiveness, and a few technical advantages such as its high longitudinal strength while relatively brittle in the traverse direction hence easily broken during excavation (Wong et al, 2000). Face pre reinforcement were usually coupled with mechanical pre-cutting (Van Walsum, 1992), pipe umbrella or jet grouting umbrella arch to maximise the overall stability of the tunnel excavation. The horizontal pipe face reinforcement had proven to be an effective technique for face stability as it was suited for varying kinds of geological and geotechnical conditions. Similar to the forepoling or pipe roof method, few numerical and analytical studies regarding the horizontal fibreglass pipe face reinforcement had been presented up to the mid 1990s. However, this technique had been used in reinforcing tunnel face stability extensively in France and Italy and the method has proven to be successful in a large number of projects that enhanced tunnelling safety regardless of ground conditions.

2.3.2.1 Physical Models and Field Studies

Lunardi et al. (1992) reported results obtained from extrusion tests on the face of the Poggio Orlandi Tunnel whereby fibreglass pipes (see Figure 2-18 to 2-20) were used as face reinforcements. It was the first instance that a face pre-consolidation method was used to stabilise the tunnel face and prevent an excessive decrease in the confining pressure. The tunnel under study was underlain by soft saturated silty clayey soils with tunnel diameter of twelve metres and eight hundred and fifty metres in length. It was found that with the inclusion of the face reinforcement, the excavation rate of the tunnel had increased. The layout of the pipes on the tunnel face and the construction sequence were defined based on soil profile, constraint state, duration of curing of the grout and depth of overburden. The sequence of the consolidation works and the layout patterns of the fibreglass pipes were executed based on the experience acquired by the site staff. An extensive monitoring and field measurement were executed to find the ground strains and axial strains experienced by the pipes. Such an extensive study had led to a better understanding of the working principle of the fibreglass pipes as face reinforcement. However, no concrete mathematical evaluation of this method of face reinforcement had been studied though its effect on face stability had proven in this field study to be highly reliable.

Similarly, the results of measurement taken from the face of the San Vitale Tunnel were also reported in a separate report by Lunardi et al.(1992) and Poma et al. (1995) where face reinforcement had been widely used during its construction.

Figure 2-18. Tunnel face reinforcement (longitudinal fibre glass tubes) (Rocksoil S.p.A).

Mitarashi et al. (2001) conducted a demonstration test to show the effectiveness of the fibreglass face reinforcement method in stabilising the tunnel face. In order to verify its work efficiency, a steel pipe long forepiling method was concurrently implemented under similar condition and their results showed that the face reinforcement was either equal or better than the long forepilings. However it was also noted that the face reinforcement poses several advantage in that it is easy to handle and implement. The fibreglass tubes have high tensile strength (600N/mm^2) despite their small diameter as observed from laboratory tests conducted and the tubes also have high load carrying capacity of 200kN or more. In addition, they are also light weighted and cheap.

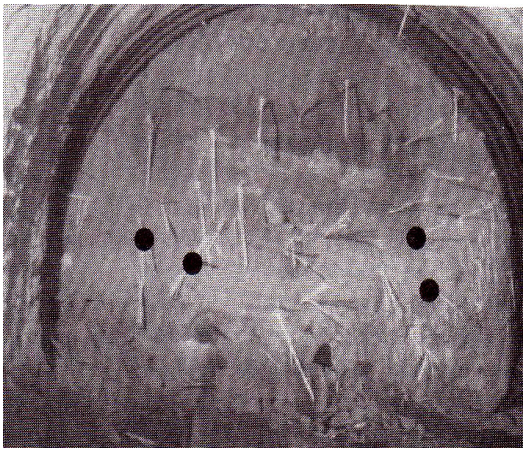

Figure 2-19. Layout of tubes.

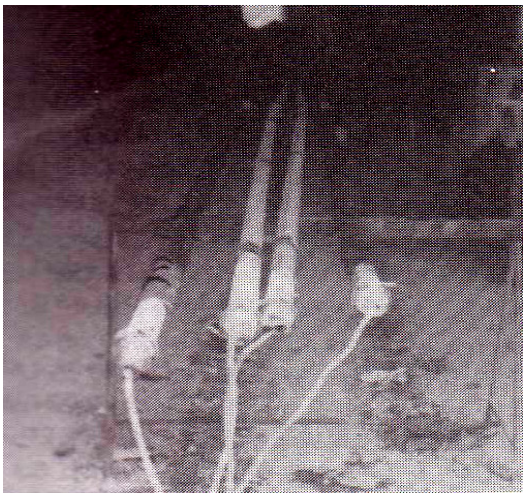

Figure 2-20. Instrumented tubes.

Limited rigorous design or analysis method had been studied and tunnel engineers usually rely on past experiences, which tend to lead to safety and cost issues. Grasso et al (1993) performed a study using axisymmetrical finite element analysis on the face reinforcing effect of horizontal pipes and proposed the concept of equivalent cohesion for the reinforcing effect of horizontal pipes. They had analysed the face stability using the numerical solution combined with the formulas based on the arching theory (Cornejo, 1989).

Peila (1994) pointed out that until his research into face reinforcement in 1994, there had been no three dimensional modelling of the face reinforcement technique to his knowledge. There were no reports or researches with the aim of

comprehending the behaviour of the face reinforcement from a theoretical aspect. A detailed analysis of the behaviour of the face reinforcement and its influence on face stability can only be obtained through a complex three-dimensional and numerical analysis (either finite element method or boundary element method). Hence, Peila (1994) conducted a parametric three-dimensional FEM analysis in a linear elasto-plastic media to study the behaviour of the horizontal pipe reinforcing technique. He developed a relationship between equivalent face pressure and face reinforcing layout after conducting extensive studies on the face stability reinforced with horizontal pipes. The main intention of developing this relationship was aimed to determine if a distributed pressure could adequately simulate the effect of face reinforcement using grouted pipes. He eventually proposed using the formula as shown in Equation (3) and developed by Bischoff and Smart (1975) because it correlated well with the numerical results obtained.

$$P_{face} = \min \{ n.A.\sigma_{adm} / S , n.s_l.\tau_{adm} / S \} \quad (3)$$

where, P_{face} = fictitious pressure on the tunnel face

n = number of pipes

A = single pipe section

σ_{adm} = maximum admissible stress in the pipe material

s_l = total lateral surface of the single pipe

τ_{adm} = maximum shear stress admissible at the interface between the pipe and the ground

S = total excavated cross section area

The above formula, after applying a reliable safety factor, can be used to calculate the number of pipes required only when the stabilising face pressure is known. The study found that eleven pipes were equivalent to 0.15MPa of face stabilising pressure. However, the face reinforcement did not significantly influence the tunnel convergence as compared to the tunnel linings. And the plastic zones and radial displacement were also affected mainly by the lining. The findings appeared to undermine the reinforcing effect of the horizontal pipes as a face-reinforcing

element even though they cause the axial stress in the reinforced core to change from tension to compression. Through the study, he also pointed out that simple limit equilibrium analysis performed by Tamez (1984) and Ellstein (1986) did not give reliable results since they defined a sliding surface ahead of the face, which does not exist.

Peila et al. (1996) conducted another numerical parametric three dimensional finite element analysis to study the behaviour of sub horizontal fibre glass pipes as reinforcing elements under varying reinforcing layouts and their respective influence on the stability of the tunnel face using the geometry and geotechnical parameters of the Saint Vitale tunnel in Italy. The study was conducted to find an optimum face reinforcement layout and pipe numbers. They recommended using three modelling approaches as described below to describe the behaviour of the reinforcement layouts. 3 types of modelling procedure were proposed to access their accuracy in representing the effect of the tunnel face reinforcement and they are:

(a) modelling the pipes singularly
(b) increasing the cohesion of the core
(c) applying a fictitious axial pressure to the tunnel face

In analysis (a), the pipes are modelled singularly as cable elements. In analysis (b), the cohesion of the core is increased with Equation (4) and taking a working force of five hundred and fifty kilo Newton for each pipe ($\Delta\sigma_3$),

$$c^* = [\, c + (1+\sin\text{Ø} / 2\cos\text{Ø}) \,]. \Delta\sigma_3 \qquad (4)$$

where, c* is the improved cohesion due to the reinforcing pipes, c is the cohesion of the ground before installation of reinforcement, Ø is the friction angle and $\Delta\sigma_3$ is the additional confining pressure provided by the reinforcing pipes. The underlying principle behind the equation is that the glass fibre tubes reinforced the rock by providing a confining pressure, which enhanced the shear resistance of the rock (Lang and Bischoff, 1984).

In the third analysis, a fictitious axial pressure was applied to the tunnel face and this pressure was calculated using the equation from Peila (1994) as shown earlier with a similar working force used to calculate the new cohesion in the reinforced core and a lateral bond of 0.3 MPa for each pipe. All three analyses were run for different pipe layouts to verify the reliability of the two modelling approaches and furthermore, the effect of different reinforcement layout could be evaluated as well. Results from the study showed that all the three analyses presented a reduction in the plastic zone ahead of the tunnel face after reinforcement installation. In addition, it was also shown that the increment of the number of pipes on the tunnel face will cause a decrease in the maximum axial forces and the position of this force along the pipe moves closer to the tunnel face. The radial stress was also found to be equal to the natural stress at a position nearer to the tunnel face when the face reinforcement was installed. However, there exists a difficulty in evaluating the pipe acting force. They concluded through a parametric study that three dimensional numerical modelling of the ground and individual pipes are necessary to investigate the behaviour of the reinforced tunnel face since simplified methods could not handle the complexity associated with the tunnel face stability conditions.

However, Poma et al (1995) had conducted an axisymmetric finite difference analysis when he studied the excavation and supporting operations of the Saint Vitale tunnel in Italy, which is characterised by swelling soils. Fibreglass tubes were used as tunnel face reinforcement and 20cm thick shotcrete is placed on the tunnel front. The field measurements obtained from the monitoring of the Saint Vitale tunnel were used to conduct a back analysis to evaluate the resistance and deformability characteristic of the rock mass. The fibreglass tubes were simulated as cylindrical shell of 1.2m and 2m in thickness with 66 and 96 numbers of tubes respectively. In the study, they concluded that the tunnel face reinforcement was effective only if it was designed like a vault and used in swelling or squeezing grounds. Furthermore, through the analysis, it was found that the concrete lining and geometry of the tunnel would affect the number of horizontal pipes used in the face stability.

Most recently, Yoo and Shin (2000) performed an investigation on the behaviour of the tunnel face reinforced with horizontal pipes using three dimensional finite element method of analysis (DIANA) of a 8m circular tunnel excavated in 3 types of ground conditions and overburden cover. Reinforcement elements were used to simulate the reinforcing bars. Through the studies they concluded that the tunnel face deformation behaviour is significantly influenced by the reinforcement layouts. However, their study was based on the assumption that face deformation was the only form of ground movement and that the radial deformation around the tunnel periphery was fully restrained since the main objective was to study the face behaviour. The nodes along the excavated tunnel wall were fixed at every step in order for the above assumption to hold. As such, by varying the boundary conditions and using a simplified excavation phase, the maximum face axial displacement were evaluated with loading steps, number of pipes and length of pipes. They found that the reinforcing effect could be maximised by a critical pattern of reinforcement layout since the face displacement tends to a constant after a certain layout. The length of pipes was also found to be a function of lateral earth pressure for a given ground condition. In addition, it was revealed that the number of pipes and length of pipes are affected by the geotechnical characteristics of the ground rather than the tunnel geometry.

Wong et al (2000) also developed an analytical model based on a spherical cavity in a medium reinforced by linear inclusions using a homogenised approach previously developed by Jassionnesse et al. (1996). The analytical model proved to be consistent with more sophisticated three-dimensional numerical approaches (Dias et al., 1998) and also with extrusion profiles developed from field data from the Tartaiguille Tunnel in France. The field study showed that a critical distance, equal to the diameter of the tunnel, where a zone of undisturbed ground exists ahead of the face. The analytical model had assumed perfect bonding between bolt and soil, and that all field quantities such as stress, strain and displacements verify spherical symmetry ahead of the face. Dias et al. (2001) conducted further analysis to understand the influence of the soil/bolt interface on the behaviour of the tunnel

face using a three dimensional finite difference method. They had used the analytical model developed by Bourdeau (1994) to derive friction law parameters. Pull-out tests were also conducted by them to determine the failure load and head displacement. Through comparisons of face displacement and axial forces in the bolts, the results showed that the type of frictional laws had no influence on the radial displacement but out of the three types of law used in the analysis (Frank-Zhao frictional law, trilinear and bilinear); the trilinear law tends to provide a more accurate picture.

2.3.3 Mechanical Pre-cutting Tunnelling Method

The technique of cutting of rocks by mechanical means has also been extensively used. The exact outlines of circular tunnels are mechanically pre-cut before any excavation of blasting takes place and these slots are then filled with shotcrete. Van Walsum (1992) provided a comprehensive explanation of the stages of Mechanical Pre Cutting Tunnelling Method (MPTM) and used field studies from several tunnels in France to show that the surface settlement is substantially reduced when using the MPTM as compared to the NATM. Furthermore full-faced advance was made possible when using the MPTM instead of the heading and bench method. Constantin (1996) also described the MPTM in the underground crossing of Toulon, France. He had provided an informative and sequential working cycle of the MPTM works in the project.

2.4 Design of Tunnel Supports

The primary action of soil or rock reinforcement is in increasing the shear capacity and stiffness of the soil rock mass. Considerable changes in the state of stress with associated strains and deformations will occur when a tunnel is excavated. Tunnel supports such as radial rock bolts will provide a stressing force in the surrounding zone. The convergence confinement method is used to evaluate the phenomenon in which the forces in the readjustment process of the surrounding soil mass after the tunnel is excavated are controlled by a competent stress distribution and rock yielding theory (Rabcewicz, 1973). The method involved the interaction between

the ground, which converges towards the excavation, and the support, which limit the closure by exerting a confining pressure. Panet and Guenot (1982) used numerical models to develop a function that gave tunnel closure in terms of the distance to the face. The derived function C(x) was described by Equation (5). A parameter λ_d was introduced to account for the delay in installing the lining was incorporated together with the use of ground reaction curves and support-load deformation curves as shown in Figure 2-21. The curves are plotted between ratio of radial stress and initial stress and ratio of radial displacement and radius of tunnel.

$$C(x) = C\omega \{ 1 - [1/ (1 - x/0.84r_p)]^2 \} \quad (5)$$

where C(x) is the tunnel closure

$C\omega$ is the final convergence

r_p is the radius of the plastic zone far behind the face

x is the distance to the face

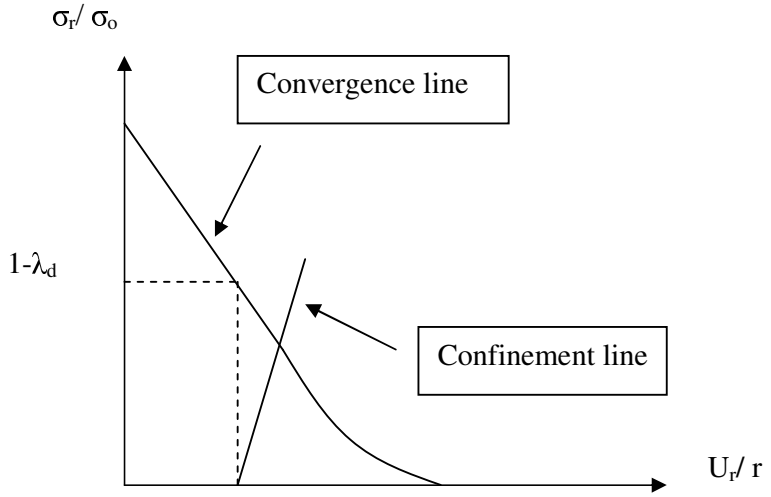

Figure 2-21. Convergence-confinement lines.

The uniform contraction and shape change of the tunnel support depend to a large extent on the relative stiffness and the shear stress transmission of the support and the ground as defined by Einstein and Schwartz (1979). Based on the original relative stiffness solution defined by Burns and Richard (1964), they developed a simplified analytical approach to tunnel support using a new relative stiffness solution. They argued that the old solution had assumed an “external loading”

condition, which meant that the tunnel opening was excavated and supported prior to the application of the load that corresponded to the free-field stresses instead of after the load was applied. This assumption would thus contribute to over estimation of the support forces. Under this new relative stiffness solution, the tunnel support is incorporated through the use of two dimensionless parameters, the compressibility (C*) and flexibility (F*) ratios.

$$C^* = ER\,(1-\nu_s^2) / E_sA_s(1-\nu^2) \qquad (6)$$

where, E, ν and E_s, ν_s = elastic constants for the ground and support

A_s = average cross-sectional area of the support per unit length of tunnel

R = tunnel radius

The compressibility ratio measures the relative stiffness of the ground support system under a uniform or symmetric loading condition. The flexibility ratio is a measure of the relative stiffness of the ground support system under an antisymmetric loading condition. The boundary conditions at the interface are full slippage and no slippage.

$$F^* = ER^3\,(1-\nu_s^2) / E_sI_s(1-\nu^2) \qquad (7)$$

where, I_s = moment of inertia of the tunnel support per unit length of tunnel.

A limitation of the relative stiffness solution is that it assumed that the supports were installed simultaneously with the excavation. Hence, the support load can vary significantly from that predicted since substantial ground displacements occurred before the support was erected. The assumption of linear elasticity was also restrictive in the relative stiffness solution.

Variations of the relative stiffness and its effect were further investigated by Peck (1969). Based on observation of several soft ground tunnels, he concluded that the earth loads acting on tunnel liners would generally be significantly smaller than the

overburden pressure at tunnel depth as a result of the load being partly carried by the surrounding ground and this in turn is due to the three dimensional deformation of the tunnel face. He had proposed a four-step semi-empirical procedure to design tunnel linings, which did not assume fixed load acting on the lining. The four steps recommended should include providing adequate ring load and anticipated distortions due to bending, accounting for possibility of buckling and allowing for significant external conditions not considered previously.

Another method developed by Bischoff and Smart (1975) assumed that a system of rock reinforcement is structurally equivalent to an internal support for the tunnel and this internal support is acted upon primarily by thrust. Hence, the increase in unit thrust capacity ΔT_A of a rock mass in a reinforced rock arch is given as:

$$\Delta T_A = q (\sigma_b A_b / S^2) t \qquad (8)$$

where $q = \tan^2 (45^\circ + Ø/2)$

σ_b = yield stress of reinforcing steel

A_b = cross sectional area of the reinforcing steel

S = spacing of the reinforcement pattern both transverse and longitudinally to the tunnel axis

t = effective thickness of the reinforced arch = L – S

L = length of fully grouted rock reinforcement

The rock stabilisation system will be structurally equivalent when the increase in unit thrust capacity of the rock mass in the reinforced rock arch is equal to the unit thrust capacity of the internal supports.

2.5 Arch Effect

The most delicate stage in tunnel excavation is during the intermediate process instead of at the final stage of the tunnel completion because at the former stage, the effects of disturbance caused by the excavations have not yet been completely

confined by the final lining (Lunardi, 2000). The pre-existing stresses in the rock mass deviated by the opening of the cavity are channelled around it in an "arch effect", creating zones of increased stress on the walls of the excavation.

A tunnel engineer has to determine if and how an arch effect can be triggered when a tunnel is excavated and then to ensure that arch effect is formed by calibrating excavation and stabilization operations appropriately as a function of the particular stress strain conditions (Lunardi, 2000).

2.6 Tunnelling induced Ground Movements

Limiting the surface settlement is the most important objective in designing tunnels in soft ground under urban infrastructures. Surface settlement due to tunnel excavation will inevitably cause disturbance to nearby buildings, services and infrastructures; hence the ultimate aim is to limit this undesirable effect. Understanding the tunnelling induced ground movements will require a three dimensional analysis of the deformational effect.

2.6.1 Loss of ground at the tunnel

When a tunnel is constructed at shallow depth, it will inevitably produce deformation of the surrounding ground, which then translates to surface settlement. The volume of loss ground at the tunnel is a dependent on the soil properties, suitability of the construction method for the range of soil conditions to be encountered in the tunnel and ground water conditions as stated by Cording et al. (1976). The volume of ground movement at the tunnel is attributed to radial movement and the movement of soil inwards at the tunnel face. Influence of the stability ratio on the displacement in clay soil was discussed by several authors. Peck (1969) noted that for stability ratio greater than five, the soil is likely to invade the tail void almost immediately after excavation, which will not permit satisfactory filling of the voids. For $N<4$, the settlement would be small if good construction methods were implemented.

From laboratory extrusion (tunnel face deformation) tests conducted by Attewell and Boden (1971) and Attewell and Farmer (1974), the rate of extrusion was found to be a function of the stability ratio and for N>4.5, the extrusion rate increased rapidly. Ground movement into the unsupported parts of the excavated soil occurs at a constant rate as stated by Attewell and Boden (1971) in their tests. Schmidt (1969) used the solutions for radial displacement around an unlined tunnel in a uniformly loaded elasto-plastic material to estimate the maximum total volume of loss ground, V_t , and found that for N between one to two, V_t is between 0.5 to 4%, and for N = 6, V_t > 4%. This study however assumes no restraint is provided at the shield or lining. Attewell et al. (1986) concluded that the loss of ground at the tunnel will exactly translate into surface settlement quantitatively in firm to stiff clay soils while in granular non-cohesive soil, the surface settlement will be lesser as a result of the effect of dilation through arching above the tunnel crown. It was also found that the greatest vertical movement is concentrated at the tunnel crown, which meant that the maximum surface settlement will also be directly above the tunnel crown. Cording et al. (1976) also discussed ground losses in fissured clay, sand and gravel overlying low permeability zones and granular, slightly cohesive soils. In a field study conducted by them in the Washington D.C. tunnel which is underlain by granular, slightly cohesive soils, they found that large displacements did not develop at the tunnel face but instead occur behind and over the shield as soil material moved immediately to fill up the voids.

Attewell et al. (1986) assumed that the overburden stress is the major driving pressure in shallow ground tunnelling and that the axial movement of the ground into the tunnel face occurs at a rate equal to that of ground movement radially around the periphery of the excavated part. The rate of tunnel advance will thus play a critical part in determining the control of ground loss. The magnitude of the soil movement at the tunnel is dependant on the type of soil, tunnel size, rate of tunnel advance and the types of support used to stabilise the tunnel. The movement of soil in cohesive and non-cohesive soil varies due to the difference in soil structure and characteristics. Dense non-cohesive soils may not dissipate the soil

movement entirely to the ground surface but may instead cause loosening of the soil at the tunnel periphery. Loose granular soil will tend to cause more surface ground loss due to closure of inter particle distances above the tunnel and hence a larger magnitude of ground loss is expected as compared to the actual loss of ground at the tunnel. The ground loss at the tunnel can be attributed primarily to four sources and they are:

(1) Face Loss, V_f

This is the axial loss at the tunnel face. It contributes both to the transverse spread and to the extent of the forward longitudinal span of the surface settlement trough. According to Attewell et al. (1986) from his studies of British tunnels, for clay soil, the face loss an be evaluated by,

$$V_f = \pi a^2 k k_1 = \pi a^2 k_1 (m'/l') \qquad (9)$$

where, a = outer radius of the shield,

l = tunnel advance distance,

m = average distance of soil movement at the tunnel,

k = soil intrusion distance per unit length of tunnel advance == m'/l',

m'= dm/dt = average rate of soil movement at the face,

l'= dl/dt = average rate of tunnel advance, and

k_1 = factor that accounts for doming effect ($0< k_1 <1$).

The loss at the tunnel face can be expressed as a percentage of the tunnel volume per unit distance of advance or in other words face area (Attewell et al., 1986), as

$$\% V_f = 100 k_1 \qquad (10)$$

where, k_1 is the factor that accounts for doming effect ($0< k_1 <1$).

In granular soils without any cohesion, the sand will slump into the face of the shield at a slope angle controlled by the inter-particle friction (Szechy, 1970).

Hence defining the slump slope angle as α degrees to the horizontal invert of the shield,

$$V_f = \pi a^2 (2a\cos\alpha)/2 = \pi a^3 \cos\alpha \qquad (11a)$$

, and

$$\%V_f = (100\ a\cos\alpha) \qquad (11b)$$

where, α = slope angle, and

a = outer radius of the shield.

Laboratory measurement of ground intrusion rate at the tunnel face conducted by Attewell et al. (1986) showed that the ground intrusion measured at the centreline are higher than those measured away from the centreline.

Ranken and Ghaboussi (1975) conducted finite element analysis of stresses and deformations around an advancing tunnel and through the results, they showed a trend of differential displacements appeared at about two times the tunnel diameter ahead of the face, and the greatest displacement took place along the tunnel centreline and progressively became less near the periphery regardless of lined or unlined tunnel and varying soil parameters. Thus, this enhances the fact that a doming effect takes place at the tunnel face.

(2) Radial Loss, V_b, over the shield

This is the radial ground loss around the perimeter of a shield and its tail due to the presence of an over cutting bead or equivalent over cutting device. Assuming a 360˚ bead, the area of the shield and tail over which radial deformation may take place is

$$A_S = 2\ \pi\ l_S\ (a+b) = 2\ \pi\ l_S\ a \quad (b<<a). \qquad (12)$$

where a = outer radius of the shield,

b = thickness of any over cutting bead or equivalent device fitted to the shield,

l_S = length of the shield and its tail,

Hence the volume of radial ground loss over the shield is

$$V_b = A_S\, m = 2\,\pi\, l_S^2\, a\, (m'/l') \qquad (13)$$

where, $m = t_S\, m'$ and t_S = time in which the soil adjacent to the shield deform inwards = $l_S/\, l'$. m' is the rate of soil movement at the tunnel face and l' is the rate of tunnel advance.

There are also other losses over the shield, which are unquantifiable. These losses are usually related to the mechanics of shield driving and are discussed further in Muir Wood, 1970; Shiraishi, 1968; Cording et al., 1976; Attewell et al., 1986.

In granular soils, there will be continuous slumping of the soil on the shield and the tail periphery. Hence, the radial ground loss will be

$$V_b = \pi\,(2ab + b^2) = 2\,\pi\, a\, b \qquad (14a)$$

or

$$\%\ V_b = 200\ b/a \qquad (14b)$$

where, a = outer radius of the shield,

b = thickness of any over cutting bead or equivalent device fitted to the shield,

(3) Postshield/ pregrout loss, V_u

This is the radial ground loss that occurs behind the tail skin after lining erection. Assuming that the soil has contacted the periphery of the tail before the shield is shoved forward,

$$V_u = 2 \pi l_u a \ (m'/l') \qquad (15a)$$

where, l_u = unsupported ungrouted tunnel length behind the tail. And expressed as a percentage of total face area,

$$\% V_u = 200 \ (l_u /a)(m'/l') \qquad (15b)$$

In granular soils, the pre-grout loss is equal to $\pi (a^2 - a_1^2)$, where a_1 is the external radius of the lining and any bead thickness is ignored. And,

$$\% V_u = 100 \ [1- (a_1/ a)^2] \qquad (15c)$$

(4) Postgrout Loss, V_g

This is the radial loss that occurs behind the tail of the shield until the set grout resists further inward movement of the ground. This value is usually measured in situ and there are no satisfactory method of estimating V_g as m' decreases (Attewell et al. 1986).

The total volume loss, V_t, at the tunnel is the summation of the individual losses as discussed above and

$$V_t = V_f + V_b + V_u + V_g + \text{other losses.}$$

There are also time dependent settlements, which should also be accounted. The long termed settlement could be due to the collapse of voids previously formed around the tunnel and the inflow of soil through holes formed in the lining. Consolidation of the soil outside the springline will also induce a downward

deflection of the tunnel crown as the horizontal diameter increases. The consolidation of the soil around the tunnel is due to the stress increase around the tunnel and drainage into the tunnel coupled with pore water pressure reduction around the tunnel as a result of excavation.

For firm to stiff clay soils, Attewell et al. (1986) concluded that the volume of the settlement depression created at the ground surface, V_S, is equal to the volume of total ground loss at the tunnel, V_t. However, the long termed settlement should also be considered since it will contribute a major portion of the total displacement.

In granular non-cohesive soil, $V_S = V_t - V_d$ where V_d is the dilation that may occur through arching above the tunnel crown. Contrary to the clayey soils, the long termed settlement will only contribute to a small portion of the displacement.

A simple overload factor can also be introduced to provide a practical estimation of V_t and V_S in cohesive soils as stated in Attewell and Yeates (1984), Glossop (1977) and Schmidt (1969). The simple overload factor is expressed in terms of $[(\gamma z_0 - \sigma_i)/ c_u]$ and using this factor, a range of values of ground loss at tunnel level and volume of transverse settlement trough can be evaluated from case studies data for different soils.

Mitchell (1983) has also attempted to evaluate the volume loss based on case studies by Peck (1969) and Schmidt (1969) in soft clay and defined

$$V_t = (c_u / E_u) \exp [(\gamma z_0 - \sigma_i)/ 2c_u] \qquad (16)$$

where E_u is the undrained deformational modulus. He had also suggested providing a safety factor of three for very sensitive soils.

2.6.2 Ground surface settlement

The usual practice to estimating deformations around a tunnel is to investigate the stress strain behaviour near the tunnel cavity theoretically. As a tunnel is advanced through the ground, changes to the initial state of stress in ground will take place and consequently followed by soil strains, which manifest as deformation of the tunnel wall and ground surface. This phenomenon will be most evident in shallow tunnel where the excavation will produce large deformations that translate to surface subsidence causing devastation to nearby structures and services. The effect of surface subsidence will be magnified in soft ground where soil is unstable and requires additional support or reinforcement. Understanding the process and the effect of ground movement is relatively easier as compared to predicting the magnitude of the ground movements at the tunnel and the corresponding surface settlement.

Analytical, empirical and numerical methods can be used to solve the problem of estimating the deformation around a tunnel cavity. Several authors had tried to model the surface depression caused by tunnelling to that of a normal probability curve. However this assumption is based primarily on the resemblance of the shape of the surface settlement to the normal probability curve, which bore no theoretical basis. However, such an assumption has provided an accurate estimate of the actual ground settlement over the years but only for cohesive soils. Table 2-3 below shows some case histories of tunnels excavated in various types of soil and their corresponding surface settlement. Non-cohesive soil tends to be dependant on workmanship factor as discussed by Attewell and Yeates (1984) and hence the magnitude of the surface settlement would be more difficult to estimate.

Table 2-3. Case histories of tunnels and the associated ground movements.

Tunnel	Ground Type	Depth (m)	Diameter (m)	Maximum vertical displacement (cm)	Maximum axial displacement (cm)	Maximum lateral inward displacement (cm)	Construction Method	Reinforcement method	Reference
Washington Metro	Granular soils	11.6	6.4	33 (at crown)		5 (at springline)	Ripper bucket on articulated arm inside shield	Steel ribs with tumber full lagging	Cording et al. (1976)
London	Stiff, fissured, heavily consolidated clay	27.2	4.1	1.65 (above crown)	<2.5 (at tunnel opening)	0.8 (at springline)	Hand excavated, shield driven	Cast iron segments	Attewell and Farmer (1974)
Willington Quay, England	Soft, saturated, silty alluvial clay	13.375	4.25	Approx. 0.8 (above tunnel centre line)		Approx. 0.7 (at tunnel face level but subsurface)	Hand excavated, shield driven	Concrete segments	Attewell et al. (1978)
Sao Paulo	Hard overconsolidated clay	13	12 (width), 10 (height),		Approx. 10 (at 10.10m above crown)	Approx. 12	Roadheader	Lattice girders and NATM	Casarin et al. (1996)

The distribution of the settlements or settlement trough at the level of the foundations approximated a normal probability law as described by Peck (1969). He had used empirical data to demonstrate that a cross section through the settlement trough over a single tunnel can be represented by a normal probability curve. He noted that such a curve cannot be justified theoretically but serves as a temporary expedient for estimating the surface settlement in the lateral direction from the tunnel centre line. As such, this will assist the tunnel designer in gauging the necessary precautions or extra reinforcement required for nearby services or buildings. The equation used to describe this probability distribution is as shown:

$$w = w_{max} \exp(-y^2/2i^2) \qquad (17)$$

where w = surface settlement at a transverse distance y from the tunnel centre line

w_{max} = maximum settlement at x=0

i = location of maximum settlement gradient or point of inflexion.

New and O'Reilly (1991), Mair et al. (1996) and Attewell et al. (1986) have described the application of this Gaussian distribution to the prediction of vertical and horizontal movements due to single and multiple tunnels. Bracegirdle et al. (1996) have also used this in evaluating the potential damage to cast iron services or pipes induced by tunnelling. Similarly, Yoshida et al. (1994) also described the behaviour of ground and adjacent underground piping during shield tunnelling. Durand et al. (1994) had used this in their design approach for the Toulon underground motorway crossing to predict surface settlements and their effects on nearby buildings.

The properties of the normal probability curve as used to represent the cross section through settlement trough above the tunnel and its relationship to the dimension of the tunnel is shown in Figure 2-22a. Extrusion tests conducted by Attewell et al. (1986) derived a longitudinal ground deformation profile that is similar to that as illustrated in Figure 2-22b.

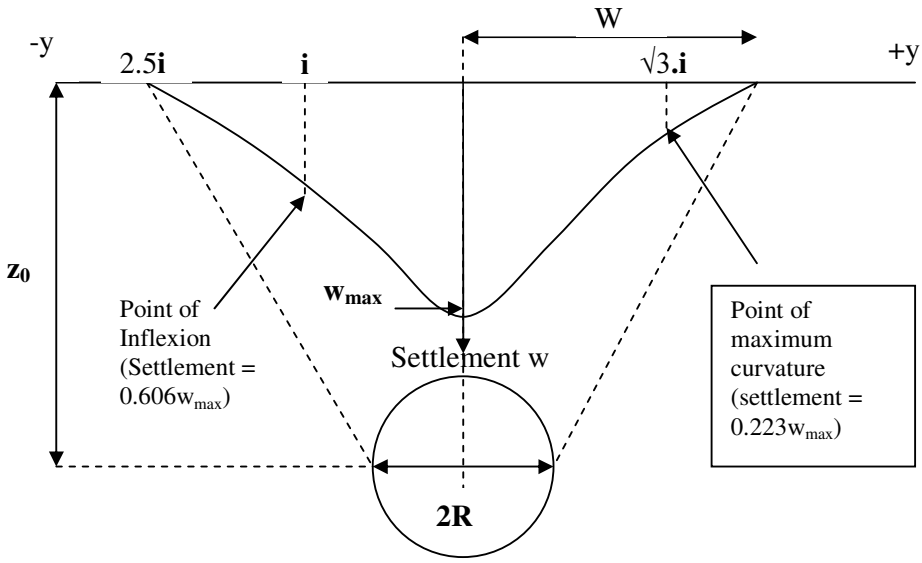

a. Transverse to tunnel

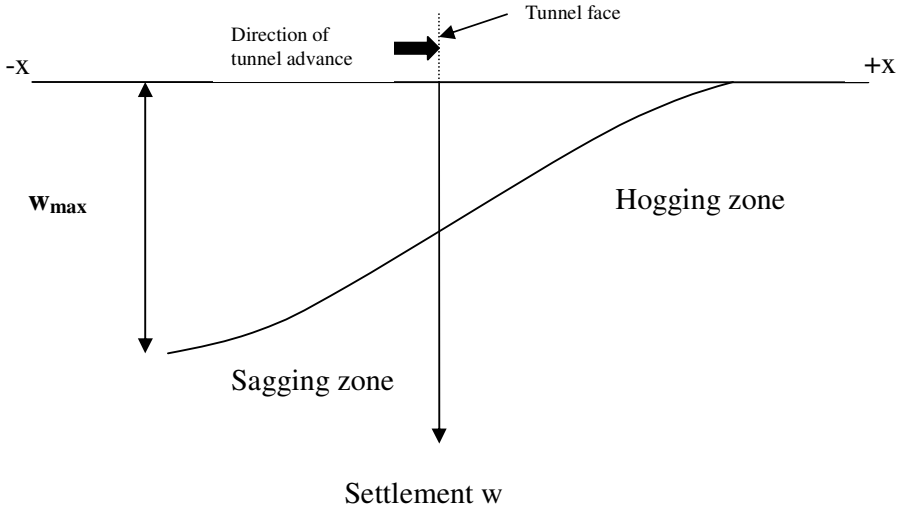

b. Longitudinal with tunnel

Figure 2-22. Transverse and longitudinal settlement trough.

The radius of the tunnel is represented by R and the depth to the centre of the tunnel by z_0. The maximum settlement is denoted by w_{max} with points of inflexion located at a distance i on either side of the centre line. i is a parameter defining the form and span of the settlement trough. The settlement ordinates at distance i is, according to

the properties of normal probability curve, equal to $0.606w_{max}$. Values of i have been calculated for tunnels based on reasonably reliable settlement data. They have been assembled and illustrated in a dimensionless plot of i/R against z/2R for various tunnels in different materials by Peck (1969). Using the relationship obtained from field observations, Peck (1969) formed the following relationship to estimate the value of i,

$$i/R = (z_o/ 2R)^{n} \qquad (18)$$

where n = 0.8 to 1.0.

He had also proposed the approximation $i = 0.2(d + z_0)$ where d is the excavated diameter. Attewell et al. (1974) had modified the empirical relationship developed by Peck (1969) and added a parameter α which is equal to one and n = 1 from his field studies of UK tunnels. However, Clough and Schmidt (1981) advocated n = 0.8 based on their studies of UK tunnels. Several other studies had developed empirical relationships that took into account of different soil types such as O'Reilly and New (1982) who suggested from case history of UK tunnels that $i = 0.43z_0 + 1.1m$ for cohesive soils with $(3 \leq z_0 \leq 34)$, and $i = 0.28z_0 - 0.1m$ for granular soils with $(6 \leq z_0 \leq 10)$. Atkinson and Potts (1976), based on model tests and field studies, suggested that $i = 0.25(z_o + R)$ for loose sand and $i = 0.25(1.5z_o + 0.5R)$ for dense sand and over consolidated clay. Leach (1985) (Attewell et al., 1986) also suggested using $i = 0.57 + 0.45z_0 \pm 1.01m$ for sites where consolidation effects are insignificant. Mair (1983) conducted extensive field studies of tunnels worldwide and centrifuge tests, and concluded that $i = 0.5z_o$ which is independent of tunnel radius.

A comparison of the various empirical methods discussed above was made assuming a hypothetical four metres diameter tunnel located at a depth of thirty metres, which experience a ground loss volume of one percent. The results are presented in Table 2-4 and Figure 2-23 below.

Table 2-4. Calculation of i values and corresponding surface settlement.

	I	w_{max} (y=0)	w (y=i)	w (y=20)	w(y=-i)	W(y=-20)
Units of measurement	metres	millimetres	millimetres	millimetres	millimetres	millimetres
Clough & Schmidt (1981)	10.0249	4.9956	0.0332	0.0000	0.0332	0.0000
Mair (1983)	15.0000	3.3387	0.0018	0.0000	0.0018	0.0000
Attewell et al. (1974)	15.0000	3.3387	0.0018	0.0000	0.0018	0.0000
O'Reilly & New (1982)	14.0000	3.5771	0.0033	0.0000	0.0033	0.0000
Atkinson & Potts (1976)	11.5000	4.3548	0.0139	0.0000	0.0139	0.0000
Leach (1985)	15.0800	3.3210	0.0018	0.0000	0.0018	0.0000

Note: $w = w_{max} \exp(-y^2/2i^2)$ and $w_{max} = 0.313V_L D^2/ i$ (Attewell et al, 1986)

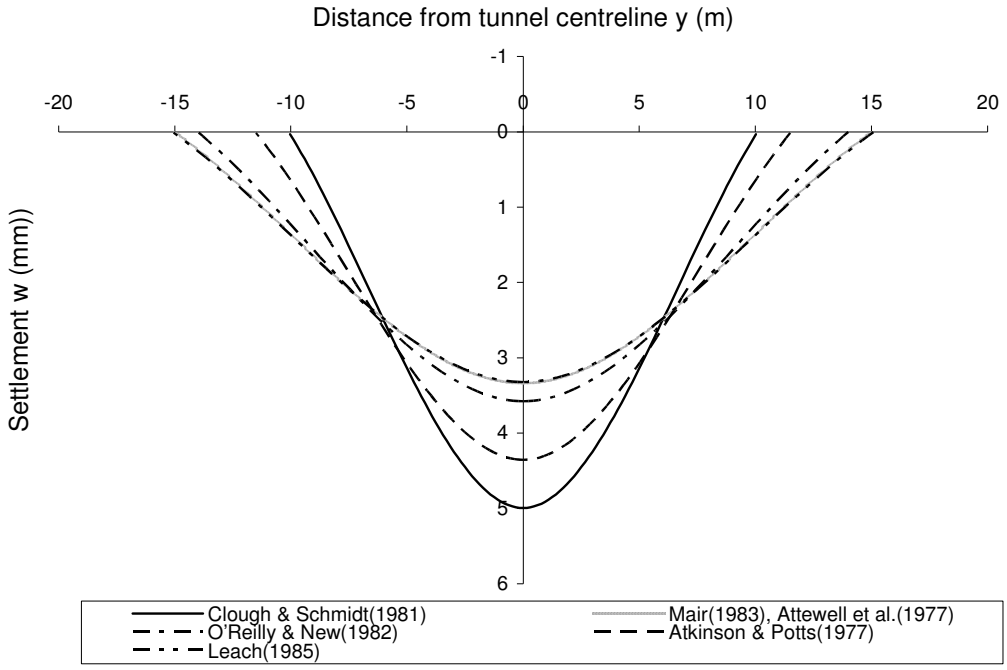

Figure 2-23. Comparison of surface settlement troughs (Tan et al., 2003).

From the comparison of various empirical solutions for surface settlement trough, the maximum settlement ranges from three to five millimetres whereas the trough width i varied between ten to fifteen metres. Hence, this shows that there are a great variety of empirical solutions to predict surface settlement trough because of different interpretation and database collection proposed by different authors.

A generalised expression for surface settlement w, assuming the settlement trough correspond to a normal probability curve, is

$$w = (V_S/ 2.5\ i)\exp [\ -y^2/ 2i^2] \{\ G[(x - x_i)/ i] - G[(x - x_f)/ i]\} \quad (19)$$

where x and y are tunnel coordinates as defined in Attewell et al.(1986) and G is the value of the cumulative normal distribution function. In order to resolve the functions $G[(x - x_i)/ i]$ and $G[(x - x_f)/ i]$, a table depicting the numerical integration of the normal probability curve has to be used. According to Attewell et al. (1986), for a tunnel face that has advanced sufficiently (approximately $3z_0$) to allow the transverse settlement profile to develop fully, the function $G [(x - x_i)/ i]$ can be re - expressed in the above equations as unity.

The volume of the settlement trough V_S can be calculated by $2.5i\ w_{max}$. This formula is obtained from the integration of the area under the normal probability curve assumed to define the form of the transverse settlement trough. This equation allows w_{max} to be calculated if V_S is known. The volume loss or ground loss is expressed as percentages of the excavated volume of the tunnel per unit distance of advance or face area,

$$\%V_L = (4/ \pi D^2)V_S.100 \quad (20)$$

The value of V_S has previously been discussed in the calculation of ground loss at the tunnel. The maximum settlement may then be calculated using the above equations,

$$w_{max} = 0.313V_L\ D^2/ i \quad (21)$$

where D = diameter of tunnel and V_L is the ground loss.

According to Cording et al. (1976), the trough width, W, defined as the width beyond tunnel centre line, of a triangular shaped trough whose volume is equal to

V_S and which has the same maximum settlement as actual settlement trough can be expressed as

$$W = V_S / w_{max} \quad (22)$$

Furthermore, for a normal probability curve, W can be related to the point of inflection i, by W = 2.5 i. Peck (1969) had tabulated an extensive field studies of tunnels excavated in dense sand above groundwater table to very stiff clay and noted that the higher ratio of settlement trough parameter to tunnel radius appeared to be associated with tunnels in plastic clay than in granular materials. He also discovered a trend that the spread of the settlement trough increases with tunnel depth.

2.6.3 Sub surface settlement

Contrary to the surface settlement, limited studies had been carried out to analyse sub surface settlement. Mair et al. (1993) had showed that sub surface settlement profiles could be approximated in the form of Gaussian distribution like the surface settlement profiles. Figure 2-24 shows the profiles of surface settlement and sub surface settlement.

They then proposed an empirical solution to measure sub surface settlement using field data collected from UK tunnels in London clay and centrifuge tests on soft clay,

$$w = w_{z,max} \exp(-y^2 / 2 i_z) \quad (23)$$

where y is the horizontal distance from the tunnel axis,

$i_z = K(z_o - z)$,

$K = [0.175 + 0.325(1- z/z_o)]/ (1- z/z_o)$.

Atkinson and Potts (1976) also studied the subsidence above shallow circular tunnels in soft ground using model tests and proposed an equation to estimate the sub surface settlement,

$$w = w_c [\ 1.0 - \alpha [(z - D/2)/ D] \qquad (24)$$

where w_c = settlement at the tunnel crown (which is also equal to the maximum settlement w_{max} .)

D = tunnel diameter

z = tunnel depth

α = slope of the line w/ w_{max} vs (z – D/2)/D and for different type of soils,

α = 0.57 (for dense sands), 0.40 (for loose sands), 0.13 (for overconsolidated clay).

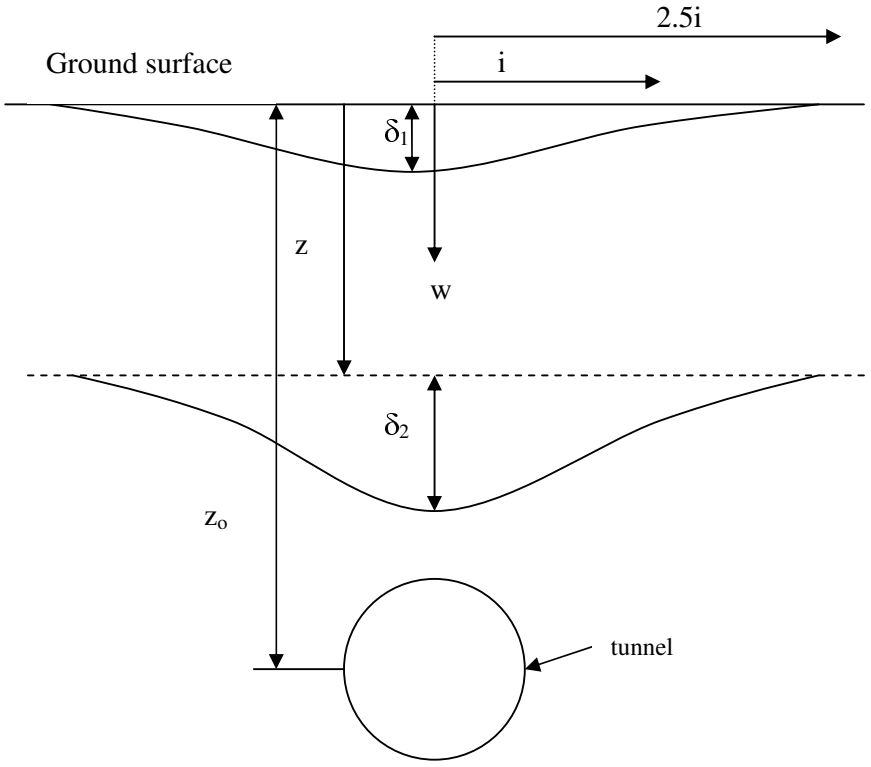

Figure 2-24. Surface and sub surface settlement profile (reproduced from Mair et al. (1993))

2.6.4 Longitudinal settlement

Besides settlement in the transverse direction, the longitudinal and lateral deformation of the ground is also attributed to tunnelling induced settlement.

However, very limited analytical studies have been conducted to understand the longitudinal behaviour of the ground along the tunnel axis. Field studies using extensometers or probes experience difficulty in installation thus few intensive monitoring of this behaviour had been carried out. Attewell et al. (1983) had conducted lab extrusion tests using undisturbed clay soil forced through a hole whilst applying a constant axial pressure to analyse the intrusion at the tunnel face. The extrusion displacement profile developed is similar to Figure 2-22(b).

Romo and Diaz (1981) had used finite element method to find the stress and deformation of different degrees of face yielding and established a relationship between safety factor, stability ratio and surface settlement at different depths that are attributable to face yielding. The settlement along a tunnel alignment due to face yielding as the tunnel progressed between two points can be calculated by Equation (25):

$$w_x = (0.0083 - 0.0014\ Z/H)(\sigma_h - p)(F_1)(Z + D)(\varepsilon_f/\ \sigma_f) \qquad (25)$$

where w_x is the settlement at a distance x from initial point of reference

Z is equal to H+D/2

H is the tunnel depth above the crown

D is the tunnel diameter

σ_h is the initial horizontal stress at tunnel axis

σ_f is the mean compressive soil strength from ground surface to depth of tunnel invert

p is fluid pressure at excavation face

ε_f is the mean axial strain at failure of soil samples from ground surface to depth of tunnel invert

F_1 is a function related to x/(Z+D).

Attewell and Woodman (1982) had assumed that the longitudinal profile of tunnelling induced settlement can be modelled as a cumulative probability curve

and drew a conclusion that the settlement directly above the tunnel face is half of S_{max}, which is the maximum transverse surface settlement.

2.6.5 Lateral settlement

Studies involving the lateral movement of the ground due to tunnelling were comparatively more extensive than studies conducted on the longitudinal behaviour. Norgrove (1979) derived an empirical equation that relate the sub surface settlement to the lateral deformations as shown below,

$$w_y / w = y / z_o \quad (26)$$

where w_y is the lateral deformation, w is the surface settlement at a distance y from the tunnel axis, z_o is the tunnel depth above the tunnel crown and y is the horizontal distance from the tunnel axis. However, these empirical equations are subjected to certain limitations and assumptions in terms of ground applicability, excavation methods and inadequate site information, thus making them inaccurate to a certain extent. O'Reilly and New (1982) assumed that the resultant vectors of ground movements are directed to the tunnel axis and proposed an empirical similar equation to Norgrove (1979) with the vertical and horizontal components of the ground movements as S_v and S_h, and the horizontal surface settlement can be calculated as

$$S_v = (y/ z_o) S_v \quad (27)$$

where, S_v is the settlement at a distance y from the tunnel axis, y is the horizontal distance from the tunnel axis and z_o is the tunnel depth above the tunnel crown.

2.6.6 Theoretical solutions of tunnelling induced settlements

In view of the limitations in using empirical solutions to predict surface, sub surface and lateral deformations, analytical solutions might prove to be useful. The normal probability curve proposed by Peck (1969) for the transverse settlement profile had

no theoretical basis but was based entirely on its similarity in shape to the observed surface settlement profiles taken from field studies. The normal probability curve was also found to be inconclusive when applied to granular soils (New and O'Reilly, 1991) and to overconsolidated clays (Eisenstein, 1981). In addition, there is very limited or no indications of measurement method with regard to sub surface settlement and lateral movements. In view of these limitations, interestingly, only a few researchers had tried to provide analytical closed form solutions to model the ground movements at the surface, sub surface and lateral to the tunnel.

A small number of authors had presented analytical predictions of tunnelling induced ground movement in clay. The most significant analytical solutions is presented by Sagaseta (1987) who proposed closed form solutions for obtaining the strain field in incompressible soil by combining fluid flow with elastic solutions for half space. Sagaseta (1987) solved for a singularity at a point of an elastic half plane and by adding the image solution for the singularity at a point located symmetrically above the soil surface, the normal or shear stresses are made to neutralise. A negative mirror image of the point with respect to the top surface will produce opposite normal stresses and the same shear stresses similar to the actual point. Conversely, a negative image will produce the same normal stresses and opposite shear stresses. A positive image will be rendered unrealistic since the half space will have a surface, which is free in the horizontal direction but cannot undergo any vertical movement. The application of this method in tunnelling process will develop equations to calculate the surface movements in the transverse, lateral and longitudinal directions:

$$S_{xo} = - (\nu / 2\pi) [x / (x^2 + h^2)] \{ 1 + [y / (x^2 + y^2 + h^2)^{½}]\} \quad (28a)$$

$$S_{yo} = (\nu / 2\pi) [1 / (x^2 + y^2 + h^2)^{½}] \quad (28b)$$

$$S_{zo} = (\nu / 2\pi) [h / (x^2 + h^2)] \{ 1 + [y / (x^2 + y^2 + h^2)^{½}]\} \quad (28c)$$

where S_{xo} , S_{yo} and S_{zo} are the surface movements in the x, y and z direction respectively; x is in the transverse horizontal direction, y is in the longitudinal horizontal direction along the tunnel of advance and z is taken as the vertical direction below the ground surface, ν is ground loss or volume per unit length and h is the tunnel depth taken from the ground surface to the tunnel crown.

An extension of the method suggested by Sagaseta (1987) for the case of ground loss in an incompressible soil was used by Verruijt and Booker (1996). Their study included solutions for various Poisson's ratio and also took into account of the effect of ovalization. The closed form solutions presented by them for the estimation of the vertical settlements (U_z) and the lateral deformations (U_x) are:

$$U_z = -\varepsilon R^2 (z_1/r_1^2 + z_2/r_2^2)+ \delta R^2 [z_1(k x^2 - z_2^2)/ r_1^4 + z_2(k x^2 - z_2^2)/ r_2^4)] + 2 \varepsilon R^2 [(m + 1) z_2 /r_2^2 + m z (x^2 - z_2^2)/ r_2^4] - 2 \delta R^2 H \{ (x^2 - z_2^2)/ r_2^4 + [m/(m+1)][2 z z_2 (3 x^2 - z_2^2)/ r_2^6] \} \quad (29a)$$

$$U_x = -\varepsilon R^2 (x/r_1^2 + x/r_2^2)+ \delta R^2 [z_1(x^2 – kz_1^2)/ r_1^4 + x(x^2 - kz_2^2)/ r_2^4)] - 2 \varepsilon R^2 x/m[1 /r_2^2 - 2m z z_2/ r_2^4] – [4 \delta R^2 x H /(m + 1)][(z_2^2/ r_2^4)] + [m z (x^2 – 3 z_2^2)/ r_2^6] \quad (29b)$$

where ε = uniform radial ground loss

δ = long term ground deformation due to the ovalization of the tunnel lining

$z_1 = z – H$

$z_2 = z + H$

$r_1^2 = x^2 + z_1^2$

$r_2^2 = x^2 + z_2^2$

R = tunnel radius

H = tunnel depth

$m = 1/ (1 – 2 \nu)$

$k = \nu/ (1 – \nu)$

ν = Poisson's ratio.

However, the third portion of the equations presented by Verruijt and Booker (1996), which is the Boussinesq stress distribution that was included to eliminate the normal stresses at the surface of the half plane, did not satisfy the boundary conditions (i.e. tend to zero) unless the Poisson's ratio is 0.5 (i.e. incompressible soil). As such, Strack and Verruijt (2000) presented modified equations for the singular solutions and its images to solve the problem. Nevertheless, with the complication of the modified equations, the solution for the Boussinesq stress distribution will also be more difficult to derive. Verruijt (1997) presented an analytical solution for problems for an elastic half plane with a circular tunnel, which underwent a certain given deformation. The solution was derived from complex variables with a conformal mapping onto a circular ring, and using Laurent series expansions to represent the complex stress functions in the transformed plane. The complex variable method was favoured because of its flexibility in solving problems with various types of boundary conditions.

A further modification of the equivalent ground loss parameter, ε, was conducted by Loganathan et al. (2001) based on initial studies reported by Loganathan and Poulos (1998). When the portion of soil above the tunnel crown touches the tunnel lining, the soil at the side of the tunnel displaces towards the bottom of the tunnel. Hence, the upward movement of the soil below the tunnel is limited. It is thus assumed that approximately 75% of the vertical ground movement occurs within the upper annulus of the gap around the tunnel and that the magnitude of the horizontal movement at the tunnel springline is approximately half of the vertical movement g at the tunnel as shown in Figure 2-25 below. The traditional ground loss parameter was redefined as the equivalent ground loss parameter, ε, with respect to a gap (g) parameter (Lo et al., 1984) and incorporated onto analytical solutions proposed by Verruijt and Booker (1996) to predict the ground movements around the tunnel in clay.

The gap parameter was first introduced by Lo et al. (1984) to quantitatively represent the components of loss of ground induced by tunnelling in cohesive soil.

The gap parameter can be estimated based on a theoretical method developed by Lo et al. (1984) where total gap (G)

$$G = 2\Delta + \delta + U \qquad (30)$$

Δ is the thickness of the tailpiece and δ is the clearance required for erection of the lining. Both these parameters arise from the geometric closure of the soil into the gap between the outer skin of the tunnel shield and the lining. U represents the three-dimensional elasto-plastic deformation ($u^*_{e,\ p}$) at the face and the loss of ground as a result of additional excavation of material due to uneven pitching by the tunnel shield (w).

Lee et al. (1992) further elaborated on the estimation of the gap parameter and used three-dimensional elastoplastic finite element analysis to develop a simple design procedure for estimating the gap parameter for tunnels excavated in cohesive soils. A set of parameters which are similar to those described by Lo et al. (1984) but with different notations are described in Lee et al. (1992) and they are represented as

$$g = G_p + U_{3D}^* + w \qquad (31)$$

where, G_p = physical gap = difference between the maximum outside diameter of the tunnelling machine and the outside diameter of the lining for a circular tunnel = $2\Delta + \delta$

Δ = thickness of tailpiece

δ = clearance for erection of lining

U_{3D}^*= 3D elastoplastic deformation into the tunnel face = $(k/2)\ \delta_x$

k = soil cutter resistance factor (k = 0.7-0.9 for stiff to soft clay and k = 1 for very soft clay)

δ_x = tunnel face soil intrusion = $\Omega R P_o / E$

Ω = dimensionless displacement factor (Lee et al.,1992)

$P_o = K_o' P_v' + P_w + P_i$

K_o'= effective coefficient of earth pressure at rest

P_v' = vertical effective stress at springline of the tunnel

P_w = pore water pressure at the springline of the tunnel

P_i = tunnel support pressure

w = workmanship factor = smallest of $0.6G_p$ and U_i

where U_i is defined as elastoplastic plane strain displacement at the tunnel crown(Lo et al., 1984).

Hence, by incorporating the gap parameter into the equivalent ground loss parameter, a modified version of the equivalent ground loss parameter incorporating the non-linear ground movement around the tunnel soil interface is derived as,

$$\varepsilon_{x,z} = \varepsilon_o \exp \{ - [1.38x^2/ (H \cot\beta + R)^2 + 0.69z^2 / H^2]\} \quad (32)$$

where, $\varepsilon_o = (4gR + g^2)/ 4R^2$

H = depth of the tunnel from the ground surface

R = radius of tunnel

The generalised modified analytical equations based on Verruijt and Booker (1996) for the estimation of the surface settlement, sub surface settlement and the lateral deformation are then given as,

$$U_{z=0} = \varepsilon_o R^2 [4 H (1-\nu) / (H^2 + x^2)] \exp \{- [1.38x^2/ (H \cot\beta + R)^2 \} \quad (33a)$$

$$U_z = \varepsilon_o R^2 \{-(z - H)/ [x^2 + (z - H)^2] + (3-4 \nu) (z + H)/ [x^2 + (z + H)^2] - 2 z [x^2 - (z +H)^2]/ [x^2 + (z + H)^2]^2 \}\exp \{ - [1.38x^2/ (H \cot\beta + R)^2 + 0.69z^2 / H^2]\} \quad (33b)$$

$$U_x = - \varepsilon_o R^2 x\{1/ [x^2 + (H - z)^2] + (3-4 \nu) / [x^2 + (H + z)^2] - 4 z (z + H) / [x^2 + (H + z)^2]^2 \}\exp \{ - [1.38x^2/ (H \cot\beta + R)^2 + 0.69z^2 / H^2]\} \quad (33c)$$

where, $U_{z=0}$ = ground surface settlement

U_z = sub surface settlement

U_x = lateral soil movement

R = tunnel radius

z = depth below ground surface

H = depth of tunnel axis level

ν = Poisson's ratio of soil

ε_o = average ground loss ratio, and

x = lateral distance from tunnel centreline.

$\beta = 45^\circ + \emptyset/2$

The ground deformation due to the ovalization term was omitted since the analysis was attributed to short termed undrained conditions (i.e. $\delta = 0$).

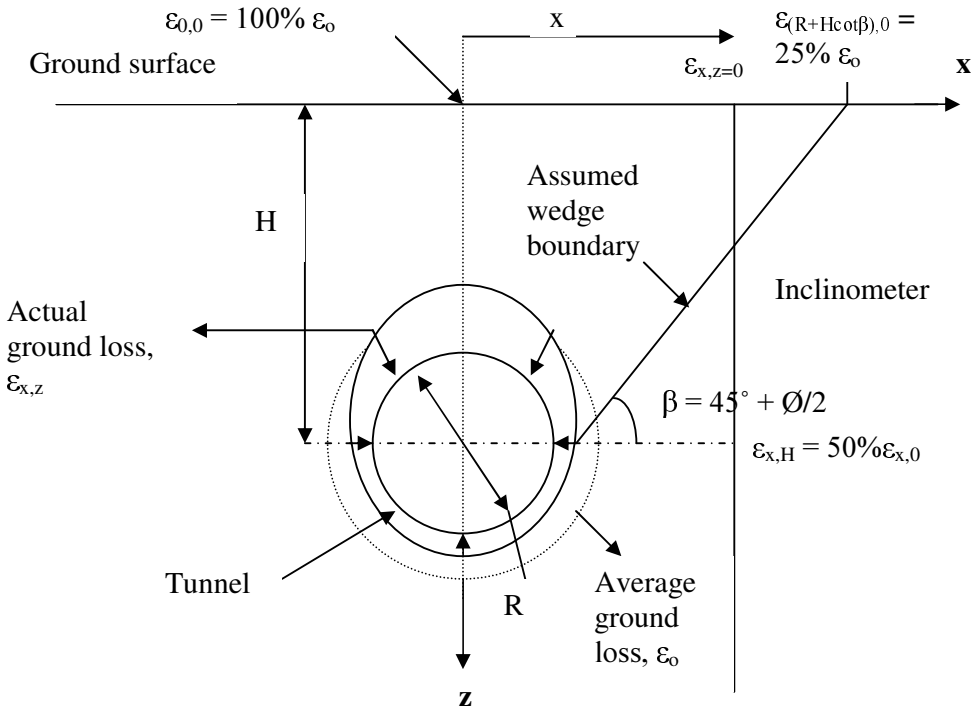

Figure 2-25. Ground deformation patterns and ground loss boundary conditions (Loganathan et al., 2001).

It should be noted that the analytical solutions are derived based on elastic solutions of the deformations induced by tunnelling as derived by Sagaseta (1989) and thus, these elastic solutions might not be readily applicable for soft ground although they have predicted creditably for some soft ground tunnelling operations as discussed in Lo et al. (1984) and Lee et al. (1992). Primarily, plasticity exists in soft ground and elastic solutions are more applicable for rock problems.

To date, Strack and Verruijt (2000) had derived complex variable solution for the ovalization of a circular tunnel in an elastic half plane and concluded that pure ovalization of shallow tunnels is not likely to occur in practice. According to Strack and Verruijt (2000), ovalization of a shallow tunnel do not exist in practice since the stresses accommodating an ovalization of the tunnel cavity did not correspond to an ovalization of the tunnel linings. Verruijt (2002) continued to derive complex variable solution for a deforming buoyant tunnel in an elastic half plane.

Sagaseta (1987) had also suggested recommendations to apply his method to that of compressible materials or drained deformation. He had proposed that the general equation be modified to become

$$S_r(r) = K\,(a/n)\,(a/r)^{\alpha} \qquad (34)$$

where, K is scaling factor.

$\alpha = n - 1$ for incompressible soil in the elastic zone,

$\alpha = (n-1)/\alpha_a$ in compressible materials in the plastic zone for a point in loose soil or

$\alpha = (n-1)\,\alpha_a$ in dense soil, where

$\alpha_a = (1 - \sin \nu)/(1 + \sin \nu)$ and ν is the angle of dilatancy of the soil.

Chapman and Rogers (1991) had applied the fluid flow analysis suggested by Sagaseta (1987) to predict undrained soil displacements caused by trenchless pipe laying operations but they had modified the analysis to account for compressibility

condition in the soil. The simple model proposed gave a good indication of the ground displacements for various conditions.

Although the empirical and theoretical solutions to tunneling induced ground movement are extensive and detailed, their application in this study is limited because in order to derive a solution that can account for the forepoling support system, extensive and comprehensive experimental analyses have to be carried out.

2.6.7 Ground movement and its effect on buried pipelines

In the analysis of using steel pipes or circular tubes to reinforce the tunnel prior to excavation, a detailed study of the effects of ground movement induced by tunnelling on buried pipes may be necessary. As there are limited studies regarding the direct effect of tunnelling induced deformation on pipes support system, hence the focus could be placed on studies involving buried services whereby several studies have been conducted by Attewell et al. (1986), Mair et al. (1996), Bracegirdle et al. (1996) and O'Rourke et al. (1982) etc. A good understanding of the potential failure modes and types of stresses induced in the pipelines during tunnelling will aid in the design of the pipe roof for tunnel pre support.

The major factor to consider in buried pipeline is their ability to withstand longitudinal bending stress as a result of ground movement. This bending stresses are associated with lateral ground movement. In addition, axial tensile and compressive forces will also affect pipelines when they are induced by parallel ground movement. The magnitude of the tensile and compressive forces induced would depend on the soil pipe bonding and the soil pipe shear strength. The ring deformation of the pipeline is also another factor which has to be accounted but since its effect is relatively small compared to the longitudinal deformation and hence can be assumed as negligible in our analysis. The joint flexibility and position of joints will also affect the restraint to ground movement and the bending moment induced in a pipeline. As our analysis is mainly on pipes aligned parallel to the

tunnel advance, hence focus will only be placed on the effects of tunnelling induced deformation on buried pipelines parallel to the tunnel drive.

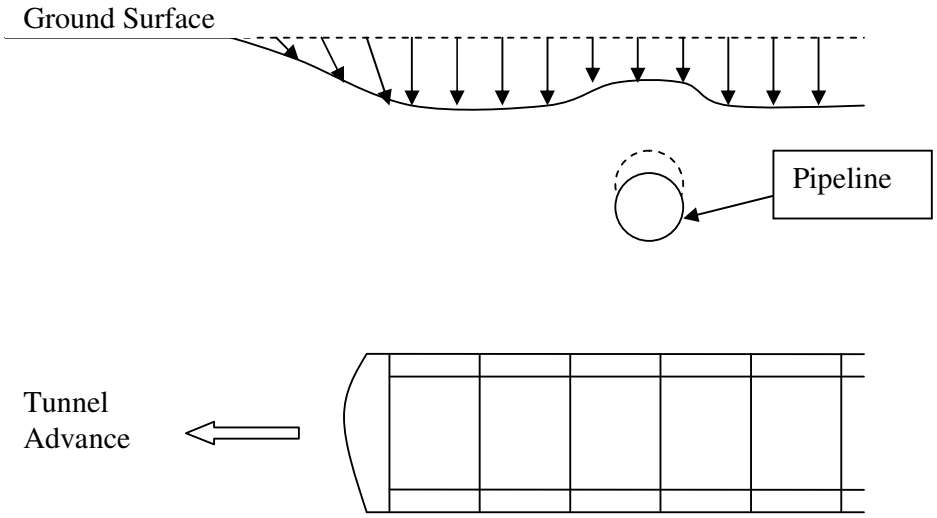

Figure 2-26. Ground movement transverse to pipeline.

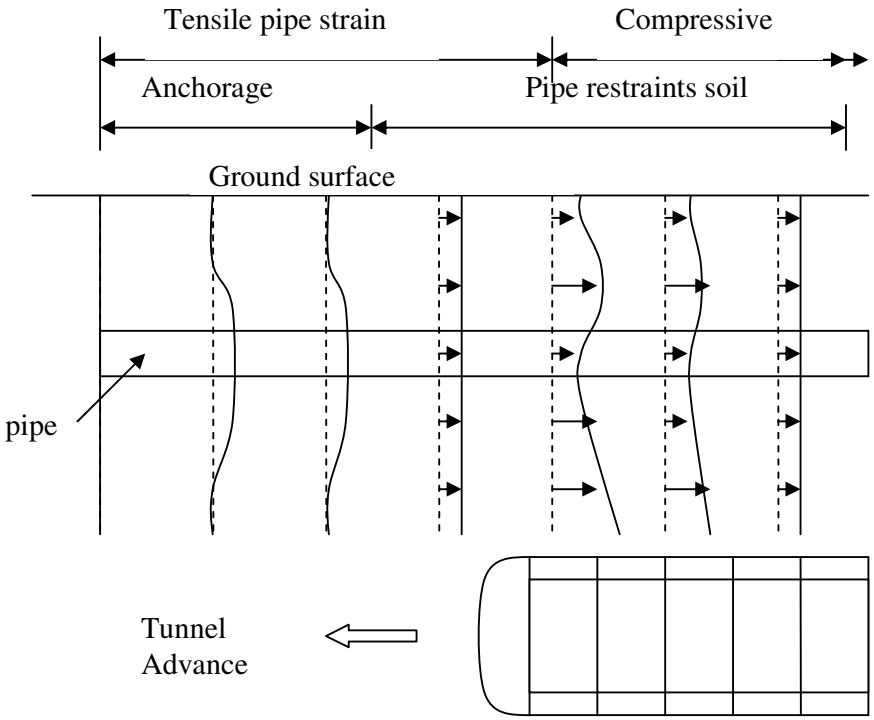

Figure 2-27. Ground movement parallel to the pipeline.

The typical restraint to ground movement due to a buried pipeline is as shown in Figures 2-26 and 2-27 for ground movements transverse and parallel to the pipeline.

(1) Ground movement transverse to a pipeline

The analysis of the longitudinal bending in a pipeline can be related to the subgrade reaction approach or Winkler foundation as stated in Attewell et al. (1986). The pressure in the foundation is proportional at every point to the deflection occurring at that point and is independent of the pressures or deflections produced elsewhere in the foundation. The pipe is assumed to be homogenous with pipe material linear elastic, homogenous and isotropic. The soil around the pipe is linear elastic and homogenous and is always in contact with the pipe.

(2) Ground movement parallel to a pipeline

The ground movement parallel to a pipeline can be analysed using the load transfer method whereby movement of the pipe at any point is related only to the shear stress at that point and is independent of stresses elsewhere on the pipe. This analysis is similar to the subgrade reaction method. The axial forces induced strains only contributes to a secondary effect as compared to those produced by longitudinal bending.

The relationship between the buried pipes and ground deformation are important to derive a theoretical solution that can determine the surface settlement induced by tunnelling when forepoling support system is used. However, comprehensive research and experiments have to be conducted.

CHAPTER 3 - CASE HISTORIES OF UMBRELLA ARCH METHOD

3.1 Case Histories

Fifty-six case histories of recent tunnels that used the Umbrella Arch method during construction have been compiled from the literature and listed in Table 3-2. Studying these cases is very important before performing any numerical analyses or parametric studies so as to understand the method of construction of the Umbrella Arch, the range of values of different material parameters used in the arch and the geometrical parameters that describes the profile of the Umbrella Arch in both the longitudinal and cross sections. Based on these compiled case histories, this chapter will describe the steel pipe specifications as used in most of these case histories and summarized in Table 3-1. The longitudinal and cross section profiles of the Umbrella Arch are summarized in Figures 3-1 and 3-2 respectively.

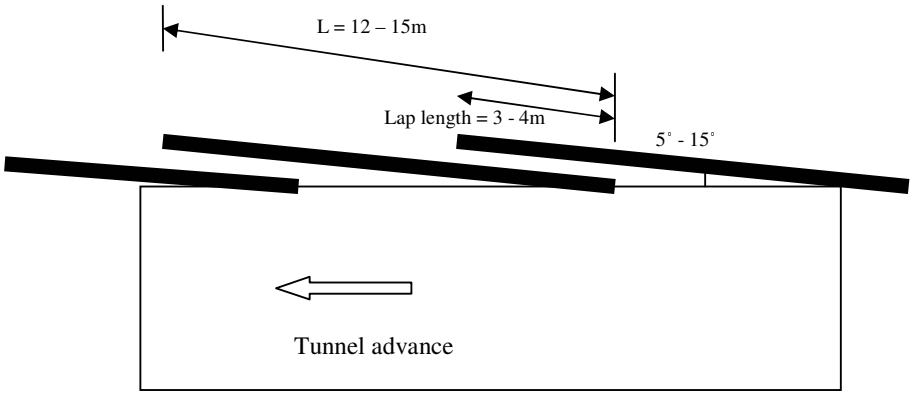

Figure 3-1. Longitudinal profile of umbrella arch method

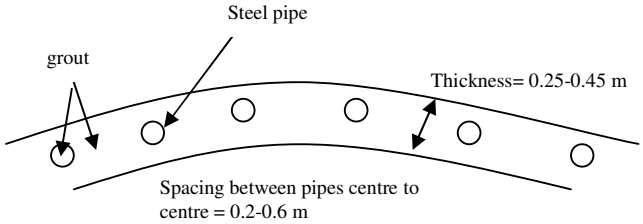

Figure 3-2. Cross section profile of umbrella arch method.

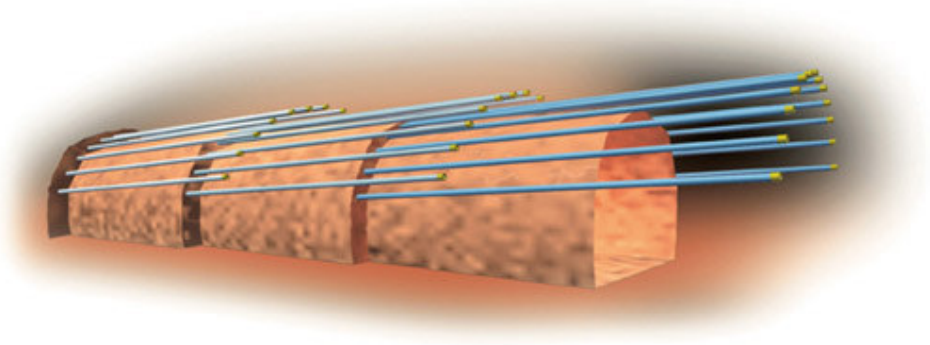

Figure 3-3. 3-D view of the Umbrella Arch (Rotex OY).

Table 3-1. Steel pipe or forepole specification.

Steel pipe diameter	Pipe thickness	Poisson's ratio	Elastic deformation	Span around tunnel crown	Nos. of pipe
114.0 – 200.0 mm	4.0 - 8.0mm	0.25 – 0.3	200 GPa	120° - 180°	20 - 40

As can be seen from Table 3-2 and Figures 3-1 and 3-2, the length of pipes usually varies between 12m and 15m with an overlapping length (lap length) of 3m to 4m. The diameter of pipes usually varies between 114mm and 200mm with thickness of between 4mm to 8mm. The pipes are usually driven longitudinally with an angle of 5º to 15º to the horizontal to cover a span of about 120º to 180º around the crown. The spacing between the pipes centre to tunnel crown usually varies between 200mm to 600mm. The grout injected inside the pipes usually forms a thickness of reinforced strip of about 0.25m to 0.45m.

3.2 Construction Procedure

The procedures followed to construct the Umbrella Arch are also summarized in this chapter. The Umbrella Arch method is an auxiliary method and is used in combination mostly with steel supports/ ribs, shotcrete, concrete lining, foot piles, jet grouting and fibre glass face reinforcement for the construction of horse shoe shape type of tunnels where weak or soft ground is encountered. New Austrian Tunnelling Method (NATM) is usually the main construction method when this

reinforcing process is used. Figure 3-4 shows a schematic diagram of the Umbrella Arch and other support system that are used in the NATM construction of a horse-shoe shape tunnel.

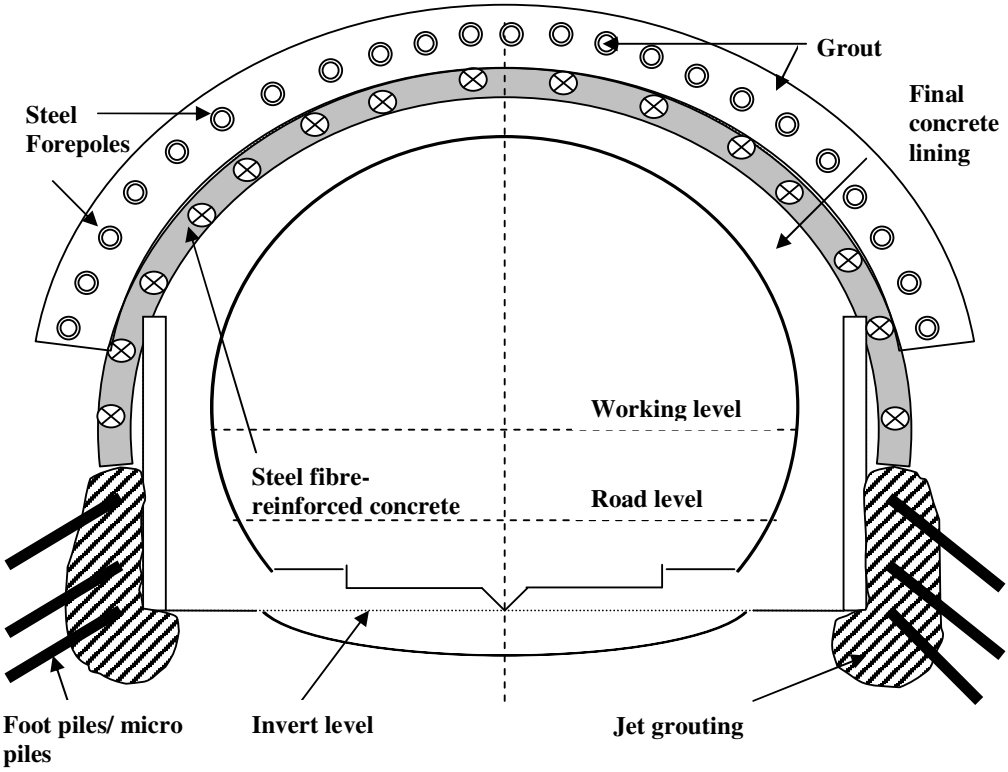

Figure 3-4. Support measures for a typical tunnel in weak ground constructed by NATM method.

Drilling is performed by forepoling rigs or drilling machines with large drills of diameter 100-180 mm (Barisone et al., 1982). The holes are drilled at an inclination to the horizontal, which never exceeds 15˚. Holes are drilled at 120˚-180˚ span with a spacing of 200-600 mm between holes.

Figure 3-5. Drilling of holes.

Figure 3-6. Insertion of steel pipes.

Forepoling rigs allow the steel pipes to be inserted into the holes with little difficulty. Pipe lengths usually range from 10-15 m depending on site requirements. Pipe dimensions are stated in Table 3-1.

Pressure grouting follows after the insertion of pipes. The steel pipes are often perforated to allow the grout to interact with the ground material outside the pipes. Since holes are usually drilled slightly larger than pipe size, the grout can occupy a substantial area to provide a stronger reinforced zone. Once all grouting is completed, the tunnel is excavated.

Figure 3-7. Grouting and excavation.

As the excavation progresses, other support measures such as steel arches and concrete linings are installed to further enhance the stability of the tunnel cavity. Figures 3-5 to 3-8 show the entire construction procedure of the Umbrella Arch method.

Figure 3-8. Completed arch.

Table 3-2. Case Histories of Umbrella Arch Method and Pipe Roof Method.

Tunnel dimension and Ground conditions	**Tunnel**	Takatoriyama north route	Takatoriyama south route	Takatoriyama north route	Takatoriyama south route	Takatoriyama north route	Whabang
	Location	Kobe, Japan	Kobe, Japan	Kobe, Japan	Kobe, Japan	Kobe, Japan	Kwangju, Korea
	Diameter	9m	9m	9m	9m	9m	6m (8m ht.)
	Implemented tunnel length	I	I	I	I	I	780m
	Ground Condition	Sat. Alluvium	weathered granite	weathered granite	sat.sand & clay	sat.sand & clay	weathered granite/soft rock
	Overburden	4m	13m	19m	20m	4-7m	<50m
	Deform. coeff.	20-40MPa	30-50 MPa	20-40 MPa	100 MPa	30-100MPa	62MPa(Gran.) 874MPa (soft rock)
	Cohesion/ Ø	I	I	I	I	I	0.02-0.3 MPa
Auxiliary Reinforcement	**Type**	Pipe roof	Pipe Umbrella	Pipe Umbrella	Pipe Umbrella	Pipe Umbrella	Pipe Umbrella (short length)
	Ø (outer/thickness)	812.8/ 12.7	114.3/6.0	114.3/6.0	114.3/6.0	139.8/6.6	60.5/4.0
	nos. (reinft. arch span)	22(180˚ span)	(180˚ span)	(180˚ span)	(120˚ span)	(120˚ span)	4 layers, each with (50/42/34/28) nos.
	Length	90.2	14	14-16	18	14	16
	Inclination	I	I	I	I	I	5˚
	overlap length	I	7	6.4-9	6	7	I
	spacing bet. Pipes	I	I	I	I	I	400mm
	rate of progress	I	I	I	I	I	I
Other supports	**steel support**	H-250@1m	H-200@1m	H-250@0.8m	H-200@1m	H-250@1m	H-125x125x65x9mm@1m
	shotcrete	300 mm	250 mm	300 mm	250 mm	300 mm	200mm
	Footpiles/rockbolts	X	X	X	x	X	Ø25 L=3m
	jet grouting	X	X	X	x	X	Urethane (at tunnel foot)
	FBG face reinft.	X	X	X	x	X	X
Tunnel shape		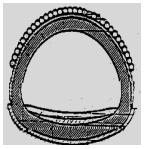	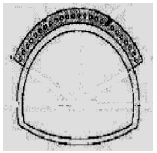	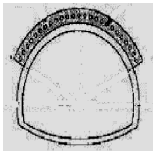	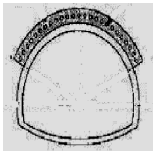	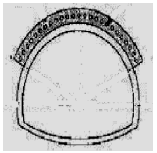	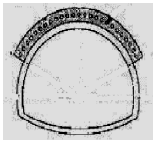
Reference		Sekimoto et al.(2001)	Sekimoto et al.(2001)	Sekimoto et al.(2001)	Sekimoto et al.(2001)	Sekimoto et al.(2001)	Shin et al. (1999)

Legend : X - not used I – not mentioned in study Implemented tunnel length – length of tunnel where Umbrella Arch method is used

Table 3-2 (cont.)

Tunnel dimension and Ground conditions	**Tunnel**	Itsukaichi	Han River	Ome	Ohme	Kokubu River Channel	Maiko
	Location	Moriaka, Japan	Seoul Korea	Tokyo, Japan	Tokyo, Japan	Matsudo, Japan	Kobe, Japan
	Diameter	approx. 6m	6.8m	14.8m, 17.7m ht.	260m2	8.8m	16.6m(width), 10.9m(ht.)
	Implemented tunnel length	72.5m	90m	2095m	x	1230m	370m
	Ground Condition	fine sand(s),tuff(t)	weathered rock	sand,silt,gravel	Loam(l), gravel(g)	fine sand(s), loam(l)	sand, gravel
	Overburden	2-5m	15.6-37m	8.6m	7-8m	10-20m	7-35m
	Deform. coeff.	X	46MPa	X	6.3MPa(l), 56MPa(g)	30MPa(s),46MPa(l)	29-171MPa
	Cohesion/ Ø	N=4(s), N=>50(t)	25.5 kPa	uni. Str.=300MPa	0.3MPa(l), 0.06MPa(g)	0.25MPa	0.28MPa
Auxiliary Reinforcement	**Type**	Pipe Umbrella	Pipe Umbrella	Pipe Umbrella	Pipe Umbrella	steel sheet,AB forepoling	Pipe Umbrella
	Ø (outer/thickness)	114.2/6.0	114.3/6.0	114.3/6.0	I	300	114.3/6.0
	nos. (reinft. arch span)	2 layers(32/33)	26 (120˚ span)	25	I	20-28	45
	Length	12.65m	12-15m	12.5m	I	2.8m	12m
	Inclination	I	I	I	I	18˚	5˚
	overlap length	6.65m	7	I	I	I	4-5m
	spacing bet. Pipes	I	300mm	600mm	I	350mm	400mm
	rate of progress	I	I	I	I	20-28 nos.installed per 4hr	I
Other supports	**steel support**	H-200@1m	H-125x125	H-200x200	H-200x200	H-125, H-150	H-250
	shotcrete	250mm	250mm	250mm	I	200mm	250mm
	footpiles/rockbolts	Ø22 L=3m	X	X	I	12nos.	/Ø114.3, thickness=8.6mm,L=6m
	jet grouting	Urethane	L.W. grouting	X	Length=10m, lap=1m	column jet grouting	urethane(2MPa)
	FBG face reinft.	Ø26 L=4m	X	X	x	x	x
Tunnel shape		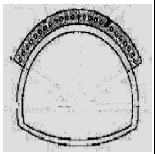	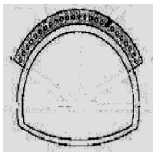	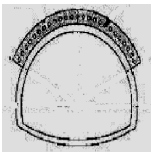	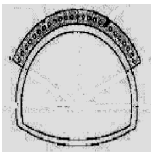	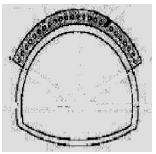	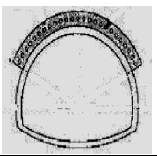
Reference		Miwa et al.(2001)	Yang et al.(2001)	Haruyama et al.(2001)	Haruyama et al.(2001)	Matsuo et al.(1996)	Murata et al. (1996)

Legend: L.W. grouting- Labiles Wasserglass grouting (this term is primarily used in Korea)

Table 3-2 (cont.)

Tunnel dimension and Ground conditions	**Tunnel**	Carbonara	Langenia	S. Ambrogio	El Goloso	Bussana
	Location	Messina-Palermo, Italy	Messina-Palermo, Italy	Messina-Palermo, Italy	Madrid, Spain	SanRemo, Italy
	Diameter	5m (110m2)	5m (110m2)	5m (110m2)	8-9m	78m2
	Implemented tunnel length	2800m	1000m	1780	x	1500m
	Ground Condition	claystone,quartz sandstone	claystone,quartz sandstone	claystone,quartz sandstone	x	Conglomerate,clay marl, flysch
	Overburden	<200m	<60m	<200m	x	x
	Deform. coeff.	12.4-20.8GPa(c),46.6-56GPa(q)	12.4-20.8GPa(c),46.6-56GPa(q)	12.4-20.8GPa(c),46.6-56GPa(q)	x	x
	Cohesion/ Ø	98-126MPa(c),226-239MPa(q)	98-126MPa(c),226-239MPa(q)	98-126MPa(c),226-239MPa(q)	x	x
Auxiliary Reinforcement	**Type**	Pipe Umbrella	Pipe Umbrella	Pipe Umbrella	Pipe Umbrella	Pipe Umbrella
	Ø (outer/thickness)	114.2/6.0	114.3/6.0	114.3/6.0	127/-	114/8.8
	nos. (reinft. arch span)	2 layers(32/33)	26 (120˚ span)	25	35	32
	Length	12.65m	12-15m	12.5m	15m	13m
	Inclination	I	I	I	7.5˚	I
	overlap length	6.65m	7	I	I	3m
	spacing bet. Pipes	I	300mm	600mm	500mm	I
	rate of progress	I	I	I	I	I
Other supports	**steel support**	H-180 or H-200	H-180 or H-201	H-180 or H-202	H-150	H-160 or H-180
	shotcrete	300mm	300mm	300mm	I	200-250mm
	Footpiles/rockbolts	I	I	I	X	/Ø80mm,thickness=7mm
	jet grouting	x	X	x	length=9m @ 0.5m spacing	x
	FBG face reinft.	x	X	x	X	x
Tunnel shape		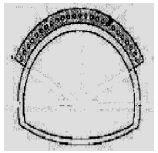	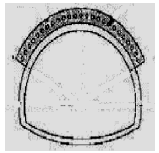	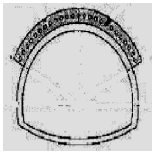	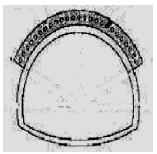	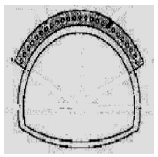
Reference		Gangale et al.(1992)	Gangale et al.(1992)	Gangale et al.(1992)	Beltran et al. (1992)	Borchi et al. (1992)

Table 3-2 (cont.)

Tunnel dimension and Ground conditions	**Tunnel**	Poggio	Ratella	Kars Iyaka	Athens Metro Line 2	Athens Metro Line 2-3
	Location	SanRemo, Italy	SanRemo, Italy	Turkey	Greece	Greece
	Diameter	82m2	93m2	16m	X	x
	Implemented tunnel length	1800m	300m	X	X	x
	Ground Condition	flysch	flysch	Rock class 4 5 & P	limestone,peridotite & black mylonitic schists	
	Overburden	x	x	X	30	10
	Deform. coeff.	x	x	X	X	x
	Cohesion/ Ø	x	x	X	X	x
Auxiliary Reinforcement	**Type**	Pipe Umbrella	Pipe Umbrella	Pipe Umbrella (short length)	Pipe Umbrella	Pipe Umbrella
	Ø (outer/thickness)	114/8.8	114/8.8	50/-	200/-	168-194/-
	nos. (reinft. arch span)	32	32	X	X	x
	Length	13m	13m	2.5-4.0m	12m	12m
	Inclination	x	x	X	X	x
	overlap length	3m	3m	X	X	x
	spacing bet. Pipes	x	x	X	X	x
	rate of progress	x	x	X	X	x
Other supports	**steel support**	H-160 or H-180	H-160 or H-180	X	X	x
	shotcrete	200-250mm	200-250mm	X	X	x
	Footpiles/ rockbolts	Ø80mm,thick=7mm	Ø80mm,thick=7mm	X	X	x
	jet grouting	x	x	X	X	x
	FBG face Reinft.	x	x	X	X	x
Tunnel shape		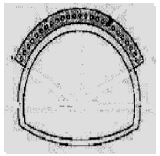	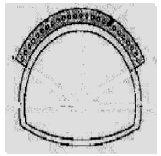	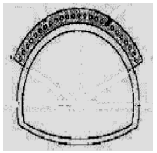	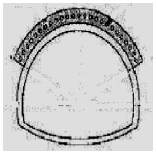	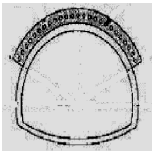
Reference		Borchi et al. (1992)	Borchi et al. (1992)	Tatar et al. (2002)	Leto et al. (1999)I	ILeto et al. (1999)

Table 3-2 (cont.)

Tunnel dimension and Ground conditions	**Tunnel**	NanLing	S Stefano	Sicily	St. Elia	Shin-Minatogawa
	Location	China	Tuscany. Italy	Italy	Messina-Palermo, Italy	Kobe, Japan
	Diameter	x	x	5.2m	5m (110m2)	14m
	Implementd tunnel length	x	x	X	1100m	85m
	Ground Condition	karst,fill,mud,clay	clay, flysch and alluvia	degraded gneiss & mylonite	sandstone, marl	Clay, sand & gravel
	Overburden	I	I	I	<150m	13m
	Deform. coeff.	I	I	I	I	80MPa-130MPa
	Cohesion/ Ø	I	I	I	I	I
Auxiliary Reinforcement	**Type**	Pipe roof	Pipe Umbrella	Pipe Umbrella	Pipe Umbrella	Pipe roof
	Ø (outer/thickness)	108/9	I	I	I	812.8/12.7
	nos. (reinft. arch span)	28	I	I	I	17
	Length	10	I	I	I	85
	Inclination	x	I	I	I	I
	overlap length	9m	I	I	I	I
	spacing bet. Pipes	I	I	I	I	I
	rate of progress	I	I	I	I	I
Other supports	**steel support**	I	I	I	H-180 or H-200	H-250@1m
	shotcrete	I	I	I	300mm	250mm
	footpiles/rock bolts	I	I	I	I	x
	jet grouting	x	x	X	X	x
	FBG face reinft.	x	x	X	X	x
Tunnel shape		X	X	X	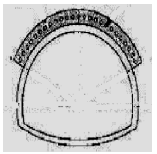	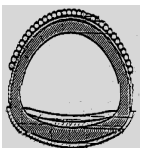
Reference		Li (1990)	http://www.tunnelbuilder.com/italy.htm	http://www.tunnelbuilder.com/italy.htm	Gangale et al.(1992)	Sasaki et al. (2001)

Table 3-2 (cont.)

Tunnel dimension and Ground conditions	**Tunnel**	Kakia Skala	Antwerp Metro	East Line Subway	Flood Control Channel	Metro Section F6b
	Location	Greece	Antwerp, Belgium	Atlanta, USA	L.A., USA	Washington, USA
	Diameter	12.6m wide, 10.8m ht.	5m	<3m	<3m	x
	Implemented tunnel length	1400m	x	approx 3-5m	X	x
	Ground Condition	fragmented rocks	medium to fine tertiary sand	variable fill, micaeous fine sand	silt,fine sand,gravel	P1 OC clay
	Overburden	10.8m	I	2m	2m	20-40m
	Deform. coeff.	I	I	I	I	I
	Cohesion/ Ø	I	I	I	I	I
Auxiliary Reinforcement	**Type**	Pipe Umbrella	Pipe roof	Pipe roof	Pipe Roof	Pipe roof
	Ø (outer/thickness)	600/-	1200-1800/-	1200-1800/-	760/-	1130/-
	nos. (reinft. arch span)	I	11	11	42	17
	Length	12m	1.0m	1.0m	6.0m	6.0m
	Inclination	I	I	Jacked horizontal	Jacked horizontal	Jacked horizontal
	overlap length	I	I	I	I	I
	spacing bet. Pipes	I	I	I	I	I
	rate of progress	I	I	I	I	I
Other supports	**steel support**	x	X	I	I	I
	shotcrete	x	X	I	I	I
	footpiles/rock bolts	x	X	X	x	X
	jet grouting	x	X	X	x	X
	FBG face reinft.	x	X	X	x	X
Tunnel shape		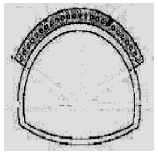	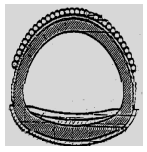	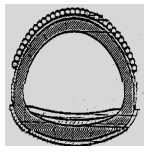	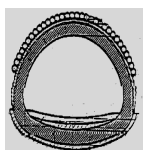	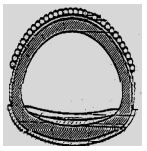
Reference		Megaw et al.(1983)	Hoste (1980)	Rhodes et al. (1996)	Rhodes et al. (1996)	Gall et al. (1998)

Table 3-2 (cont.)

Tunnel dimension and Ground conditions	**Tunnel**	Almeda Station	Senseki Line	Mito	Fiumelatte	Satsuma Tagami
	Location	Lisbon, Portugal	Sendai, japan	Ibaraki, Japan	Italy	Kyushu, Japan
	Diameter	I	I	102m2	10.5m wide (100m2)	I
	Implemented tunnel length	I	I	I	640m	I
	Ground Condition	grey limestone,silty clay	organic clay, tuff, gravel	gravel, clay	limestone debris	volcanic fill (shirasu)
	Overburden	4.0m	3.5m	6-11m	I	20-70m
	Deform. coeff.	I	I	I	I	I
	Cohesion/ Ø	I	I	I	I	I
Auxiliary Reinforcement	**Type**	Pipe roof	Pipe roof	Pipe Umbrella	Pipe Umbrella	Pipe roof
	Ø (outer/thickness)	1600/-	1000/-	140/-	95/4.5	1016/-
	nos. (reinft. arch span)	14	21	25	12	13
	Length	7m	I	12.5m	12m	2m
	Inclination	I	I	I	15˚	I
	overlap length	I	I	I	4m	I
	spacing bet. Pipes	I	I	I	700mm	I
	rate of progress	I	I	I	24 nos. installed per hr	I
Other supports	**steel support**	I	I	X	2xNP-160	x
	shotcrete	I	I	X	I	x
	footpiles/rock bolts	X	X	X	I	x
	jet grouting	X	X	X	x	x
	FBG face reinft.	X	X	X	x	x
Tunnel shape		Box shape	x	x	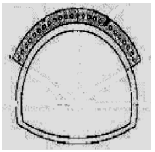	x
Reference		Mcfeat-Smith (2001)	Satoh et al. (1996)	Itoh et al. (2001)	Barisone et al. (1982)	Matsumoto et al. (2001)

Table 3-2 (cont.)

Tunnel dimension and Ground conditions	**Tunnel**	Merone	Delle Tanze	Cernobia	Serre la Voute	Pietratagliata
	Location	Como,Italy	Italy	Italy	Italy	Italy
	Diameter	8m wide (70m2)	6.5m wide (60m2)	10.5m wide(100m2)	12m wide (100m2)	12.5m wide (100m2)
	Implemented tunnel length	185m	1630m	240m	160m	32m
	Ground Condition	marls	limestone	gravel cobbles alluvium	gneiss	clay
	Overburden	I	I	I	I	I
	Deform. coeff.	I	I	I	I	I
	Cohesion/ Ø	I	I	I	I	I
Auxiliary Reinforcement	**Type**	Pipe Umbrella	Pipe Umbrella	Pipe Umbrella	Pipe Umbrella	Pipe Umbrella
	Ø (outer/thickness)	150/6	9.5/4.5	150/6	180/10	160/10
	nos. (reinft. arch span)	17	12	18	18	13
	Length	18m	12m	18m	14m	18m
	Inclination	15˚	15˚	15˚	15˚	4˚
	overlap length	4m	3m	5m	4m	4m
	spacing bet. Pipes	600mm	600-800mm	500mm	750mm	800mm
	rate of progress	72 nos. installed per hr	16 nos. installed per hr	72 nos. installed per hr	60 nos. installed per hr	80 nos. installed per hr
Other supports	**steel support**	2xNP-160	2xNP-160	2xNP-160	2xNP-160	2xNP-160
	shotcrete	I	I	X	x	x
	footpiles/rock bolts	I	I	I	I	I
	jet grouting	x	x	X	x	X
	FBG face reinft.	x	x	X	x	X
Tunnel shape		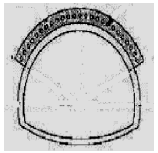	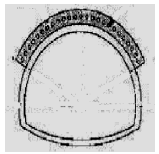	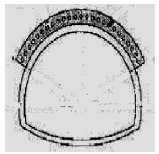	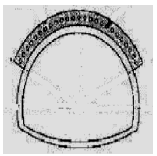	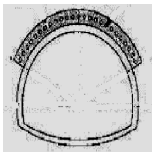
Reference		Barisone et al. (1982)	Barisone et al. (1982)	Barisone et al. (1982)	Barisone et al. (1982)	Barisone et al. (1982)

Table 3-2 (cont.)

Tunnel dimension and Ground conditions	**Tunnel**	Spallanzani	S. Bernardino	Il Bricco	Lonato	Serena
	Location	Italy	Italy	Italy	Italy	Italy
	Diameter	100m2	I	I	90m2	20m
	Implemented tunnel length	18m	266m	40m	1660m	50m
	Ground Condition	flysch, weak rock	schists,weak rock	Landslide	morainic deposit	alluvial deposit
	Overburden	I	I	I	0-70m	20m
	Deform. coeff.	I	I	I	I	I
	Cohesion/ Ø	I	I	I	I	I
Auxiliary Reinforcement	**Type**	Pipe Umbrella	Pipe Umbrella	Pipe Umbrella	Pipe Umbrella	Pipe Umbrella
	Ø (outer/thickness)	140/3.2	200/8	120/-	120/7	120/7
	nos. (reinft. arch span)	22	30	19+21	40	30-44
	Length	15m	11m	21m	12m	12m
	Inclination	2˚	X	X	x	X
	overlap length	I	8m	9m	9m	9m
	spacing bet. Pipes	600mm	I	I	I	I
	rate of progress	140/hr	I	I	I	I
Other supports	**steel support**	2xNP-160	I	I	I	2xIPN-160
	shotcrete	I	I	I	I	I
	footpiles/rock bolts	x	X	X	I	X
	jet grouting	x	X	X	x	X
	FBG face reinft.	x	X	X	x	X
Tunnel shape		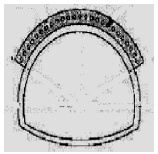	X	X	X	X
Reference		Barisone et al. (1982)	Barisone et al. (1982)	Piepoli (1976)	Fasoli and Pastore (1976)	Carrieri et al. (1990)

Table 3-2 (cont.)

Tunnel dimension and Ground conditions	**Tunnel**	Alpe	Ceresole	Chabodey	La Perosa	Ramat
	Location	Liguria, Italy	Italy	Italy	Turin, Italy	Italy
	Diameter	14.5m	90m2	70m2	I	12m wide, 10m ht.
	Implemented tunnel length	955m	50m	70m	400m	500m
	Ground Condition	calcareous mica schists	detritus	schists, weak rock	morainic	weak rock, morainic
	Overburden	I	I	I	20m	I
	Deform. coeff.	I	I	I	I	I
	Cohesion/ Ø	I	I	I	I	I
Auxiliary Reinforcement	**Type**	Pipe Umbrella	Pipe Umbrella	Pipe Umbrella	Pipe Umbrella	Pipe Umbrella
	Ø (outer/thickness)	I	120/7	120/7	120/10	120/10
	nos. (reinft. arch span)	I	40	30	33-39	33
	Length	I	12m	12m	12m	12m
	Inclination	I	I	I	I	I
	overlap length	I	9m	9m	9m	9m
	spacing bet. Pipes	I	I	I	I	I
	rate of progress	I	I	I	I	I
Other supports	**steel support**	I	I	I	I	I
	shotcrete	I	I	I	I	I
	footpiles/rock bolts	I	I	I	I	I
	jet grouting	x	x	X	x	X
	FBG face reinft.	x	x	X	x	X
Tunnel shape		X	X	X	X	X
Reference		Grasso et al. (1990)	Carrieri et al. (1991)	Carrieri et al. (1991)	Eusebjo et al. (1990)	Barisone et al. (1989)

Table 3-2 (cont.)

Tunnel dimension and Ground conditions	**Tunnel**	Lange Issel	Irlahull	Stammham	Euerwang
	Location	Cologne-Nuremberg, Germany	Cologne-Nuremberg, Germany	Cologne-Nuremberg, Germany	Cologne-Nuremberg, Germany
	Diameter	I	I	I	I
	Implemented tunnel length	I	I	I	I
	Ground Condition	Weathered slate	Deposits of sand, boulders, silt, clay	Deposits of sand, silt, clay	Decomposed sandstone above siltstone
	Overburden	6-7m	6-20m	6-10m	
	Deform. coeff.	80-150 MN/m2	30-50 MN/m2	20-30 MN/m2	60 & 50 MN/m2
	Cohesion/ Ø	0.13 MN/m2 / 25	0.005 MN/m2 / 32.5	0.005-0.02 MN/m2 / 20-30	0.005 & 0.05 MN/m2 / 32.5 & 20
Auxiliary Reinforcement	**Type**	Pipe Umbrella	Pipe Umbrella	Pipe Umbrella	Pipe Umbrella
	Ø (outer/thickness)	114.3/ 6.3	88.9/ 8.0	114.3/ 6.3	114.3/ 6.3
	nos. (reinft. arch span)	I	I	I	I
	Length	17.5m	12 / 9m	15m	15m / 13m
	Inclination	I	I	I	I
	overlap length	4.3m	5.9m	6.7m	3.9m
	spacing bet. Pipes	0.4m	0.3m	0.3m / 0.4m	0.4m
	rate of progress	I	I	I	I
Other supports	**steel support**	I	I	I	I
	shotcrete	I	I	I	I
	footpiles/rock bolts	X	X	Drainage pipes 25m	X
	jet grouting	X	x	X	X
	FBG face reinft.	X	Face bolts 12-15m	Face bolts 12-15m	Face bolts 9-12m
Tunnel shape		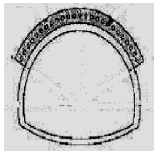	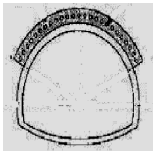	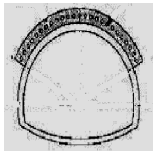	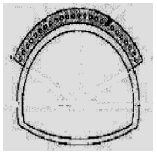
Reference		John. M & Mattle, B (2002)	John. M & Mattle, B (2002)	John. M & Mattle, B (2002)	John. M & Mattle, B (2002)

CHAPTER 4 – ANALYSIS OF A CASE HISTORY OF UMBRELLA ARCH IN WEAK ROCKS USING DIFFERENT APPROXIMATIONS: COMPARISON OF RESULTS

4.1 Numerical Analysis for Umbrella Arch Method

Currently, most tunnel engineers would use their experience to decide on the design of the Pipe Umbrella Arch instead of by theoretical or numerical methods. When numerical methods are implemented, most often crude approximation using 2-D analysis, such as the equivalent strength of the components to simulate the Pipe Umbrella Arch, is adopted. However, the results derived from such crude approximations should not be used in any detailed design (Hoek, 2000). The effect of Umbrella Arch method is without doubt a three-dimensional problem. Nevertheless, a two-dimensional model which can effectively provide a suitable solution to the problem will be invaluable. Using a crude two-dimensional (2-D) model to analyze a three-dimensional (3-D) problem will require numerous assumptions and approximations that might erase the actual effect of the field condition. The Pipe Umbrella Arch can be used in both fractured rocks and soil and in this chapter, a case history of the Umbrella Arch is studied in weak rocks and FLAC, a finite difference program commonly used for numerical analysis in rock engineering, is used. Unfortunately, this case history in weak rocks does not have any records of field measurements which will thus make comparison of results difficult. 2 case histories of Pipe Umbrella Arch in soil are also studied in the next chapter using a 3-D finite element program, ABAQUS.

The objective of the study presented in this chapter is to assess and compare the results generated by different approximations of the Umbrella Arch method when it is used as pre-support for tunnel excavation in weak rock at shallow depth.

4.1.1 Problem Description

The problem investigated is a simplified version of a real case study of the Egnatia Highway in Greece (Hoek, 2000) and is schematically defined in Figure 4-1. A horse-shoe shaped transportation tunnel of 10m height and 6m width is to be excavated by a top heading and bench method. The tunnel is situated at a shallow depth of 15 m from the ground surface in a highly weathered and disturbed rock mass. The construction is separated into the excavation of the top heading which is a semi circular tunnel of 6m diameter followed by the bottom bench of a rectangular 6m x 7m tunnel. Pre-support reinforcement was required to stabilise the top heading construction in this weak ground and the umbrella arch method was chosen. The umbrella arch spans 180˚ around the tunnel crown. It was anticipated that the Umbrella Arch would minimise the surface settlement during the excavation of the top heading. The method uses 18 steel forepoles with 150 mm outer diameter and 136 mm inner diameter. The forepoles are approximately 12 m in length and spaced at 500 mm centre to centre. The tunnel is advanced at 8 m intervals before installation of the next set of Umbrella Arch, thus allowing for 4 m of overlap.

4.1.2 Ground conditions of case study

The tunnel is excavated in a highly weathered rock mass. For simplification, the surrounding rock mass is assumed to be homogeneous and the rock mass properties are given by Hoek (2000) and shown in Table 4-1.

Table 4-1. Rock mass properties.

Geological strength index, GSI	20
Hoek-Brown constant m_i	8
Intact rock strength σ_{ci}	3MPa
Friction angle, Ø	30˚
Cohesive strength, c	28 kPa
Deformation modulus, E	308 MPa
Tensile strength	1.0 kPa

4.1.3 Geometry and Boundary Conditions

2-D finite difference (FD) modeling using Fast Lagrangian Analysis of Continua (FLAC) code (Itasca, 1997) is used to study the ground behaviour using different approximations for the Umbrella Arch. The model to be studied is shown in Figure 4-1 with its associated boundary conditions. A 60m wide by 30m deep model space is constructed to model the tunnel and the surrounding rock. A semi-circular tunnel of 6m diameter is to be excavated in the highly weathered rock mass. The overburden height from the tunnel crown to the ground surface is 15m. The model only considered the excavation of the top heading, which is the semi circular part of the horse shoe tunnel. This is because the forepoling system is installed prior to excavation of the top heading over the entire stretch of the tunnel crown to control the collapse of the rock mass and to control the induced ground surface settlement. The bottom bench is excavated after the top heading has been excavated and after other stabilizing measures had been installed for the top heading.

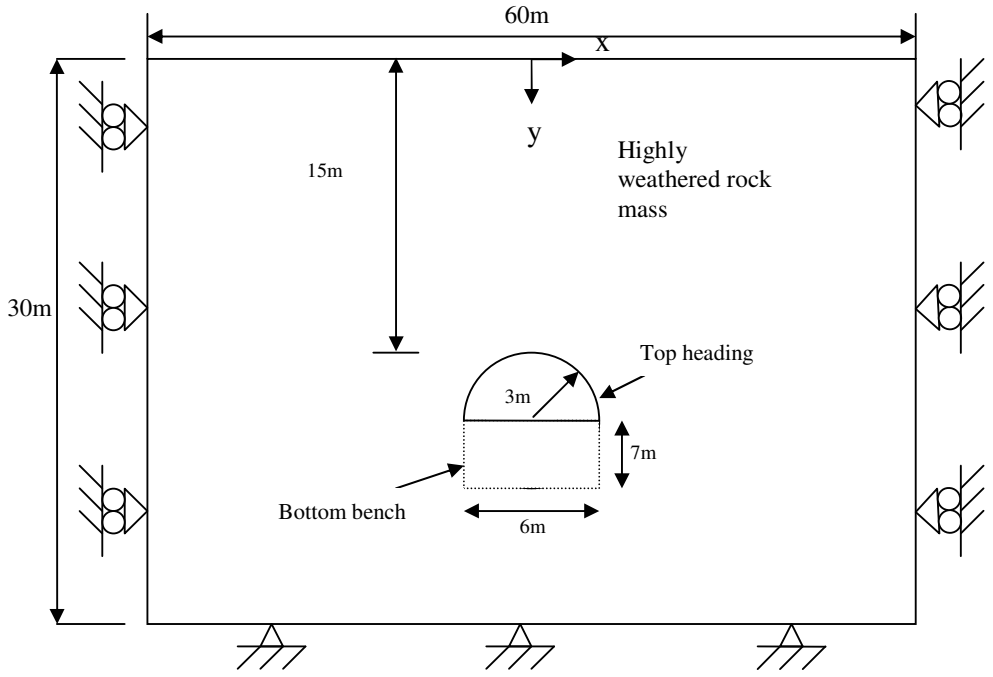

Figure 4-1. Boundary conditions employed in the numerical study.

From this 2-D numerical analysis, the vertical displacements induced by tunnelling at the tunnel crown and ground surface as well as the vertical (displacement difference between tunnel crown and foot) and horizontal (displacement difference between the left and right springline) closures are determined and compared for the different approximation models.

4.1.4 2-D Mesh and element types

A. Soil model

Due to geometrical symmetry of the tunnel section, only half the problem is considered. A 120 x 60 grid mesh is generated using 0.5m x 0.5m zones. The vertical in-situ stress at any point is assumed to be due to gravity and is calculated by multiplication of the depth below the ground surface with the unit weight of the rock mass. The stress gradient is linear with zero stress at the ground surface. The horizontal in-situ stresses in the x and z (into tunnel) directions are assumed to be equal to the vertical stresses (K_o = 1) (Hoek, 2000). The rock is at equilibrium under gravity loading prior to making the excavation.

B. Steel pipe

Steel pipes were assumed to be elastic and homogenous and were modelled using beam elements. The steel beam has an elastic modulus of 200 GPa.

4.1.5 Material Constitutive Model

An elasto-ideally plastic behaviour with an associated flow rule was assumed for the calculations of the weathered rock layer. The tunnel section consists mainly of weathered rocks. The density for weathered rocks is assumed to be 1900kg/m^3 with a Poisson's ratio of 0.49 and strength of 160 kPa (Hoek, 2000). The deformation modulus and shear modulus are 308MPa and 103MPa respectively. The cohesion of

the rock is 28kPa. The friction angle is 30º. The coefficient of earth pressure at rest, K_o, is assumed to be 1.0 (Hoek, 2000). The properties of the composite strip, steel pipes and composite beam are discussed in Section 4.2.

4.1.6 Initial Conditions and Modelling steps

The numerical analyses were conducted according to field construction procedures and the Pipe Umbrella Arch is installed prior to excavation of the tunnel. The sequential modelling consists of initial installation of an umbrella arch prior to any excavation and followed by the removal of the tunnel. The procedures used for the sequential modelling follows very closely to the actual field construction and is tabulated in Table 4-2. Each construction step is run for 3500 cycles to reach an equilibrium state.

Table 4-2. 2-D modelling procedure.

Step	Stage of construction	Descriptions
1	Geostatic state of stress	Model is subjected to initial stresses & gravity
2	Installation of U	Activate Pipe Umbrella Arch elements
3	Excavation of tunnel	Tunnel elements are deactivated

4.2 Approximations used for modelling Umbrella Arch

Three different approximations of the Umbrella Arch are identified from case histories and evaluated using the numerical modelling procedures as mentioned in Section 4.1. The ideology and calculation steps for each method are explained in details as follows:

1. Method (1) - Steel pipes, grout and rock material properties are combined using weighted averages and an equivalent rock mass strength is derived (Hoek, 2000). Using the Hoek-Brown criterion, corresponding rock mass parameters are used. These parameters only apply to a strip of rock material around the tunnel crown (Figure 4-2a).

2. Method (2) - Steel pipes are modelled using beam elements. Grout and rock material properties are combined using weighted averages and an equivalent rock mass strength is derived (Hefny et al., 2004). Using the Hoek-Brown criterion, the equivalent rock mass parameters are derived as in Section 4.2.1. These parameters only apply to a strip of rock material around the tunnel crown. Steel pipes are installed within the reinforced zones (Figure 4-2b).

3. Method (3) - Steel pipes are modelled using beam elements and grout is also modelled as beam elements around the tunnel periphery (Figure 4-2c) (Hefny et al., 2004).

The methods of approximation are adopted based on Hoek (2000) and Hefny et al. (2004). Hoek (2000) discussed the effects of using Method (1) for design of Pipe Umbrella Arch while Hefny et al. (2004) investigated the effect of different approximations of Pipe Umbrella Arch (Method (1), (2) and (3)) on ground behaviour in weak rocks. In Methods (2) and (3), a generic simulation of steel pipes is used in the study to model the effect of steel pipes as opposed to the conventional method of combining the ground, pipes and grout as an equivalent material. Steel pipes are individually modelled using beam elements while grout is modelled either as beam elements or as elements of material with equivalent rock strength in numerical analysis. By separating the steel pipes from the “equivalent material”, the steel pipes will be isolated and hence it will enable the investigation of the reinforcing effect of the steel pipes alone. Although the process of modelling individual steel pipes is tedious and time consuming, it is expected that this method will provide a more accurate representation of the behaviour of the steel pipes in umbrella arch support system.

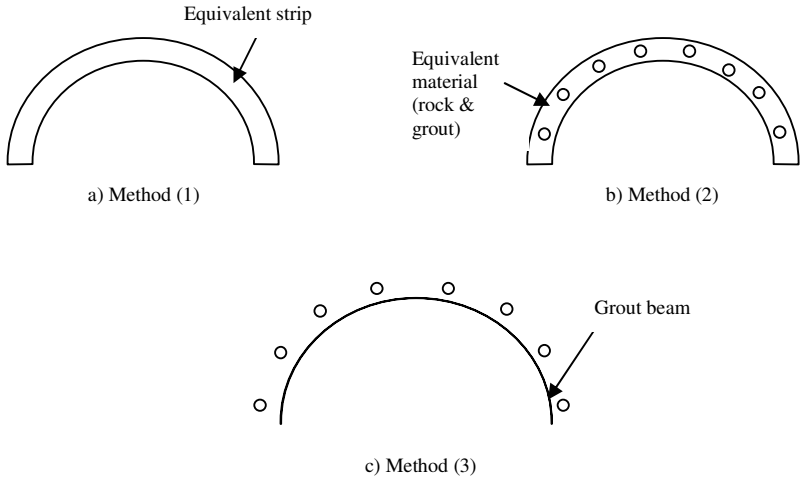

Figure 4-2. Approximations used for simulating Umbrella Arch.

4.2.1 Calculation steps for the various methods of approximations

(1) <u>Modelling steel pipes, grout and rock as a composite strip for Method (1)</u>

Method (1) is the conventional approach used to approximate the Umbrella Arch, where the process of weighted averages is used to calculate an equivalent rock mass strength for the reinforced rock zone above the tunnel crown. The strength is estimated through the multiplication of the strength and the cross sectional area of individual components in the reinforced zone and then dividing the sum of all products by the total area. Figure 4-3 shows the dimensions of the composite strip used in Method 1.

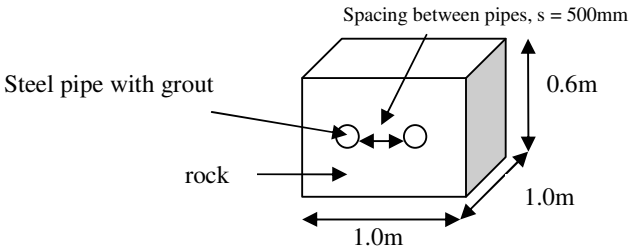

Figure 4-3. Dimensions of the composite strip (grout, rock & steel pipes).

Table 4-3. Specifications of the composite strip (grout, rock & steel pipes).

Component	Area (m^2)	Strength (MPa)	Product	Remarks
Rock	0.6*1.0 = 0.6	0.16	0.1	
Steel pipes	2*0.00314= 0.00628	200	1.26	Cross sect. area of single pipe = $3.142*(.150^2 - .136^2)/4=0.00314$
Grout	2*0.0145=0.029	30	0.87	Cross sect. area of grout in a single pipe= $3.142*(0.068)^2=0.0145$
Sum	0.635		2.23	
Rock mass strength = 2.23/0.635 = 3.5 MPa				

Table 4-3 shows the specifications and calculation steps for the equivalent rock mass strength. Using the Hoek-Brown failure criterion, the equivalent rock mass parameters for the composite strip can be derived using the calculated rock mass strength. Roclab (Rocscience Inc., 2004), a software program for determining rock mass strength parameters based on the generalized Hoek-Brown failure criterion, is used to calculate the associated rock mass parameters. RocLab provides a simple and intuitive implementation of the Hoek-Brown failure criterion, allowing users to easily obtain reliable estimates of rock mass properties and to visualize the effects of changing rock mass parameters on the failure envelope. The calculated rock mass parameters are tabulated in Table 4-4.

Table 4-4. Rock mass parameters for composite strip (grout, rock & steel pipes).

Geological strength index, GSI	20
Hoek-Brown constant m_i	8
Intact rock strength σ_{ci}	48 MPa
Friction angle, Ø	20˚
Cohesive strength, c	1.2 MPa
Deformation modulus, E	1230 MPa
Tensile strength	14 kPa

(2) Modelling steel pipes as single components for Methods (2) and (3)

Table 4-5. Properties of steel pipe.

Deformation modulus, E	200GPa
Second moment of area, $I = (1/12).t^3$	2.86E-08 m^4
Cross sectional area, $A = b.t$	0.00628 m^2

Note: b = per unit length of pipe

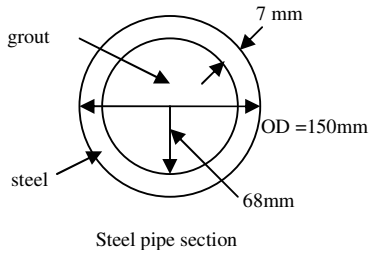

Figure 4-4. Description and dimension of steel pipe.

The steel pipes are modelled using 2-noded beam elements. The steel pipes have an outer diameter of 150 mm and thickness of 7 mm. The properties and dimensions of the steel pipe are clearly shown in Table 4-5 and Figure 4-4 respectively.

(3) Modelling of grout material for Method (2)

The grouted interior of the pipe and rock material are modelled as a composite strip with equivalent rock mass strength using the method proposed by Hoek (2000) and it is simulated with thickness of 0.6 m around the tunnel crown for 180˚ span and the steel pipes are embedded in the composite strip. This approach is used for simulation of the Umbrella Arch in Method (2). Figure 4-5 shows the calculations and ideology.

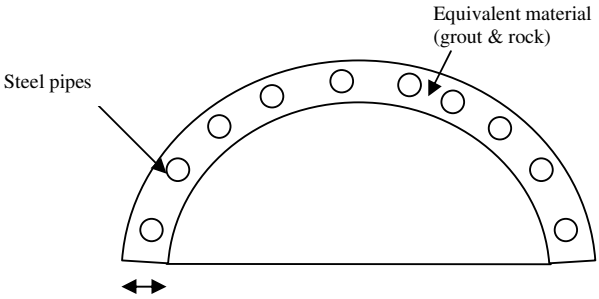

	Area(m^2)	Strength(MPa)	Product
Rock	0.6x1.0= 0.6	0.16	0.1
Grout	0.029	30	0.87
Total	0.629		0.97
Equivalent rock mass strength = 0.97/0.629 = 1.54MPa			

Figure 4-5. Simulation of equivalent material (grout & rock).

Using the Hoek-Brown criterion, the calculated equivalent rock mass strength translates into the parameters listed in Table 4-6. These generated estimates of rock mass properties are used for the reinforced zone for Method (2).

Table 4-6. Rock mass parameters of composite strip (grout & rock).

Geological strength index, GSI	20
Hoek-Brown constant m_i	8
Intact rock strength σ_{ci}	21MPa
Friction angle, Ø	20˚
Cohesive strength, c	0.5 MPa
Deformation modulus, E	815 MPa
Tensile strength	0.006 MPa

(4) Modelling of grout material for Method (3)

Table 4-7. Properties of grout material.

Elastic modulus, E	2.0 GPa
Second moment of area, I	$0.018m^4$
Cross sectional area, A	$0.6\ m^2$

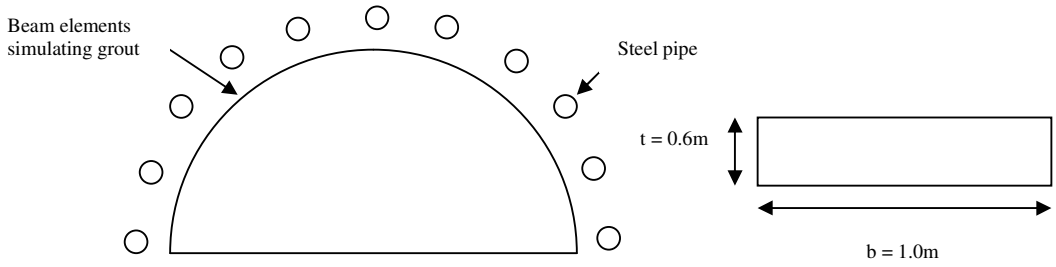

Figure 4-6. Simulation of grout as beam elements.

The grouted region of the Umbrella Arch is modelled by the conventional method of using beam elements to simulate concrete linings as shown in Figure 4-6. The beam element is assumed to have a thickness of 0.6 m which is similar to the thickness of the zones used in the method proposed by Hoek (2000). The properties of grout are listed in Table 4-7. The grout beam is modeled using beam elements in FLAC.

4.3 Results and Discussions

The ground surface settlement profile obtained from using Method (1) (Figure 4-7) showed that the maximum value developed directly above the tunnel crown is approximately 4 mm. Ground surface settlement plots of Methods (2) and (3) presented good correlation with each other but varied widely from the ground surface settlement of Method (1). Method (1) produced 4 mm of ground surface settlement whilst Methods (2) and (3) yielded approximately 2 mm which is half of that estimated by Method (1). It was observed that the equivalent strip of Method (1) acted upon the tunnel footings and created greater deformations at the tunnel crown and inevitably led to greater ground surface deformations.

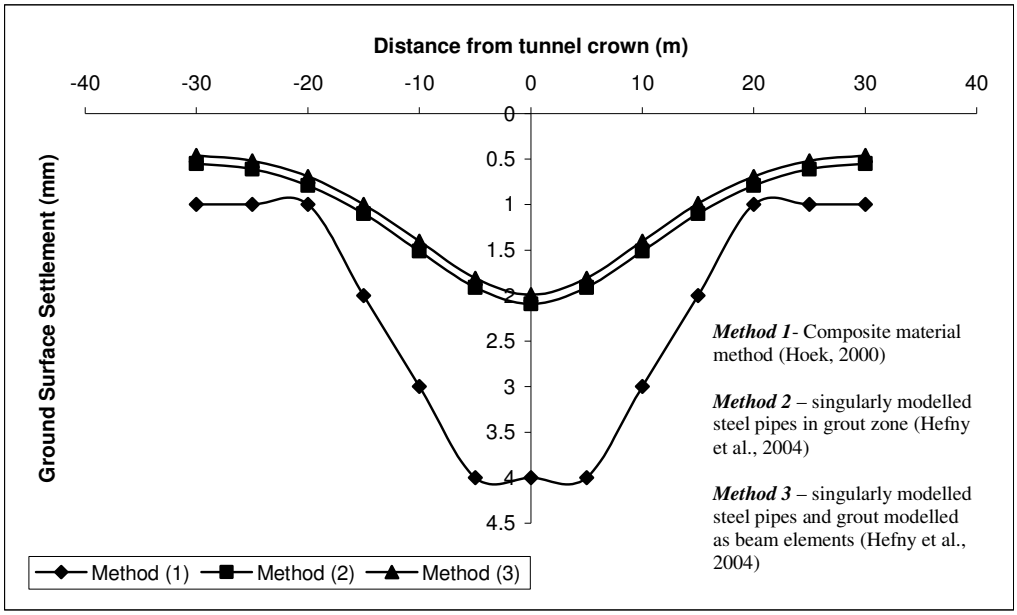

Figure 4-7.Comparsion of ground surface settlement using various methods of analysis.

Table 4-8. Vertical and horizontal tunnel closures.

Method	Vertical closure (mm)	horizontal closure (mm)
1	20	7
2	15	6.5
3	14.5	6.2

Table 4-8 shows the vertical and horizontal tunnel closures for the tunnel studied. Vertical closure is the change in vertical distance between the tunnel crown and the tunnel base after tunnel excavation. Horizontal closure is the change in the horizontal distance between the left and right side of the tunnel wall at the tunnel springline.

Methods (2) and (3) showed close correlation with each other. Method (1) yielded vertical closure of 20 mm which is about 5 mm or 33% higher than Method (2) and (3). Such significant variations are due to different approximations of Pipe Umbrella Arch used.

By comparing the tunnel crown settlement as shown in Figure 4-8 using Methods (1), (2) and (3), it was observed that all 3 methods produced different results.

Method (1) yielded the highest tunnel crown settlement of 9 mm whilst Method (3) yielded the lowest tunnel crown settlement of approximately 4 mm (44% of the value estimated by Method (1)). This further emphasizes that different approximations produce different results and that case studies and 3-D numerical analyses are required to accurately derive a better approximation.

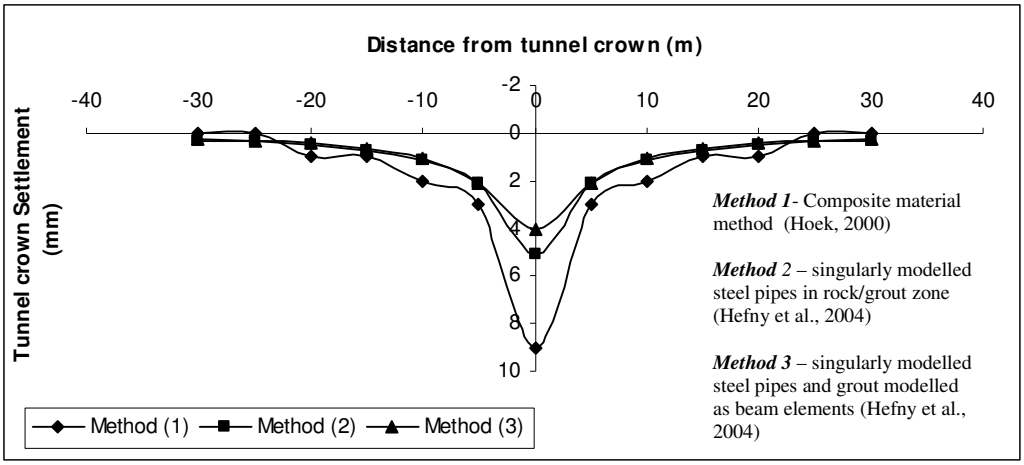

Figure 4-8. Comparison of tunnel crown settlement with various methods.

By observation of the comparison of ground surface and tunnel crown settlements generated by the different methods, the difference in the obtained results could be due to the different approach used by the different methods. Methods (2) and (3) had modelled the steel pipes singularly, which practically should yield more accurate results of surface settlement since in actual field execution, the steel pipes and the grout are separate components in the Umbrella Arch method. Unfortunately, this case history of the Pipe Umbrella Arch in weak rocks does not have records of field measurement and thus, comparison of results is not possible.

CHAPTER 5 – 3-D NUMERICAL ANALYSIS FOR 2 CASE STUDIES OF THE PIPE UMBRELLA ARCH METHOD

The different approximations for the Pipe Umbrella Arch were studied in the previous chapter and it was shown that they produced significantly different results and settlement profiles. These are crude approximations because they do not consider several intricate mechanism of the Pipe Umbrella such as the effect of the overlap length on the overall stability of the tunnel face, the interaction of the grout/steel pipes and pipe/soil interfaces and the phased construction stages of tunnel excavation when the Pipe Umbrella is installed. The analysed case study (in Chapter 4) was for the case of Umbrella Arch in weak rocks. In this chapter, 3-D analyses have been performed on two well-documented case studies for the Umbrella Arch method in soil. Comparison between numerical results and field measurements are made.

5.1 Case History and Description

Preliminary studies are conducted in this chapter to calibrate a three dimensional numerical model to the case study of the Maiko tunnel in Kobe, Japan, where the Umbrella Arch method was used during construction in soil. For this project, both the measured soil displacement and construction of the Pipe Umbrella Arch were well documented at some excavation sections. The Pipe Umbrella Arch method was used at 2 sites along the Maiko Tunnel. Murata et al. (1996), Muraki (1997) and Harazaki et al. (1998) presented details of the phased construction of the project and reported the longitudinal ground surface settlements during the construction of the tunnel through very shallow ground at the Fukuda Junior High School section. The 2 sites are the Fukuda Junior High School site and the Maikodai site as shown in Figure 5-1. The details of the excavation of the Maikodai site are incomplete. Thus, the numerical analyses conducted in this chapter are for the excavations at the Fukuda Junior High School site of the Maiko Tunnel. At the Fukuda Junior High

School site, 2 sections of different ground conditions are studied and they are known as Zone A and Zone B.

5.1.1 Fukuda Junior High School site of the Maiko Tunnel

The Maiko Tunnel is a twin highway tunnel with three lanes in each direction that passes through a few residential areas (see Figure 5-2). The tunnel is 3.3 km long and has an average excavated cross section of 150 m^2, i.e. approximately 16m in width and 12m in height. Approximately 70% of the tunnel passes through the Osaka soil formation and the rest through Rokko Granite. The tunnel at the Fukuda Junior High School site of the tunnel passes through relatively shallow overburden which is situated below a school and residential areas. An aerial view for Maiko Tunnel is shown in Figure 5-2.

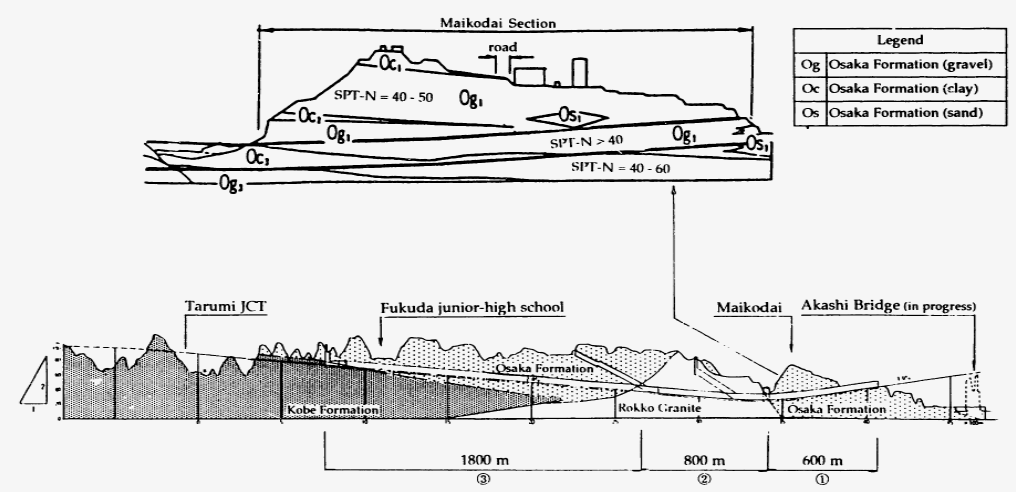

Figure 5-1. Maiko Tunnel, Kobe, Japan (Murata et al., 1996).

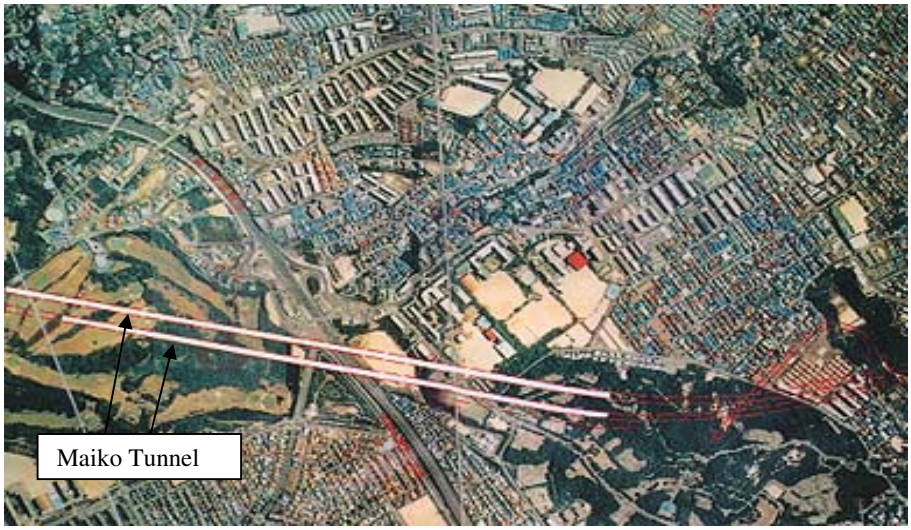

Figure 5-2. Aerial view of a section of the Maiko Tunnel through the city of Kobe. (www.gel.civil.nagasaki-u.ac.jp)

The Fukuda Junior High School is situated near the north portal of the Maiko Tunnel and the tunnel passes at a shallow depth of 6m under the athletic field of the high school.

5.1.2 Ground Conditions

Excavations at the Fukuda Junior High School site are executed in 2 different types of ground conditions (Zone A and Zone B). Generally, the soil in the Fukuda High School area consists of the Osaka formation which is mainly gravel with silt and clay with alluvial gravel and fill encountered in certain sections as shown in a schematic drawing in Figure 5-3. The Osaka formation is underlain by a much stiffer layer of sandstone and shale called the Kobe formation as shown in Figure 5-1. The ground being excavated is laden with a mixture of gravely clay, clayey gravel and clay. Zone A consists of a thin layer of weaker alluvial fills underlain by stiffer Kobe Formation. Zone B is situated in the Osaka Formation and underlain by the Kobe formation.

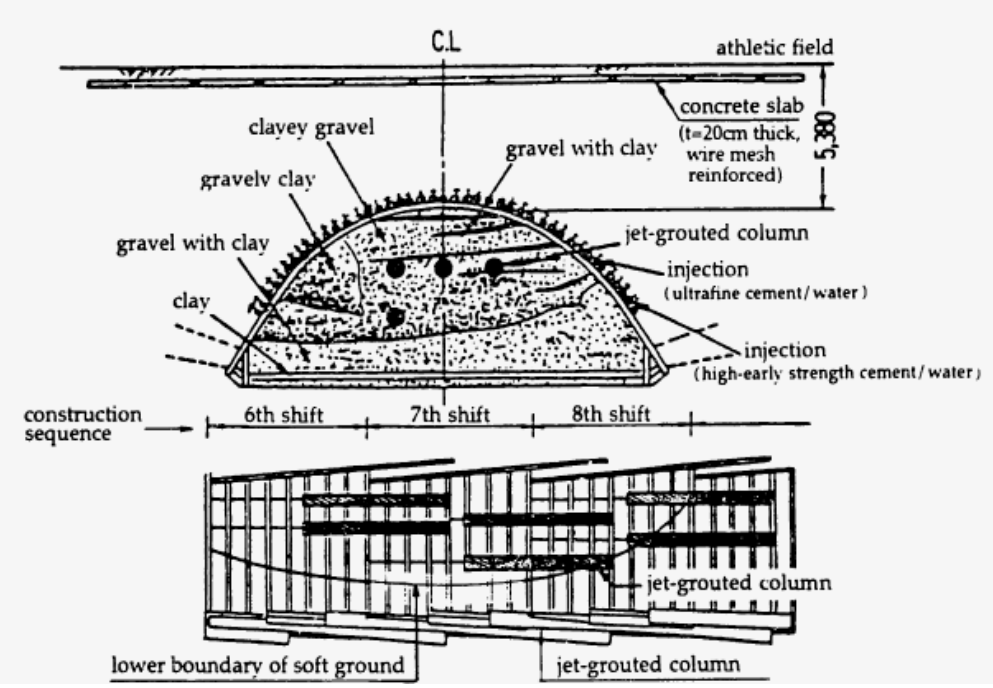

Figure 5-3. Type of soil generally encountered at the excavated tunnel under Fukuda Junior High School.

5.1.3 Construction Details

In order to minimise ground movement in the shallow sensitive area, the pipe umbrella arch was installed prior to tunnel excavation. Figures 5-4 and 5-5 show the cross sectional and longitudinal view of the tunnel, respectively, and the types of tunnel stabilisation methods that were used. The properties of the pipe umbrella arch reinforcement are tabulated in Table 5-1. A total of 42 pipes of 12m length are installed at an inclination of 5˚ to the horizontal. The pipes are evenly separated over a span of 140˚ of the tunnel periphery.

The tunnel is excavated using the centre drift method. 8m of the tunnel was excavated before installation of the next Umbrella Arch to maintain a 4m overlap for the protection of the tunnel face. The bottom bench only proceeded with excavation after every 200m of excavation of the top heading and installation of reinforcing support measures. Part of the tunnel cross section is shown in Figure 5-6.

Table 5-1. Dimension of steel pipes used.

Length	Outer Diameter	Thickness	Number used	Span
12m	114mm	6mm	42	140˚

The excavated tunnel was further supported by a primary concrete lining of 250mm and H-200 section steel arches with wing ribs installed at every 1m interval. In addition, a secondary concrete lining of 450mm is also employed over the primary lining. A tunnel invert of 250mm was also installed.

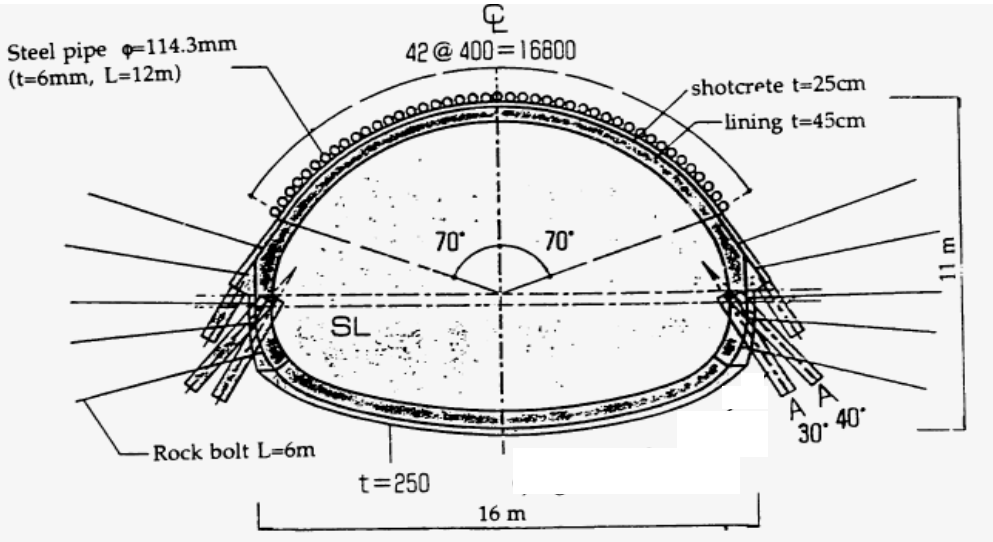

Figure 5-4. Cross sectional view of Maiko Tunnel under Fukuda Junior High School.

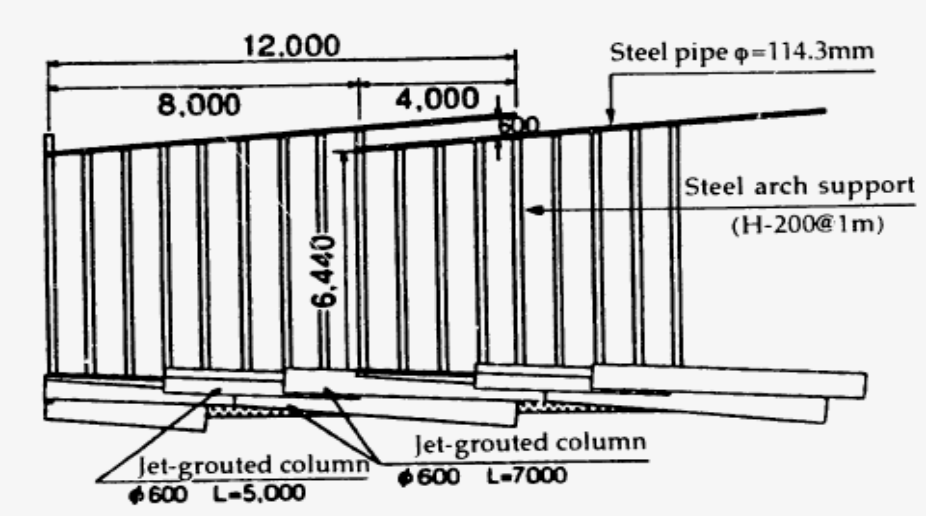

Figure 5-5. Longitudinal view of Maiko Tunnel under Fukuda Junior High School.

Figure 5-6. Tunnel cross section.

5.1.4 Field Measurements

The longitudinal ground surface settlements for the two excavation sites (Zone A and Zone B) are reported as shown in Figure 5-7 (Muraki, 1997).

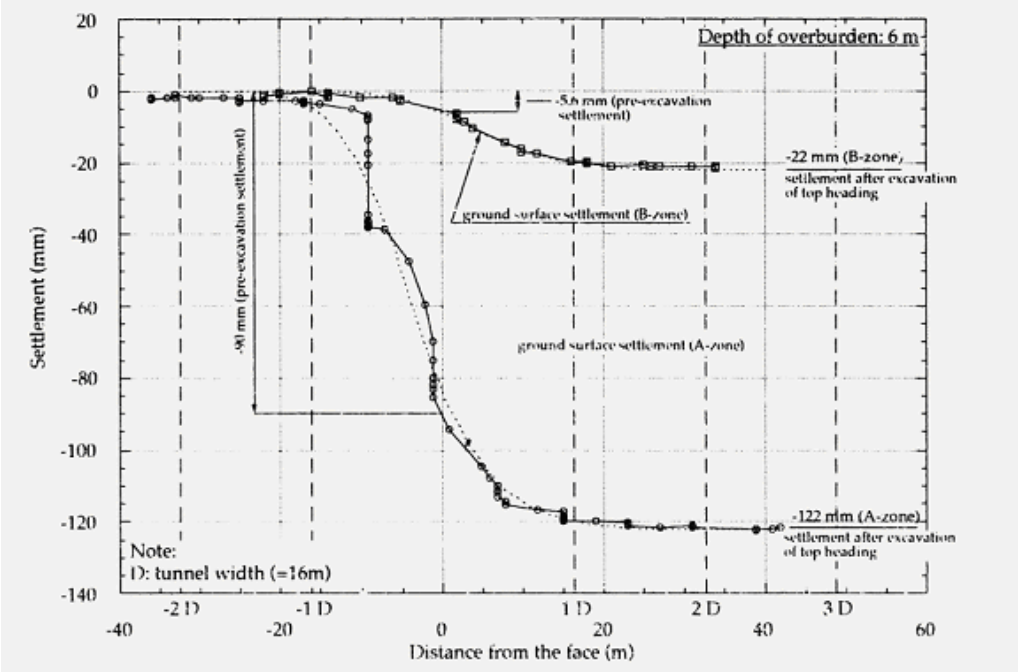

Figure 5-7. Longitudinal ground surface settlement for Zone A and B of the Maiko Tunnel (Muraki, 1997).

5.2 3-D FEM Analysis of the Fukuda Junior High School site

The purpose of this analysis is to calibrate three dimensional numerical models to the construction of tunnels in Zone A and Zone B of the Fukuda Junior High School site of the Maiko Tunnel. After verifying the models, parametric studies are conducted to determine the optimum pipe number, pipe diameter and pipe lap length (i.e. overlapping length of steel pipes). The tunnels were excavated in alluvial fills in Zone A and in Osaka Formation in Zone B. Every shift of the tunnel was excavated and reinforced with concrete linings, steel arches and concrete tunnel inverts. Subsequently before the next shift was excavated, Pipe Umbrella Arch was installed to reinforce the periphery of the tunnel.

The finite element program ABAQUS/ STANDARD version 6.4 (Hibbitt, Karlsson and Sorensen, Inc., 2003 & 2004) running on Sun Microstations platform was used for the analyses. The software package ABAQUS/CAE version 6.4 was used to perform the pre-processing and post-processing. ABAQUS provides a versatile capacity to model activation and deactivation of elements, sophisticated geometrical details, and embedment of solid elements into other solid elements.

5.2.1 Case Study 1 - Fukuda Junior High School (Zone B)

5.2.1.1 Geometry and boundary conditions (Zone B)

Figures 5-8 and 5-9, respectively, show the geometry and boundary conditions considered for the problem. Due to the geometrical symmetry of the tunnel section that was excavated in Zone B of the Fukuda Junior High School section of the Maiko Tunnel, only half of the problem was considered. As shown in Figure 5-8, a volume of soil of 200m length (in tunnel direction) by 60m width by 40m depth was modelled. The top 28m represented the Osaka Formation (gravel with clay) and the underlying 12m represented the stiffer Kobe Formation. The tunnel exists in the top layer with its crown at 6m below the ground surface. 96m (12D, where D is the tunnel diameter) of tunnel excavation was modelled in the analysis. 12 sets of Pipe

Umbrella Arches (21 steel pipes with grout interior for each Umbrella Arch), concrete linings (250mm thickness) and concrete tunnel inverts (250mm thickness) and 96 sets of steel arches (H-200 profile) were installed throughout the phased excavation of the tunnel. The tunnel was excavated sequentially in 8m shifts whereby

(1) concrete lining, concrete tunnel invert and 8 sets of steel arches were installed to further support the already excavated section and,

(2) Umbrella Arch is installed to pre-support the next section.

In Figure 5-9, the right (RIGHT) surface represented the symmetrical face with symmetrical constraints (U_1=0, in which U_1 is the displacement in the 1-direction). The left (LEFT) surface was restraint from moving in the 1-direction (U_1=0), and the front (FRONT) and back (BACK) surfaces were restraint from moving in the 3-direction (U_3=0). The bottom (BOTTOM) surface was fixed in all 3 directions to restrict any movement.

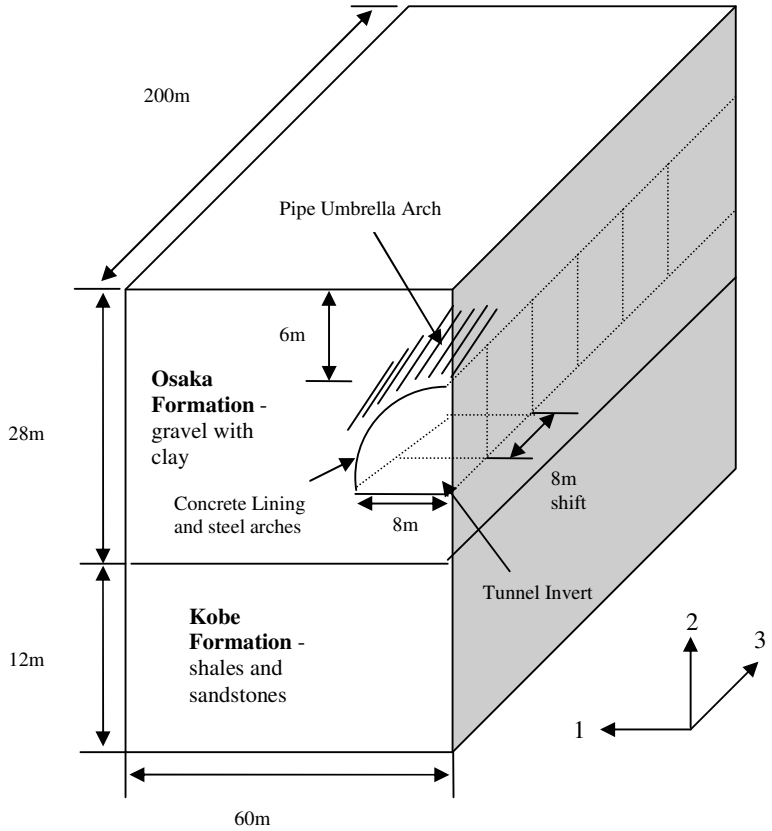

Figure 5-8. 3-D geometry for Zone B.

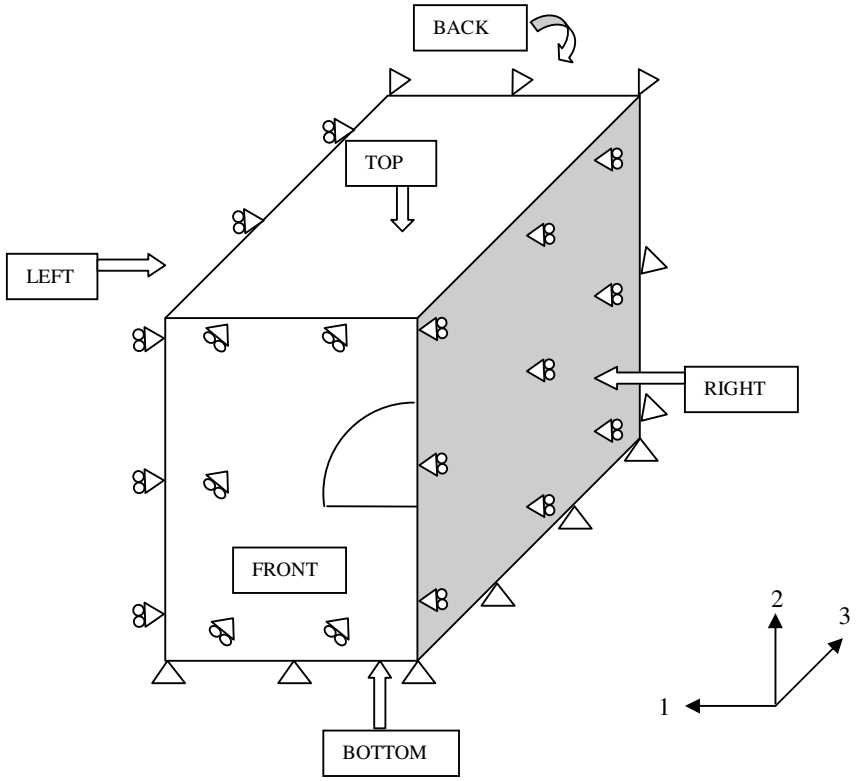

Figure 5-9. Boundary Conditions for 3-D model.

5.2.1.2 3-D Mesh and element types (Zone B)

A. Soil Model

A model of 60m width by 40m depth by 200m length with twelve 8m shifts of tunnel excavations was considered in the analysis (Figure 5-10). A total of 136956 8-node linear stress/displacement brick elements (C3D8) were used to model the soil and reinforcements. Stress/displacement elements had only displacement degrees of freedom. C3D8 elements are three-dimensional solid (continuum) elements in ABAQUS. It should be noted that the simulation of excavation takes place for 96m of the tunnel. As can be seen from Figure 5-10, the first 128m was meshed equally (at 1m intervals) in the longitudinal direction. The last 72m of the model has coarser mesh (at 7.2m intervals) in the longitudinal direction.

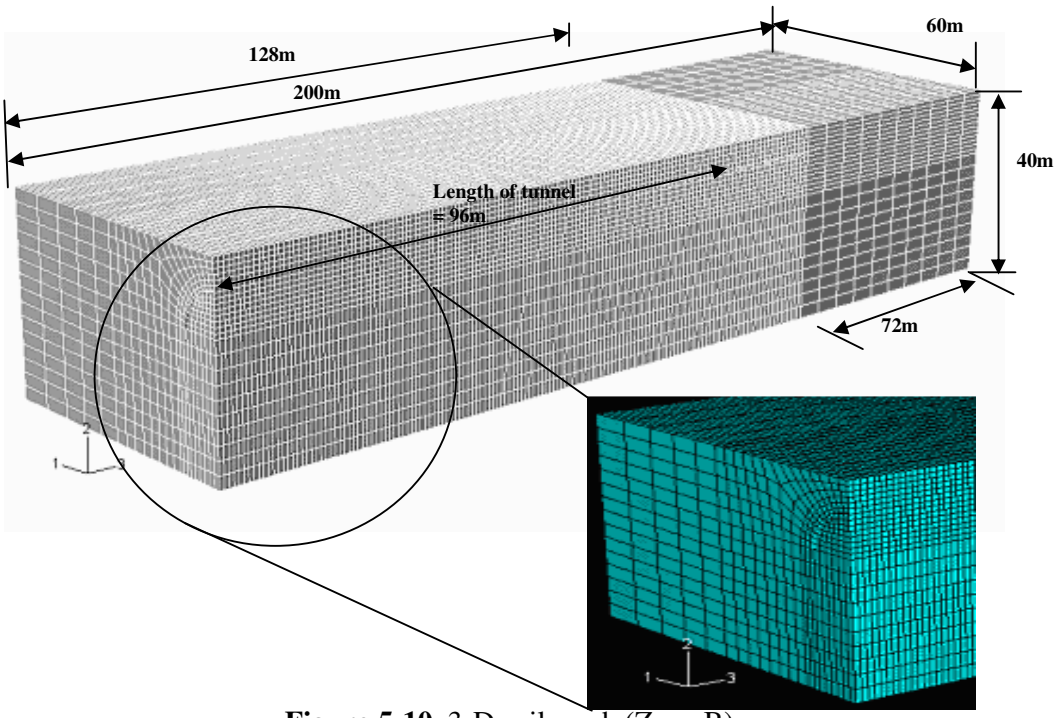

Figure 5-10. 3-D soil mesh (Zone B).

The cross section of the model was meshed in a biased manner whereby the area nearer to the tunnel was finer. The monitoring section for the ground surface displacements in the 3-D model was selected to be at a distance of 3D (i.e. 48m) from the face of the first tunnel shift.

B. Steel pipes and Grout interior

A set of the Pipe Umbrella consists of 21 steel pipes with grout interior was installed at a spacing of 150mm from the tunnel periphery at a span of 70˚ from the vertical. The steel pipes were arranged at an oblique angle of 5˚ to the longitudinal axis. A total of 12 sets of the Pipe Umbrella arches were installed along 96m (i.e. 6D) of the model where tunnel excavation took place. Figure 5-11 shows the arrangement of the Pipe Umbrella. The outside diameter of the pipe was 114mm and the pipe wall thickness was 6mm. The pipes were modelled using 8-node linear stress/displacement brick elements (C3D8). Grout interior of 102mm diameter was also meshed using 8-node linear stress/displacement brick elements (C3D8) as shown in Figure 5-11.

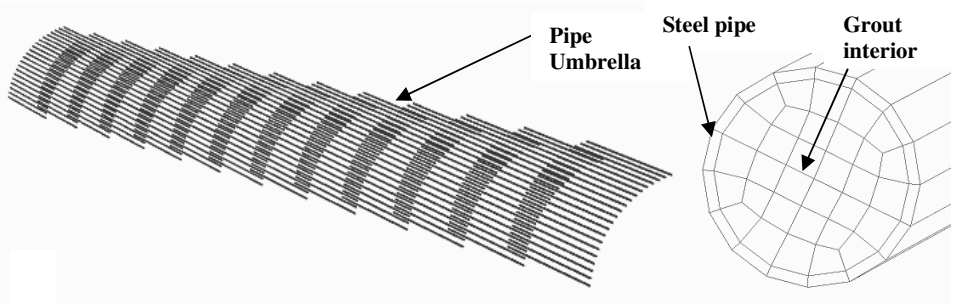

Figure 5-11. 3-D view of the Pipe Umbrella (Zone B).

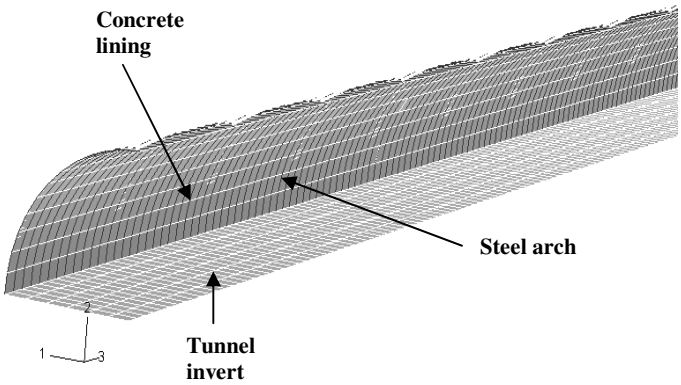

Figure 5-12. 3-D view of the arrangement of linings, inverts and arches (Zone B).

C. Concrete Linings, Tunnel Inverts and Steel Arches

In addition to the Umbrella Arch, primary lining of 250mm thickness were installed, and H-200 steel arches were installed at every 1m interval. A concrete tunnel invert of 250mm was also placed at the foot of the tunnel according to actual construction procedures. 4-node quadrilateral stress/displacement shell elements (S4R) were used to model the linings and inverts. S4R elements were three dimensional shell elements in ABAQUS. A total of 2592 S4R elements were used to model the concrete lining and inverts. 2-node linear open-section beam elements (B31OS) with H-profile were used to model the H-200 steel arches. B31OS elements were open section beams in space in ABAQUS. A total of 1728 B31OS elements were used to model the steel arches. The 2-node linear beam elements (steel arches) were

selected for its compatibility with the 8-node linear brick elements (soil model) whereby the arches had to be integrated.

5.2.1.5 Material Constitutive Model (Zone B)

A. Soil Model

A Mohr-Coulomb elasto-plastic constitutive model with associated flow rule was used for modelling the soil layers. The soil density for the Osaka Formation is 2000kg/m^3 with a Poisson's ratio of 0.49. Kobe formation has a density of 2200kg/m^3 with a Poisson's ratio of 0.4. The Young's modulus and cohesion of the soils are tabulated in Table 5-2 (Muraki, 1997). As the Osaka layer was reported to have a range of deformation modulus of 20 – 60 MPa, several analyses with different values of deformation modulus were performed to cover the range.

B. Steel pipes and Grout interior Models

The steel pipes and grout are assumed to be linearly elastic. The pipes are made of an elastic metal (steel) with a density of 7860kg/m^3, Young's modulus of 200GPa, a Poisson's ratio of 0.4 and a yield stress of 413.7MPa. The grout interior is made of grout with a density of 2500kg/m^3, Young's modulus of 50GPa and a Poisson's ratio of 0.35. The cohesion of the respective soil type is calculated based on the empirical formula (by Terzaghi-Peck) in Design Codes for Foundation and Earth Retaining Structures of Japan Railway (1997). Cohesion (c), in MPa, is equal to the SPT-N value divided by 160 and the calculated median values are used and tabulated in Table 5-2.

Table 5-2. Geotechnical properties of the Fukuda High School section of the Maiko Tunnel (Zone B).

Zone	Layer	Description	Soil type	SPT-N	c (kPa)	E (MPa)
B	**Top**	Osaka formation	Clayey gravel	20-60	250	20-60
	Bottom	Kobe formation	Sandstone, shale	> 70	625	640

C. Concrete Lining and Concrete Tunnel Inverts Models

The lining and inverts are made of an elastic material (concrete) with a density of 2500kg/m^3, Young's modulus of 20GPa and a Poisson's ratio of 0.3.

D. Steel Arches Model

The steel arches are assumed to be linearly elastic. The arches are made of an elastic metal (steel) with a density of 7860kg/m^3, Young's modulus of 200GPa, a Poisson's ratio of 0.4 and a yield stress of 413.7MPa.

5.2.1.6 Initial Conditions and Sequence of Modelling (Zone B)

The numerical analyses were conducted to follow closely the field construction procedures and the excavation and installation of reinforcement were conducted in stages. During construction of the tunnel, the excavation of a single shift consisted of initial installation of a set of umbrella arch prior to any excavation and this was followed by excavating the soil to form the tunnel. Then, concrete lining, steel arches and concrete invert were installed. The procedures used for the numerical modelling follows very closely the actual field construction and are tabulated in Table 5-3. Geostatic state of stress was initially created in the soil model before any installation of reinforcement or excavation. The initial effective stresses were specified using *INITIAL CONDITIONS, TYPE=STRESS, GEOSTATIC option in the first step of analysis. This step included application of gravity loads

corresponding to the weight of the soil materials. K_o is taken to be 1.0. The *GEOSTATIC option is then used to re-establish initial equilibrium so as to ensure that the load and initial stresses generated are in equilibrium before other steps are processed. Subsequently, the first set of umbrella arch was installed. The *MODEL CHANGE, ADD=STRAIN FREE option is used to activate the first set of strain-free Pipe Umbrella to the soil model which is in equilibrium. Then the first shift of 8m of the tunnel was removed and the rest of the stabilisation supports (concrete lining, steel arches and inverts) were activated. These processes are repeated for subsequent shifts. The model was run until steady state is reached as shown in Fig. 5-13.

Table 5-3. 3-D modelling procedure (Zone B).

Step	Stage of construction	Descriptions
1	Geostatic state of stress	Model is subjected to initial stresses
2	Installation of U1	Install pipe umbrella arch 1
3	Excavation of tunnel	Shift 1 (8m) of the tunnel is excavated
4	Installation of LIA1	Install lining(L1), invert(I1) & steel arch(A1) for the 8m excavated tunnel
5	Installation of U2	Install pipe umbrella arch 2
6	Excavation of tunnel	Shift 2 (8m) of the tunnel is excavated
7	Installation of LIA2	Install lining(L2), invert(I2) & steel arch(A2)
8-37		Repeat steps 2-4 until U12, L12, I12 & A12 are installed

5.2.1.7 Results and Discussions (Zone B)

Several analyses were performed by changing the values of the deformation modulus of the Osaka Formation to cover the behaviour of the ground under the reported range of deformation modulus (20 to 60MPa). Figure 5-13 shows the longitudinal surface settlement profile, above the tunnel centreline, generated from 3 analyses of different elastic modulus (20, 40 and 60MPa). Curves EB20, EB40 and EB60 are the longitudinal settlement profiles generated for excavation in Zone B with modulus of deformation for the Osaka layer of E = 20MPa, 40MPa and

60MPa respectively. For comparison, the field measurements for the longitudinal settlement profile due to excavation in Zone B are also shown in Figure 5-7 and represented by Curve FB.

From the results shown in Figure 5-13, it can be seen that the longitudinal ground surface settlement profile for E = 60MPa (i.e. Curve EB60) agrees with the longitudinal settlement profile measured in the field (FB). A final vertical settlement of about 21mm (where steady state is reached) is obtained from the numerical model whilst the field measurement was about 22mm. The pre-excavation settlement profile has a smooth decrement from 0 to 7mm which correlates well with the measured settlement of 6mm. Therefore it is concluded that the soil parameters of analysis EB60 (E=60MPa, c_u= 250kPa (from Table 5-2) and E/c_u = 240) can be used to represent the behaviour of the soil in this section of the tunnel (Zone B) and they are used for subsequent analyses described in the following sections.

The 3D vertical ground surface displacement (vertical ground surface displacement at the tunnel face (d_{fp})) is approximately 40% of the final ground surface settlement away from the tunnel face (d_f) for EB20. This percentage is 25% for EB60.

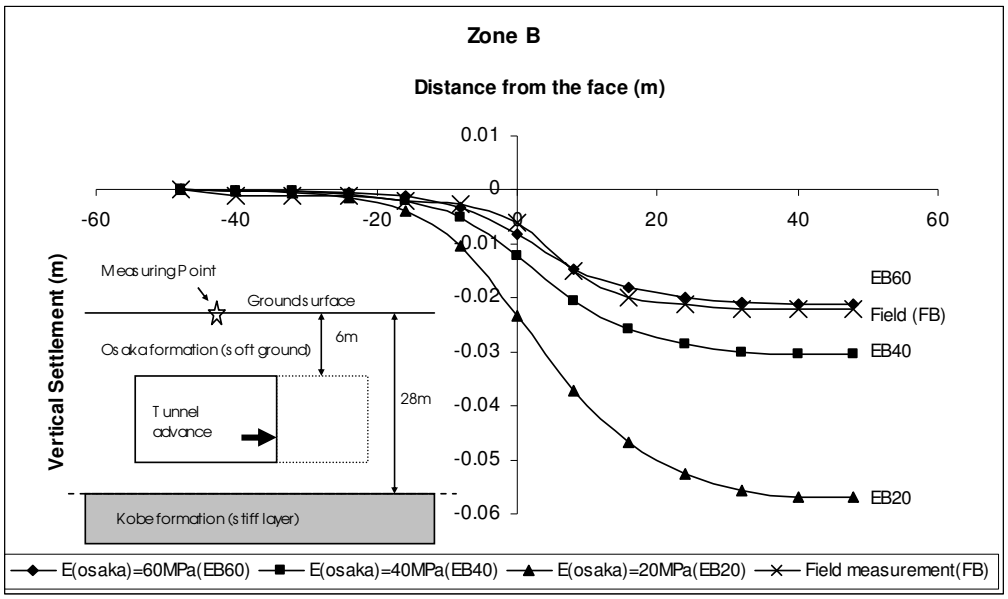

Figure 5-13. Longitudinal ground surface settlement profiles for different modulus of deformation (Zone B).

5.2.1.8 Effect of various tunnel supports on the tunnel excavation at Zone B

Upon successful calibration of the model that represents the actual effect of the installation of the Pipe Umbrella Arch, the reinforcing effect of the various structural elements used in supporting the tunnel is studied. The objective is to identify and distinguish the contribution of each structural support element in providing stability to the tunnel during excavation. In this study, structural elements are used individually and in combinations in six analyses. An analysis for excavation of the ground for the unlined case is also performed. Figure 5-14 shows the longitudinal settlement profiles for the analyses of different combinations of structural support elements. As seen in Figure 5-14, a decrease of approximately 40% in soil settlement is achieved when only the Pipe Umbrella is installed (Curve P) as compared to the case of unsupported tunnel (Curve NR). The results also shows that the Umbrella Arch controlled soil settlement more efficiently than when only lining (Curve L) or steel arch beams (Curve A) were installed. Thus it can be established that the pipe umbrella arch can provide significant control of soil movement during tunnel excavations and it is the most efficient structural support system during excavation as compared to the installation of concrete lining and steel arches after excavation. The steel arches (Curve A) provide the least stabilisation as compared to the concrete lining (Curve L) and Umbrella Arch (Curve P). Installation of the arches only provided a slight improvement to the final settlement and hence, it could be omitted from the design.

The percentage [(d_{fp} / d_f) x 100%] of the 3D vertical ground surface displacement (vertical ground surface displacement at the tunnel face (d_{fp})) is 40% of the final ground surface settlement away from the tunnel face (d_f) for the case of LP (lining and pipes), LA (lining and arches) and L (lining only). This percentage is 35% for the cases of P (pipes only) and A (arches only). This means that when only Pipe Umbrella Arch are installed, the ground surface at the tunnel face displaces

vertically by 35% of the expected final ground surface settlement when the tunnel first passes the measuring point.

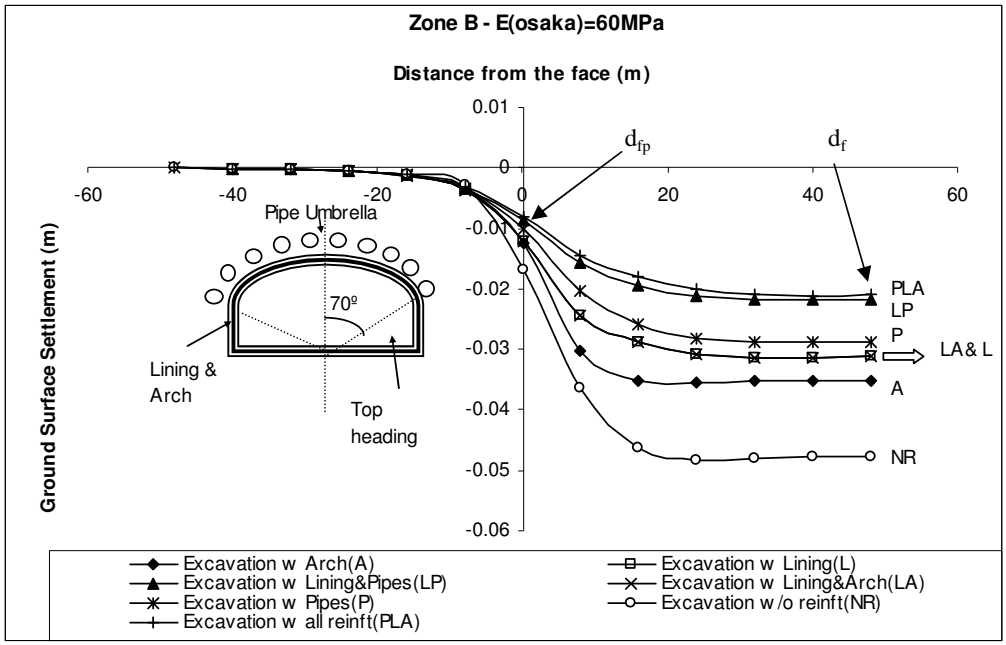

Figure 5-14. Longitudinal ground surface settlement profiles for different combinations of structural support element installed (Zone B).

Generally, it was found that the Pipe Umbrella Arch, when used individually without any other complementary support, contributed significantly to the overall stability of the tunnel during excavation. This could be attributed to its installation prior to excavation as well as its high structural stiffness which provided a reinforced arch that reduces the caving of the surrounding soil. The overlapping of the pipes could also have contributed significantly in stabilising the longitudinal movement of the soil into the tunnel face. Nevertheless, the structural supports studied complemented one another and heterogeneity of field conditions might support their usage although numerical results showed small effect of the steel arch.

5.2.2 Case Study 2 - Fukuda Junior High School (Zone A)

5.2.2.1 Geometry and boundary conditions (Zone A)

Figures 5-15 and 5-16, respectively, show the geometry and boundary conditions considered for the problem. Due to the geometrical symmetry of the tunnel section that was excavated in Zone A of the Fukuda Junior High School section of the Maiko Tunnel, only half of the problem was considered. As shown in Figure 5-15, a volume of soil of 200m length (in tunnel direction) by 60m width by 40m depth was modelled. The top 28m represented the alluvial fills (gravel with clay) and the underlying 12m represented the stiffer Kobe Formation. The tunnel existed in the top layer with its crown at 6m below the ground surface. The tunnel excavation was modelled similarly to the case of Zone. 12 sets of Pipe Umbrella Arches (21 steel pipes with grout interior for each Umbrella arch), concrete linings (250mm thickness) and concrete tunnel inverts (250mm thickness) and 96 sets of steel arches (H-200 profile) were installed throughout the phased excavation of the tunnel. The tunnel was excavated sequentially in 8m shifts whereby

(1) concrete lining, concrete tunnel invert and 8 sets of steel arches were installed to further support the already excavated section and,
(2) Umbrella Arch is installed to pre-support the next section.

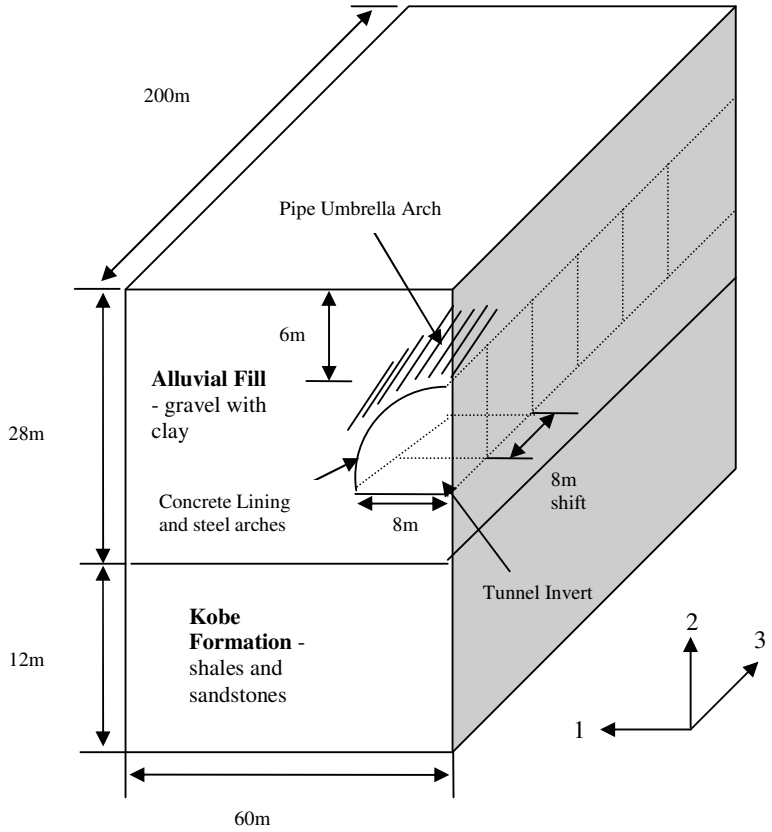

Figure 5-15. 3-D soil model (Zone A).

In Figure 5-16, the right (RIGHT) surface represented the symmetrical face with symmetrical constraints (U_1=0, in which U_1 is the displacement in the 1-direction). The left (LEFT) surface was restraint from moving in the 1-direction (U_1=0), and the front (FRONT) and back (BACK) surfaces are restraint from moving in the 3-direction (U_3=0). The bottom (BOTTOM) surface is fixed in all 3 directions to restrict any movement.

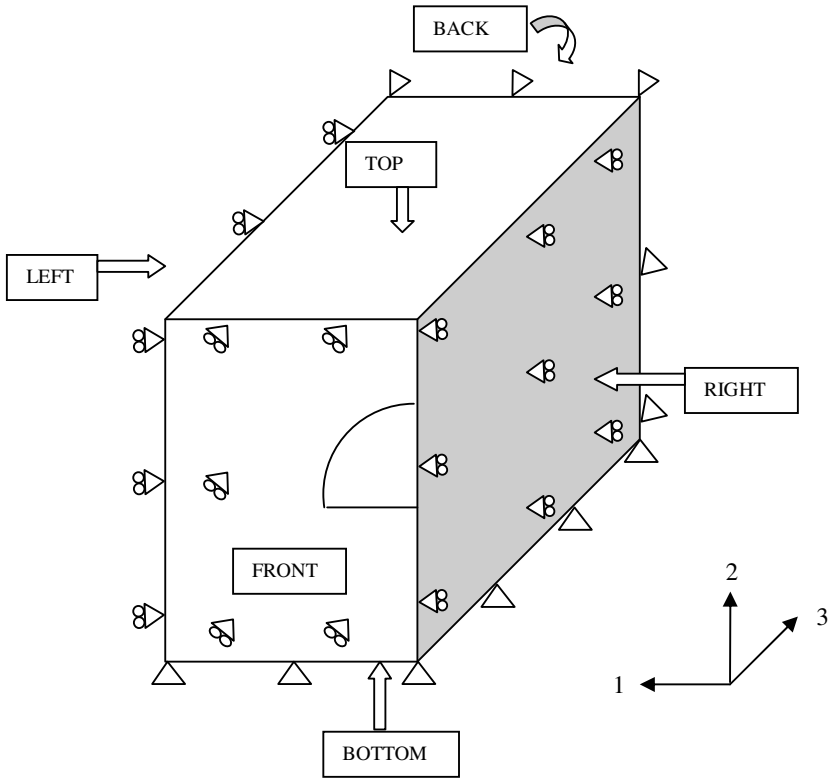

Figure 5-16. Boundary Conditions for 3-D model.

5.2.2.2 3-D Mesh and element types (Zone A)

A. Soil Model

A model of 60m width by 40m depth by 200m length with twelve 8m shifts of tunnel excavations was considered in the analysis (Figure 5-10). A total of 136956 8-node linear stress/displacement brick elements (C3D8) were used to model the soil and reinforcements. Stress/displacement elements had only displacement degrees of freedom. C3D8 elements were three-dimensional solid (continuum) elements in ABAQUS. It should be noted that the simulation of excavation takes place for 96m of the tunnel. As can be seen from Figure 5-10, the first 128m was meshed equally (at 1m intervals) in the longitudinal direction. The last 72m of the model has coarser mesh (at 7.2m intervals) in the longitudinal direction. The cross section of the model was meshed in a biased manner whereby the area nearer to the tunnel was finer.

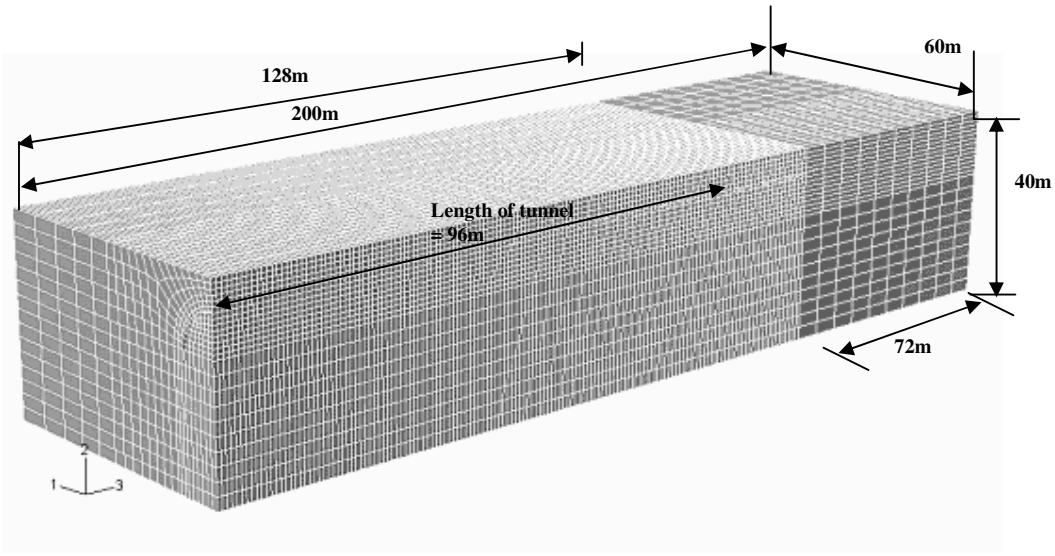

Figure 5-17. 3-D soil model (Zone A).

The meshes generated are very similar to that generated for Zone B. This is because Zone A and Zone B of the Fukuda High School site of the Maiko Tunnel are excavated using the same phases and reinforcing supports but in different ground conditions.

B. Steel pipes and grout interior

A set of the Pipe Umbrella consists of 21 steel pipes with grout interior installed at a spacing of 150mm from the tunnel periphery at a span of 70˚ from the vertical. The steel pipes were arranged at an oblique angle of 5˚ to the longitudinal axis. A total of 12 sets of the Pipe Umbrella arches were installed along 96m tunnel section (i.e. 6D) of the total 200m length of the model. The pipes were modelled using 8-node linear stress/displacement brick elements (C3D8). Grout interior of 102mm diameter was also meshed using 8-node linear stress/displacement brick elements (C3D8). A uniform cross section of a pipe with grout interior is shown in Figure 5-18.

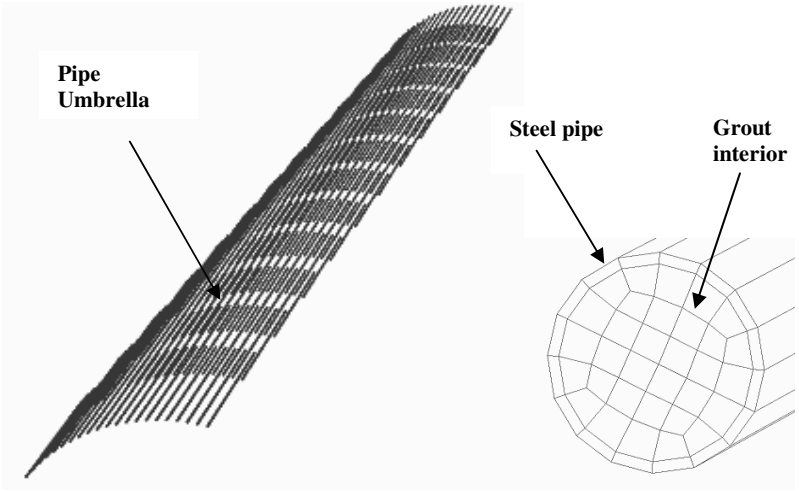

Figure 5-18. 3-D view of the arrangement of the Pipe Umbrella (Zone A)

C. Concrete Lining, Concrete Tunnel Inverts and Steel Arches

In addition to the umbrella arch, primary lining of 250mm thickness were installed, and H-200 steel arches were installed at every 1m interval as shown in Figure 5-19. A concrete tunnel invert of 250mm was also placed at the foot of the tunnel according to actual construction procedures. 4-node quadrilateral stress/displacement shell elements (S4R) were used to model the lining and invert while the steel arches were modelled using tri-node linear beam elements. A total of 2592 S4R elements were used to model the concrete lining and inverts.

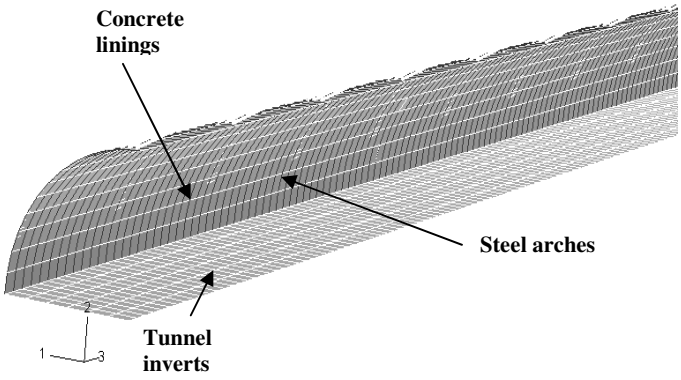

Figure 5-19. 3-D view of the arrangement of linings, inverts and arches (Zone A).

2-node linear open-section beam elements (B31OS) with H-profile were used to model the H-200 steel arches. A total of 1728 B31OS elements were used to model the steel arches.

5.2.2.3 Material Constitutive Model (Zone A)

A. Soil Model

A Mohr-Coulomb elasto-plastic constitutive model with associated flow rule was used for modelling the soil layers. Zone A of the Maiko Tunnel consisted mainly of alluvial fills and small stretches of gravely clay. The soft ground is also underlain by a stiffer layer of the Kobe formation, which has similar properties as that used for Zone B. The soil density for alluvial fill is 2000kg/m^3 with a Poisson's ratio of 0.49. Kobe formation has a density of 2200kg/m^3 with a Poisson's ratio of 0.4. The geotechnical properties of Zone A are as shown in Table 5-4 (Muraki, 1997). The cohesion of the respective soil type is calculated based on the empirical formula (by Terzaghi-Peck) in Design Codes for Foundation and Earth Retaining Structures of Japan Railway (1997). Cohesion (c), in MPa, is equal to the SPT-N value divided by 160 and the calculated median values are used and tabulated in Table 5-4.

B. Steel pipes and grout interior Models

The steel pipes and grout are assumed to be linearly elastic. The pipes are made of an elastic metal (steel) with a density of 7860kg/m^3, Young's modulus of 200GPa, a Poisson's ratio of 0.4 and a yield stress of 413.7MPa. The grout interior is made of grout with a density of 2500kg/m^3, Young's modulus of 50GPa and a Poisson's ratio of 0.35.

Table 5-4. Geotechnical properties of the Fukuda High School section of the Maiko Tunnel (Zone A).

Zone	Layer	Description	Soil type	SPT-N	c (kPa)	E (MPa)
A	**Top**	Alluvial fill	Gravel with clay	5-40	125	0.5-30
	Bottom	Kobe formation	Sandstone, shale	> 70	625	640

C. Concrete Lining and Concrete Tunnel Inverts Models

The lining and inverts are made of an elastic material (concrete) with a density of 2500kg/m^3, Young's modulus of 20GPa and a Poisson's ratio of 0.35.

D. Steel Arches Model

The steel arches are assumed to be linearly elastic. The arches are made of an elastic metal (steel) with a density of 7860kg/m^3, Young's modulus of 200GPa, a Poisson's ratio of 0.4 and a yield stress of 413.7MPa.

5.2.2.4 Initial Conditions and Sequence of Modelling (Zone A)

The numerical analyses were conducted to follow closely the field construction procedures and the excavation and installation of reinforcement were done in stages. The excavation of a single shift consisted of initial installation of a set of Pipe Umbrella Arch prior to any excavation and followed by the removal of the tunnel and installation of the concrete lining, steel arches and concrete invert.

The procedures used for the numerical modelling follows very closely the actual field construction and are tabulated in Table 5-5. The staged constructions were sequentially modelled and similar to that as described in details for Zone B and hence will not be further elaborated.

Table 5-5. 3-D modelling procedure (Zone A).

Step	Stage of construction	Descriptions
1	Geostatic state of stress	Model is subjected to initial stresses
2	Installation of U1	Install pipe umbrella arch 1
3	Excavation of tunnel	Shift 1 (8m) of the tunnel is excavated
4	Installation of LIA1	Install lining(L1), invert(I1) & steel arch(A1) for the 8m excavated tunnel
5	Installation of U2	Install pipe umbrella arch 2
6	Excavation of tunnel	Shift 2 (8m) of the tunnel is excavated
7	Installation of LIA2	Install lining(L2), invert(I2) & steel arch(A2)
8-37		Repeat steps 2-4 until U12, L12, I12 & A12 are installed

5.2.2.5 Results and Discussions (Zone A)

Several analyses were performed by changing the values of the deformation modulus of the alluvial fill to cover the behaviour of the ground under the reported range of deformation modulus (0.5 to 30MPa). Figure 5-20 shows the longitudinal settlement profile, along the tunnel centreline, generated from 4 analyses of different elastic modulus (4, 10, 20 and 40MPa). Curve EA4, EA10, EA20 and EA40 are the longitudinal settlement profiles generated for excavation in Zone A with modulus of deformation for the alluvial fill layer of E = 4MPa, 10MPa, 20MPa and 40MPa respectively. By using a plot of the elastic modulus and maximum ground surface settlements generated for various E values (Figure 5-21), it was shown that the softer alluvial layer can be represented by the soil parameters of modulus of deformation of approximately 15MPa and cohesion of 125kPa. Thus, an E/c_u ratio of 120 was established for this weaker zone of soil. These soil parameters (E=15MPa, c_u=125kPa and E/c_u=120) are used for subsequent analyses in the following sections. The longitudinal ground surface settlement profile for E=15MPa agreed with the measured field longitudinal settlement profile as shown in Figure 5-20.

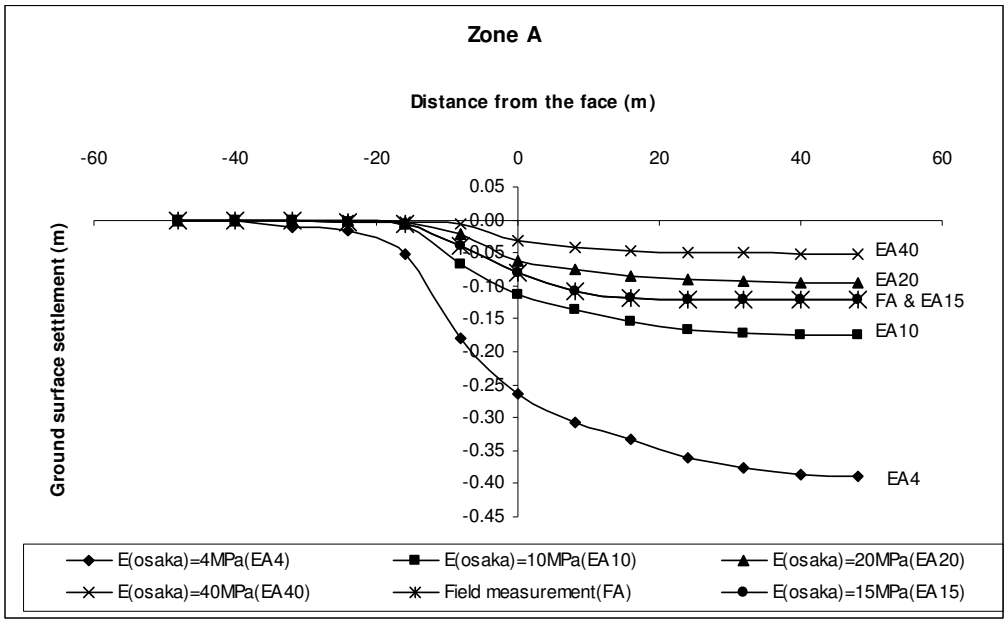

Figure 5-20. Longitudinal ground surface settlement profiles for different modulus of deformation (Zone A).

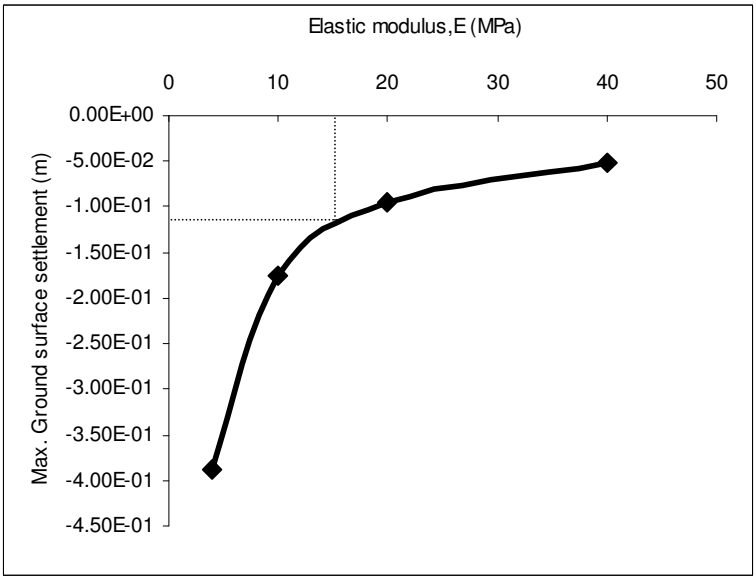

Figure 5-21. Elastic modulus versus maximum vertical ground surface settlement (Zone A).

CHAPTER 6 – PARAMETRIC STUDIES ON THE PIPE UMBRELLA ARCH

Upon successful calibration of the two models for the Pipe Umbrella Arch presented in Chapter 5, parametric studies are conducted to investigate the effect of pipe numbers, pipe diameter and lap lengths (i.e. overlapping pipe length) on the reinforcing capability of the Umbrella Arch. In order to fully establish and understand the reinforcing effect of the pipe umbrella arch, other structural elements such as the concrete lining and steel arches are omitted from the parametric studies. A clear understanding of the stabilising mechanism of the pipe umbrella arch will help to improve the cost and design efficiency for this pre-reinforcement.

Table 6-1 shows the parameters and values used in the parametric study. The number of pipes chosen for the analysis is 6, 14, 28, 42, 56 and 70. The pipe diameters are varied at 30mm, 70mm, 100mm, 114mm, 128mm and 142mm. Lap lengths of 0m, 2m, 4m, and 6m are also studied. These variations are applied to the 2 calibrated models of Zone B and Zone A.

Table 6-1. Parameters and values used in the parametric study.

Parameters	**Values**					
Number of pipes	6	14	28	42	56	70
Diameter of pipes (mm)	30	70	100	114	128	142
Lap length (m)	0	2	4	6		

6.1 Variation of number of pipes

The number of pipes used in the Pipe Umbrella Arch was studied to understand the extent of influence of this parameter in the overall reinforcing effect of the Umbrella Arch. It should be commonly understood that the greater the number of pipes used, the more the reinforcing effect of the Umbrella Arch. However, by consideration of cost effectiveness and design efficiency, an optimum number is desired. Optimisation in this context is defined as achieving both economic efficiency and attaining a state of consistent differential ground surface settlement of less than 5mm. In this study, the pipe numbers are varied and their pipe spacings are adjusted accordingly for all analyses. The longitudinal settlement profiles generated for various numbers of pipes in the Pipe Umbrella Arch for excavation in Zone B are as shown in Figure 6-1. The number of pipes used in the field is 42.

In order to have a clearer view of the effect of the pipe numbers on the vertical settlement, a plot of pipe number versus maximum vertical ground surface settlement is generated and shown in Figure 6-2. As observed from Figures 6-1 and 6-2, the optimum pipe number is approximately between 40 and 50 and this optimum range coincides with the number of pipes used in the field (42 pipes).

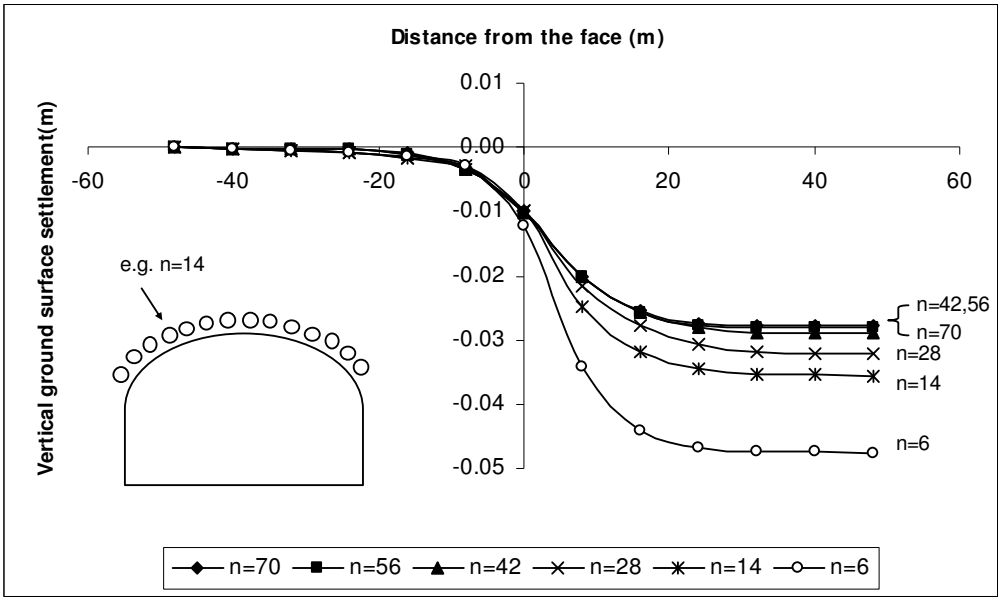

Figure 6-1. Longitudinal ground surface settlement profiles for varying number of pipes (Zone B).

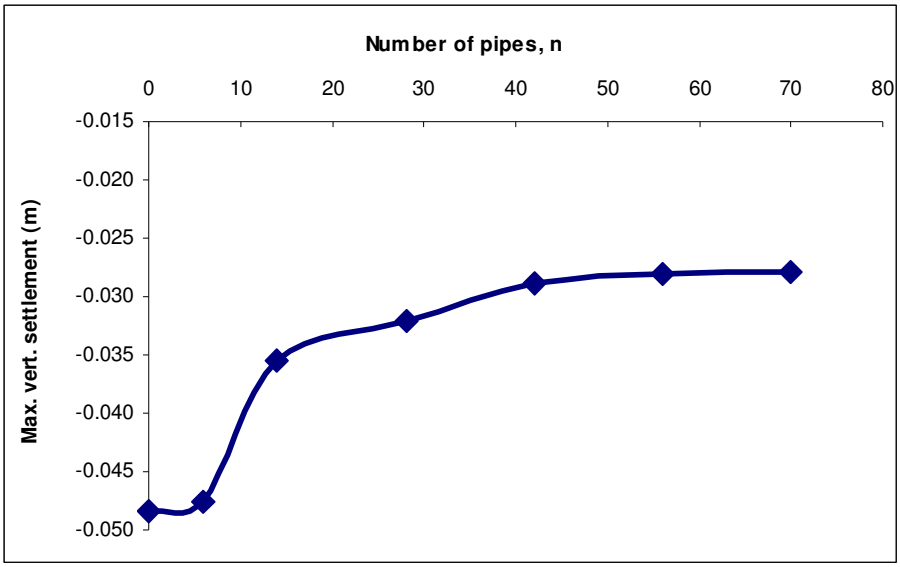

Figure 6-2. Pipe numbers versus maximum vertical ground surface settlement (Zone B).

It can also be noted that between n=6 and n=14, there is a sudden dip in the maximum vertical ground surface settlement. Installation of n=14 pipes will create a 27% improvement in the vertical ground surface settlement as compared to the optimum installation of n=42, which provides a 40% improvement. The difference in improvement of vertical ground surface settlement between 14 and 42 pipes is about 10%. In addition, it was observed from Figure 6-1 that the 3D vertical ground surface displacement (vertical ground surface displacement at the tunnel face (d_{fp})) is within the range of 33% of the final ground surface settlement away from the tunnel face (d_f) for n=42 and greater. For n=14 and n=28, the percentage of (d_{fp}/d_f) is approximately 30% and for n=6, it is 24%.

Figure 6-3 shows the longitudinal settlement profiles for various numbers of pipes installations in Zone A model. From Figure 6-3, it can be shown that from n=28 to n=70, the vertical settlement profiles differs only minimally. Thus it can be concluded that an optimum number of pipes lies within this range. In order to have a clearer comparison of the number of pipes and their respective vertical settlements,

a plot of the pipe numbers versus maximum vertical ground surface settlement is presented in Figure 6-4. From this plot, it is clearly shown that the optimum number of pipes that can be used in reinforcing the tunnel in Zone A is about 42 (approximately 38% improvement). It should also be noted that a sudden dip in vertical ground surface settlement is experienced between n=14 and n=6. For n=14, there is a significant 34% improvement of the vertical ground surface settlement as compared to only 3% for n=6.

In addition, it was observed that the 3D vertical ground surface displacement (vertical ground surface displacement at the tunnel face) is 29% of the final ground surface settlement away from the tunnel face for n=42 and greater. For n=14 and n=28, the percentage is approximately 28%. For n =6, the percentage is 26%.

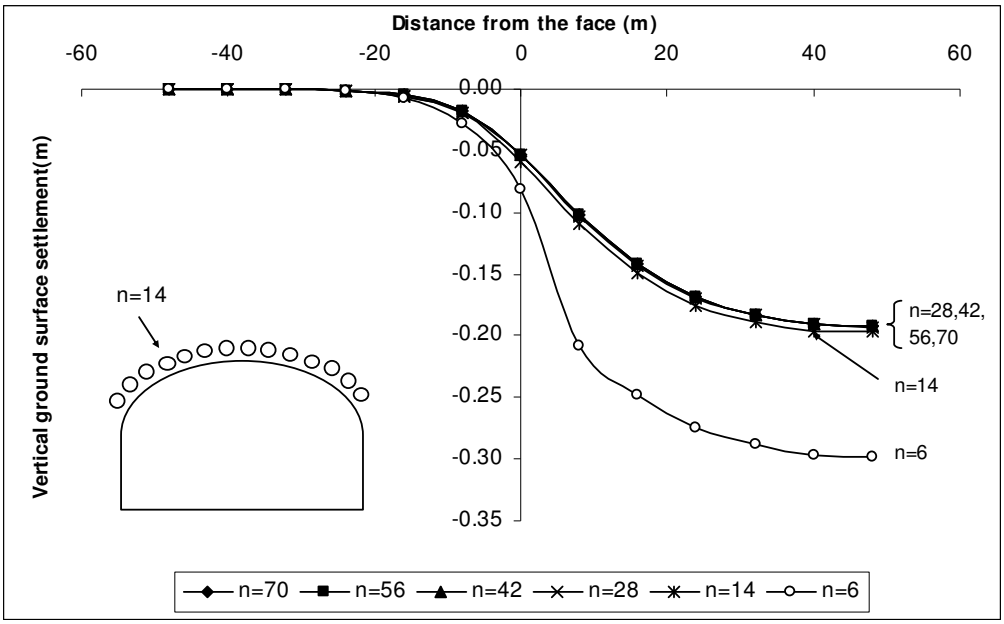

Figure 6-3. Longitudinal ground surface settlement profiles for varying number of pipes (Zone A).

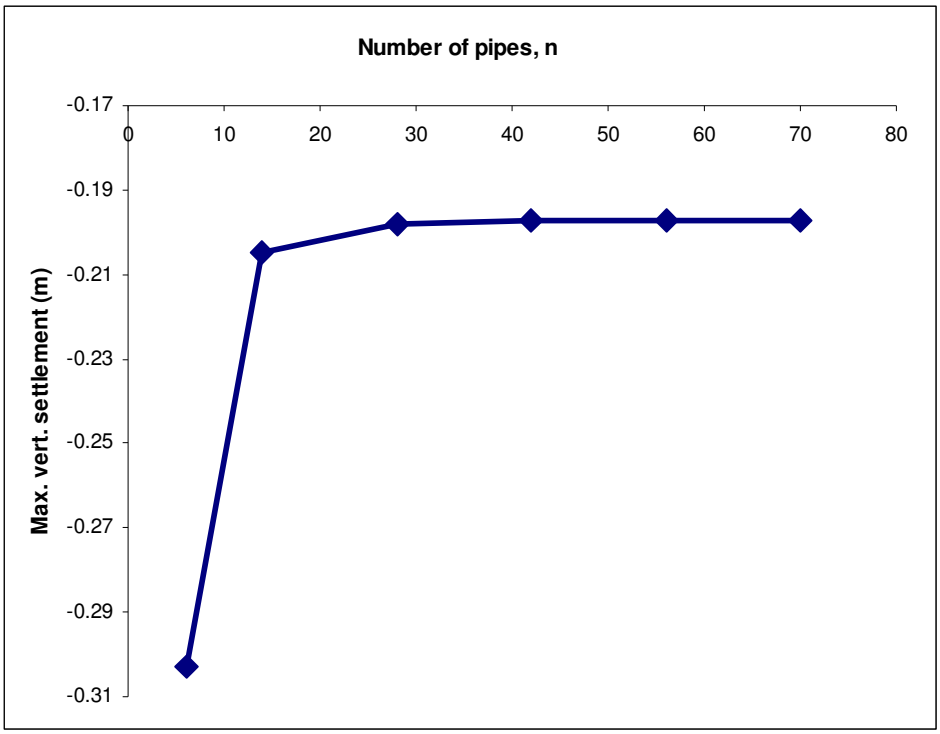

Figure 6-4. Pipe numbers versus maximum vertical ground surface settlement (Zone A).

6.2 Variation of pipe diameter

The pipe diameter was varied to study the effect of different pipe sizes on the overall reinforcing effect of the Pipe Umbrella Arch. In this study, the pipe diameter was varied with pipe thickness kept constant at 6mm. With an increase in pipe diameter, it should be noted that the diameter of the grout interior is also increased. The generated longitudinal settlement profiles for various pipe diameters are presented in Figure 6-5 and Figure 6-7 for Zone B and Zone A respectively. Figures 6-6 and 6-8 show the plot of pipe diameters versus maximum vertical ground surface settlement for Zone B and A respectively.

From Figure 6-6, it can be seen that the optimum pipe diameter is approximately between 100 to 120 mm for Zone B. Thus the selected field design of 114mm is considered to be an optimum design. There is no significant improvement obtained for the vertical ground surface settlement when pipe diameters above 114mm are installed as shown in Figure 6-7. When steel pipes of outer diameter of 114mm are

installed, it provided about 40% decrease in the vertical ground surface settlement for Zone B.

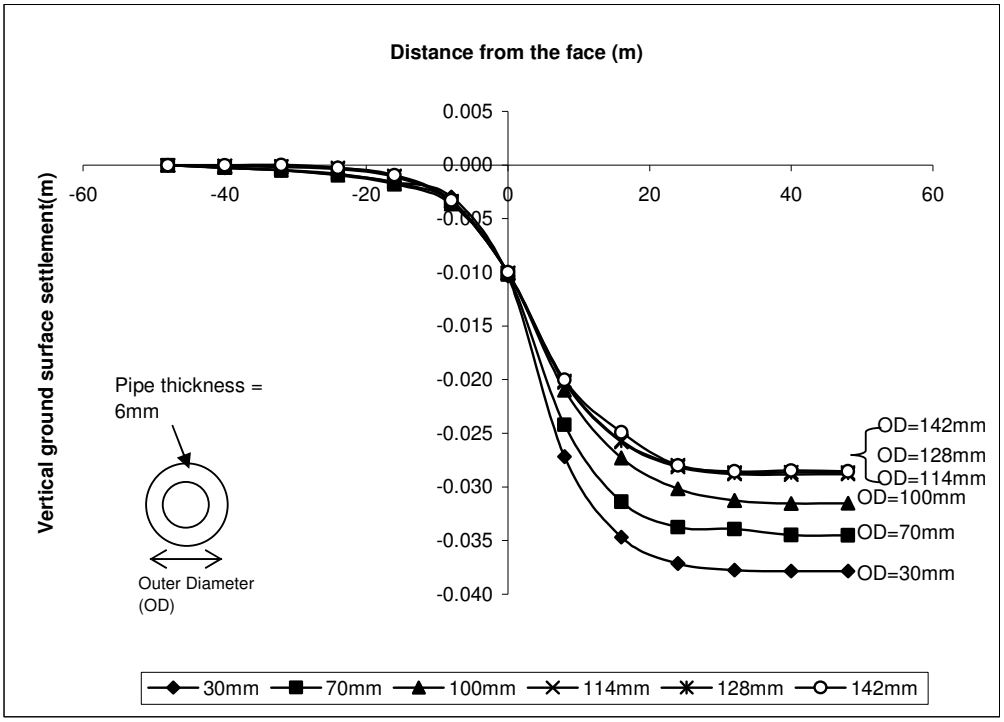

Figure 6-5. Longitudinal ground surface settlement profiles for varying pipe diameters (Zone B)

In addition, it was observed that 3D vertical ground surface displacement (vertical ground surface displacement at the tunnel face(d_{fp})) is 37% of the final ground surface settlement away from the tunnel face (d_f) for OD=114mm and greater, for Zone B. For OD=100mm and OD=70mm, the (d_{fp}/ d_f) is approximately 33% and 29% respectively. This percentage is 27% for OD=30mm.

From Figure 6-6, it can be observed that for Zone B, pipe diameters larger than 114mm do not affect the final maximum vertical settlement. The optimum pipe size is about 114mm.

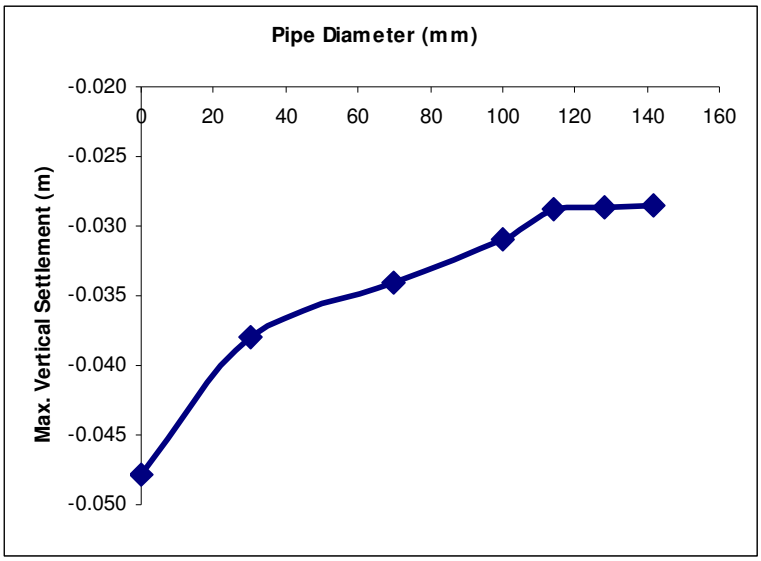

Figure 6-6. Pipe diameter versus maximum vertical ground surface settlement (Zone B).

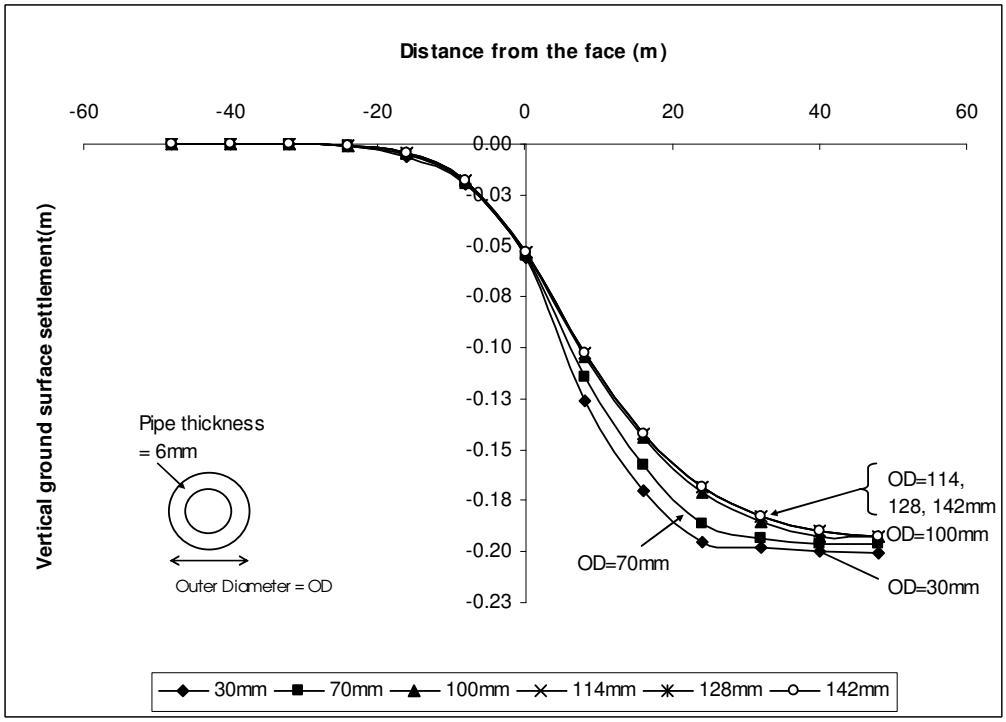

Figure 6-7. Longitudinal ground surface settlement profiles for varying pipe diameters (Zone A)

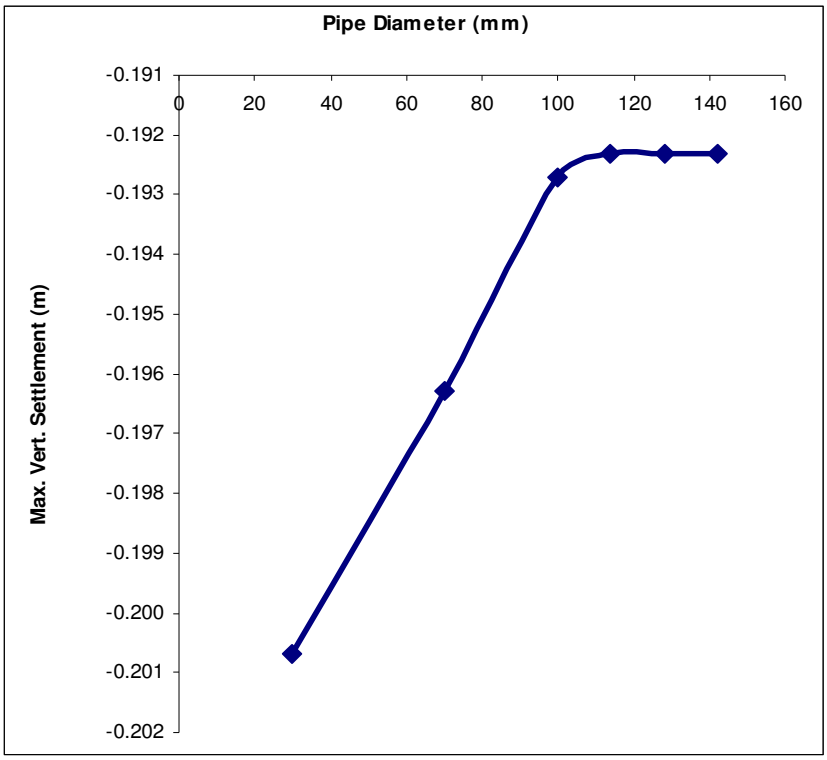

Figure 6-8. Pipe diameter versus maximum vertical ground surface settlement (Zone A).

From Figure 6-8, it can be seen that the optimum pipe diameter for Zone A is about 114mm, which is also similar to the field design for Zone A. Pipe diameters larger than 114mm do not affect the final maximum vertical settlement.

The optimum design (pipe diameter=114mm) provides about 38% improvement in controlling the vertical soil settlement for Zone A. From the study of pipe diameters, it is observed that this parameter do not affect the overall settlement results as much as varying the number of pipes. The ground surface displacement decreases as the pipe diameter increases for Zone A. The rate of decrease in ground surface displacement decreases as the pipe diameter increases. The percentage of (d_{fp}/d_f) is 27% for OD=114mm or greater. For OD=100mm, the percentage of (d_{fp}/d_f) is 26.5%. In addition, it was observed that the percentage of (d_{fp}/d_f) is 26% for OD=70mm and greater and 25% for OD=30mm.

6.3 Variation of lap length (Overlapping pipe length)

The overlapping length of the pipes is considered to have a significant effect on the overall soil movement during tunnel excavation. This is because the overlapped region has 2 layers of reinforcement as compared to other parts which has only one. Thus, the 2 layers of reinforcement should provide greater interlocking effect and provide greater face stability. For this analysis, the number of pipes and their diameter are kept constant at 42 and 114mm respectively. Figure 6-9 shows the longitudinal ground surface settlement profiles generated for various lap lengths for Zone B and Figure 6-10 shows the plot of the lap lengths versus their respective maximum vertical settlement for Zone B.

From Figures 6-9 and 6-10, it can be observed that the optimum lap length is about 4m which is similar to that used in the field during construction for Zone B. It can also be seen that any increment of the lap length beyond this point will have negligible effect on the overall vertical ground surface settlement. The optimum value of lap length (4m) provides about 40% improvement in vertical ground surface settlement as compared to only 20% improvement when the lap length is zero.

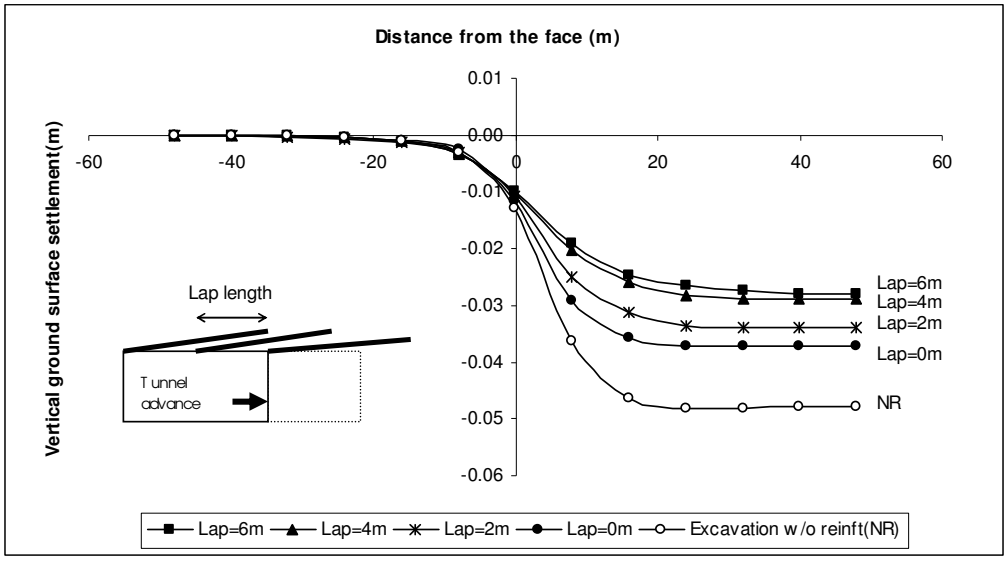

Figure 6-9. Longitudinal ground surface settlement profiles of varying lap lengths (Zone B).

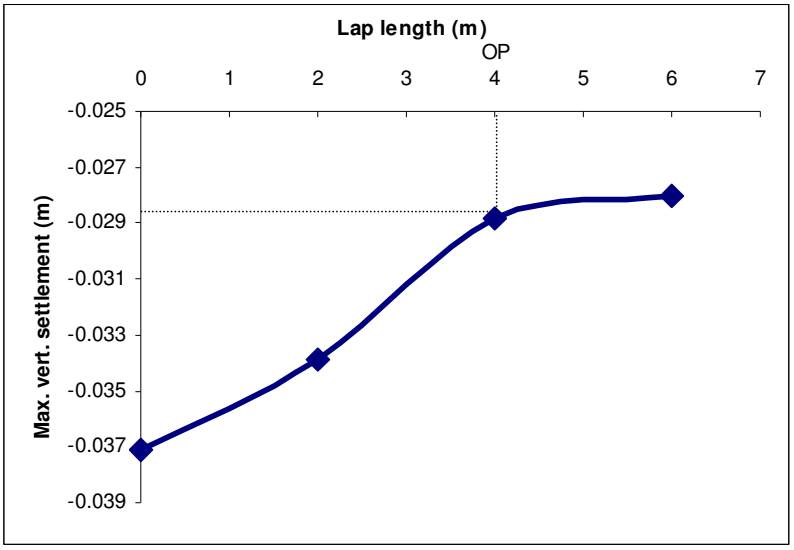

Figure 6-10. Lap length versus maximum vertical ground surface settlement (Zone B).

In addition, it can be observed that the percentage of (d_{fp}/d_f) is 36% for lap length=4m or greater and 33% for lap length=2m for Zone B. For lap length=0m, the percentage (d_{fp}/d_f) is 29%.

It can be concluded that the lap length plays an important part in controlling the overall vertical ground surface settlement during tunnel excavation for Zone B.

Figure 6-11 shows the longitudinal settlement profiles for varying lap lengths in Zone A of the Maiko Tunnel. The variation of lap length versus maximum vertical ground surface settlement is shown in Figure 6-12 and it can be seen from Figure 6-12 that the optimum lap length in this case is 4m for Zone A. This value is also similar to that used in the field during construction.

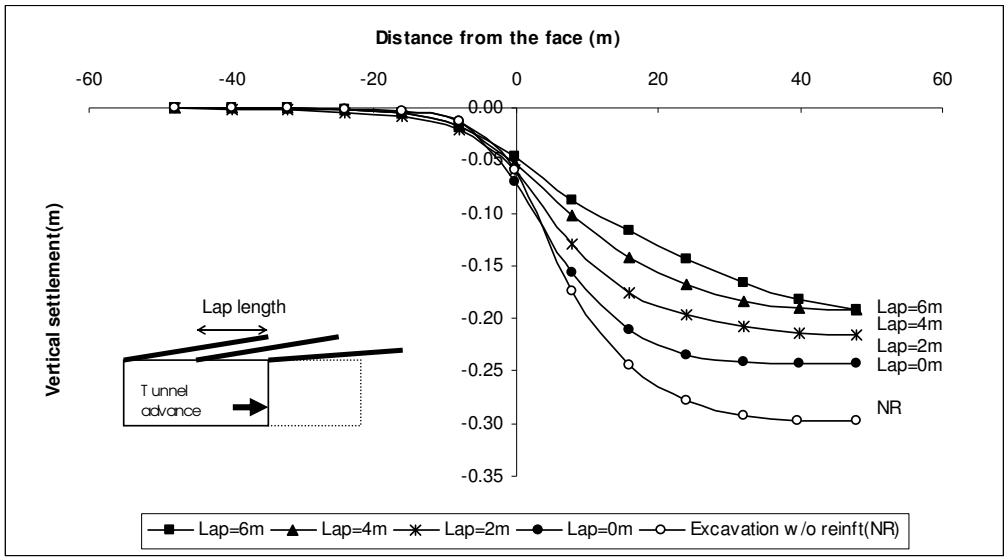

Figure 6-11. Longitudinal ground surface settlement profiles of varying lap lengths (Zone A).

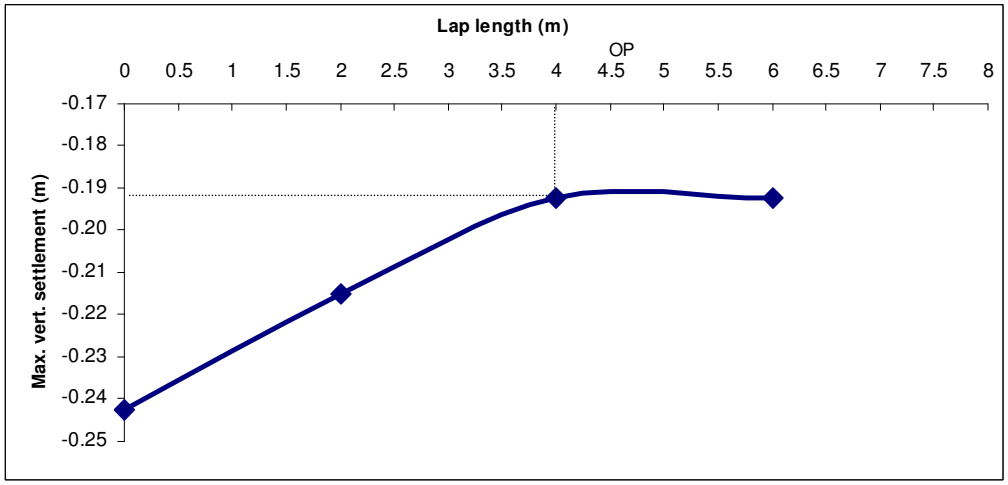

Figure 6-12. Lap length versus maximum vertical ground surface settlement (Zone A).

The optimum value of the lap length (4m) provided a decrease of 38% for the vertical ground surface settlement as compared to 18% decrease when the lap length is zero. In addition, it was observed that the percentage of (d_{fp}/d_f) is 29% for lap length=4m or greater. For lap length=2m and lap length=0m, the percentage is approximately 27.5% and 25% respectively. This result further reinforced the fact

that the lap length of the pipes is a significant factor to be considered during reinforcement design for the Pipe Umbrella Arch.

For Zone A, the Pipe Umbrella Arch produced 38% less ground surface settlement for lap length of 4m (i.e. according to actual field construction) than when the tunnel was unsupported at all.

CHAPTER 7 – COMPARISON OF 2D & 3D NUMERICAL ANALYSIS FOR 2 CASE STUDIES

Although 3-D numerical analyses can produce accurate results in the prediction of settlement profiles, sophisticated commercial software are required for modelling the Pipe Umbrella Arch. Most simulations of the Pipe Umbrella Arch are conducted by considering the arch as a generalised reinforced strip with an equivalent strength. To date, simulations of the steel pipes and grout interior of the Pipe Umbrella Arch as separate components have not been studied. In view of the cost of sophisticated software such as ABAQUS, the long tedious process of producing each individual structural elements and the long running time of the program, a simpler 2-D numerical method is more appealing to tunnel designers. The objective of the study performed in this chapter is to investigate the reliability of analysing the Pipe Umbrella Arch problem using a 2-D analysis instead of the tedious 3-D analysis.

Two 3-D models of the Pipe Umbrella Arch are calibrated using two actual case studies in Chapter 5. 2-D numerical analyses of 3 approximations for the Pipe Umbrella Arch are also conducted for the same case studies to compare the maximum vertical ground surface settlement results to the three dimensional results obtained. By comparing and analysing the difference between the results generated from two and three dimensional models, the ability of the different 2-D models to produce results in agreement with those obtained from the 3-D models is explored.

7.1 2-D Finite Element Analysis

7.1.1 Problem Description

The problem is the Fukuda Junior High School site of the Maiko Tunnel. 2 excavated sections (Zone A and Zone B) in this site are studied. 2-D finite element analyses for these 2 case studies are carried out using ABAQUS. The description of the case histories including the field results were given in Chapter 5.

7.1.2 Geometry and Boundary Conditions

For both case studies, only the top heading which is the semi circular part of the horse shoe tunnel as shown in Figure 7-1 is considered. Zone A and Zone B have geometry as shown in Figure 7-1. The top 28m layer of the soil model consists of Osaka Formation which is underlain by 12m of the stiffer Kobe Formation. Concrete linings, tunnel inverts and steel arches are not modelled in these analyses because the focus of these analyses is to study the behaviour of the ground surrounding the excavated tunnel under the reinforcement of the Pipe Umbrella Arch only.

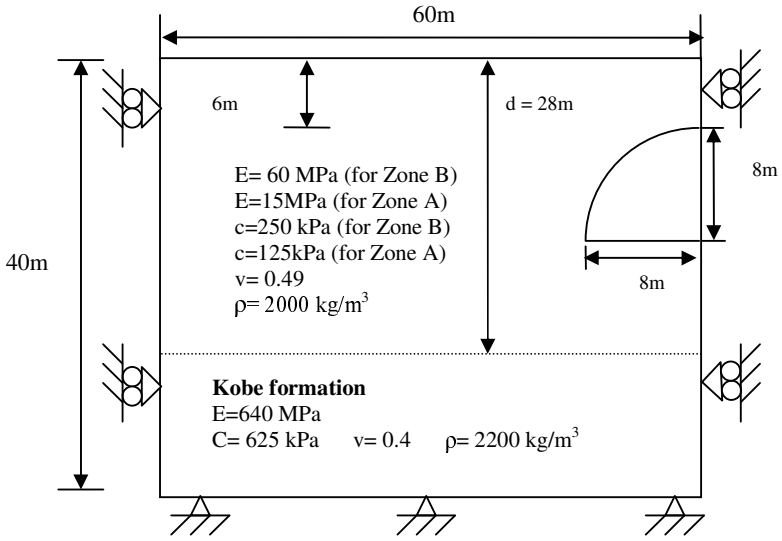

Figure 7-1. Geometry and boundary conditions.

7.1.3 2-D Mesh

A total of 1478 8-node biquadratic plane strain elements (CPE8) were used for the soil model. CPE8 elements are two-dimensional planar solid (continuum) elements in ABAQUS. The soil model was meshed as closely as possible to the cross section of the 3-D model so as to enable accurate plane strain analysis to be conducted.

The composite strip, steel pipes and grout interior are modelled according to the approximations described in Section 7.1.6. The types of elements used are also described in Section 7.1.6.

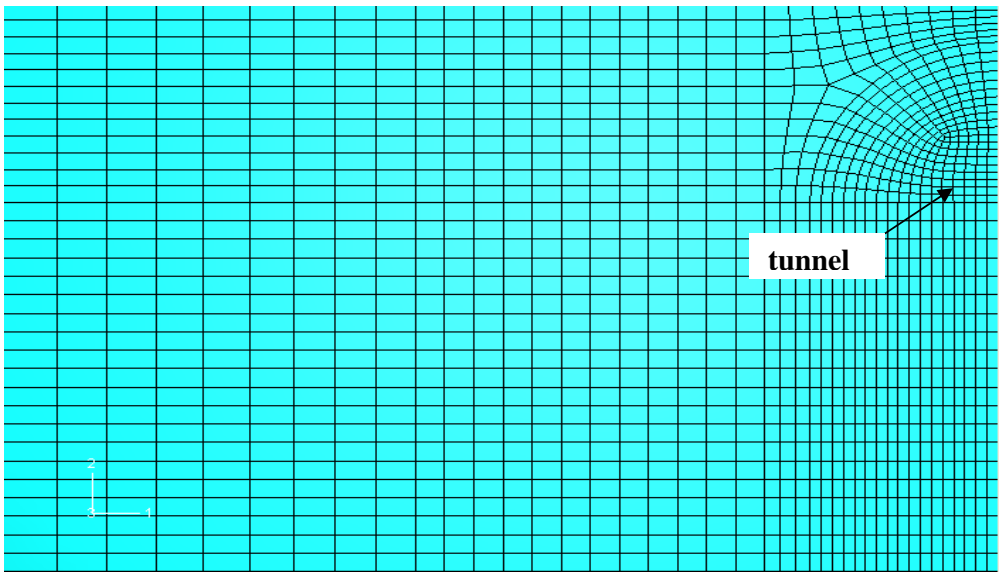

Figure 7-2. 2-D soil mesh.

7.1.4 Material Constitutive Model

A. Soil Model

A Mohr-Coulomb elasto-plastic constitutive model with associated flow rule was used for modelling the soil layers. Geotechnical parameters for Zone A and Zone B are taken as those established for the 3-D models.

The geotechnical properties of the soil formations in Zone A and Zone B were given in Chapter 6 and summarised in Table 7-1 for convenience.

B. Steel pipes and Grout interior Models

The steel pipes and grout are assumed to be linearly elastic. The pipes are made of an elastic metal (steel) with a density of 7860kg/m^3, Young's modulus of 200GPa and a Poisson's ratio of 0.4. The grout interior is made of grout with a density of 2500kg/m^3, Young's modulus of 50GPa and a Poisson's ratio of 0.35. Other

approximations used to simulate the Pipe Umbrella Arch and their associated material properties are described in subsequent sections.

Table 7-1. Geotechnical properties of the Fukuda High School section of the Maiko Tunnel.

Zone	Layer	Description	Soil type	SPT-N	c (kPa)	E (MPa)
A	**Top**	Alluvial fill	Gravel with clay	5-40	125	15
	Bottom	Kobe Formation	Sandstone, shale	>70	625	640
B	**Top**	Osaka formation	Clayey gravel	20-60	250	60
	Bottom	Kobe formation	Sandstone, shale	> 70	625	640

7.1.5 Initial Conditions

The modelling is conducted sequentially and consists of initial installation of a set of umbrella arch prior to any excavation and followed by tunnel excavation. The procedures used for the sequential modelling followed very closely the actual field construction and are tabulated in Table 7-2.

Geostatic state of stress is initially created in the soil model before any installation of reinforcement or excavation. The initial effective stresses are specified using *INITIAL CONDITIONS, TYPE=STRESS, GEOSTATIC option. In the first step of analysis, gravity loads corresponding to the weight of the soil materials are applied. The *GEOSTATIC option is then used to re-establish initial equilibrium so as to ensure that the load and initial stresses generated are in equilibrium before other steps are processed. Subsequently, the Umbrella Arch was installed. The *MODEL CHANGE, ADD=STRAIN FREE option is used to activate the strain-free Pipe Umbrella to the soil model which is in equilibrium.

Table 7-2. 2-D modelling procedure.

Step	Stage of construction	Descriptions
1	Geostatic state of stress	Model is subjected to initial stresses & gravity
2	Installation of U	Install Pipe Umbrella Arch
3	Excavation of tunnel	Tunnel is excavated

7.1.6 Approximations for Pipe Umbrella Arch

3 types of simulation for the Pipe Umbrella Arch were conducted as follows:

1. A strip of reinforced composite material with an equivalent strength derived from the soil, steel pipe and grout (**Method 1**).
2. 21 individual steel pipes with grout interior were arranged along the tunnel periphery at a spacing of 400mm (centre to centre) between one another at a distance of 150mm from the tunnel periphery (**Method 2**).
3. Reinforced strip is replaced by beam elements of equivalent strength (**Method 3**).

7.1.6.1 Method 1 – Equivalent Material

In the first simulation, a strip of width of 300mm was arranged at an angle of 70˚ from the vertical along the tunnel periphery. The equivalent strength of this reinforced strip is derived based on the process of weighted averages of the components used in the Umbrella Arch. The thickness of the reinforced strip is twice the distance between the pipe centre and the tunnel periphery. Tables 7-3 to 7-5 and Tables 7-6 to 7-8 show the calculation procedures for deriving the equivalent soil properties used for the reinforced strip for Zone B and Zone A respectively. The sum of product of the Young's modulus and the area are divided by the sum of the area of each component in order to derive the equivalent Young's modulus. The equivalent cohesion of the strip of equivalent material is also derived similarly as shown in Table 7-4 for Zone B and Table 7-7 for Zone A. The strip of

equivalent material is modelled using Mohr-Coulomb failure criterion with an associated flow rule.

Table 7-3. Calculation of the Young's modulus for the strip of equivalent material (Zone B).

Component	**Area (m^2)**	**Young's Modulus, E (MPa)**	**Product ($x10^6$)**	**Remarks**
Clayey gravel	0.3*1.0 = 0.3	60	18	
Steel pipes	($\pi 0.057^2$*2.5)=0.00512	200000	1024	Per metre of strip consists of 2.5 pipes
Grout	($\pi 0.051^2$*2.5)=0.0204	50000	1020	Cross sect. area of single pipe= $3.142*(0.051)^2$=0.00817
Sum	0.32552		2062	
Equivalent modulus, E_{equiv} = $2062x10^6$ /0.32552 = 6.334 GPa				

Table 7-4. Calculation of the cohesion for the strip of equivalent material (Zone B).

Component	**Area (m^2)**	**Strength (MPa)**	**Product ($x10^6$)**	**Remarks**
Clayey gravel	0.3	0.5	0.15	Cohesion of the soil=250kPa. For undrained analysis, compressive strength=2*c=500kPa
Steel pipes	0.00512	200	1.024	
Grout	0.0204	30	0.612	
Sum	0.32552		1.786	
Equivalent strength, S_{equiv} = $1.786x10^6$ /0.32552 = 5.486 MPa C_{equiv} = 5.486/2 = 2.7MPa, where C is the cohesion of the reinforced strip				

Table 7-5. Calculation of the density for the strip of equivalent material (Zone B).

Component	**Area (m^2)**	**Density (kg/m^3)**	**Product**	**Remarks**
Clayey gravel	0.3	2000	600	
Steel pipes	0.00512	7860	40.24	
Grout	0.0204	2500	51	
Sum	0.32552		691.24	
Equivalent density, ρ_{equiv} = 691.24 /0.32552 = 2123 kg/m^3				

Table 7-6. Calculation of the Young's modulus for the strip of equivalent material (Zone A).

Component	Area (m^2)	Young's Modulus, E (MPa)	Product ($x10^6$)	Remarks
Clayey gravel	0.3*1.0 = 0.3	15	4.5	
Steel pipes	(π0.057^2*2.5)=0.00512	200000	1024	Per metre of strip consists of 2.5 pipes
Grout	(π0.051^2*2.5)=0.0204	50000	1020	Cross sect. area of single pipe= 3.142*(0.051)^2=0.00817
Sum	0.32552		2049	
Equivalent modulus, E_{equiv} = 2049x10^6 /0.32552 = 6.295 GPa				

Table 7-7. Calculation of the cohesion for the strip of equivalent material (Zone A).

Component	Area (m^2)	Strength (MPa)	Product ($x10^6$)	Remarks
Clayey gravel	0.3	0.25	0.075	Cohesion of the soil=125kPa. For undrained analysis, compressive strength=2*c=250kPa
Steel pipes	0.00512	200	1.024	
Grout	0.0204	30	0.612	
Sum	0.32552		1.711	
Equivalent strength, S_{equiv} = 1.711x10^6 /0.32552 = 5.256 MPa C_{equiv} = 5.256/2 = 2.6MPa, where C is the cohesion of the reinforced strip				

Table 7-8. Calculation of the density for the strip of equivalent material (Zone A).

Component	Area (m^2)	Density (kg/m^3)	Product	Remarks
Clayey gravel	0.3	2000	600	
Steel pipes	0.00512	7860	40.24	
Grout	0.0204	2500	51	
Sum	0.32552		691.24	
Equivalent density, ρ_{equiv} = 691.24 /0.32552 = 2123 kg/m^3				

The methodology used in generating the model is shown in Figure 7-3 and the generated mesh using ABAQUS FEM programme code is shown in Figure 7-4. 8-node biquadratic plane strain elements (CPE8) are used to model the composite strip. CPE8 elements are two-dimensional planar solid (continuum) elements in ABAQUS.

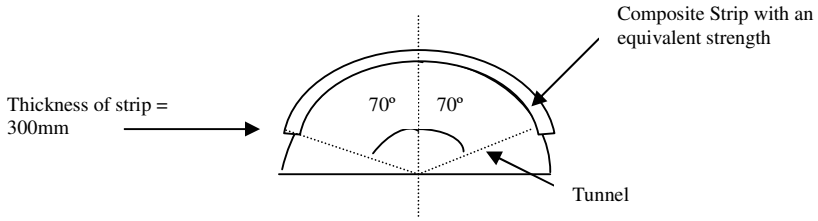

Figure 7-3. Methodology for Method 1 – Equivalent Material.

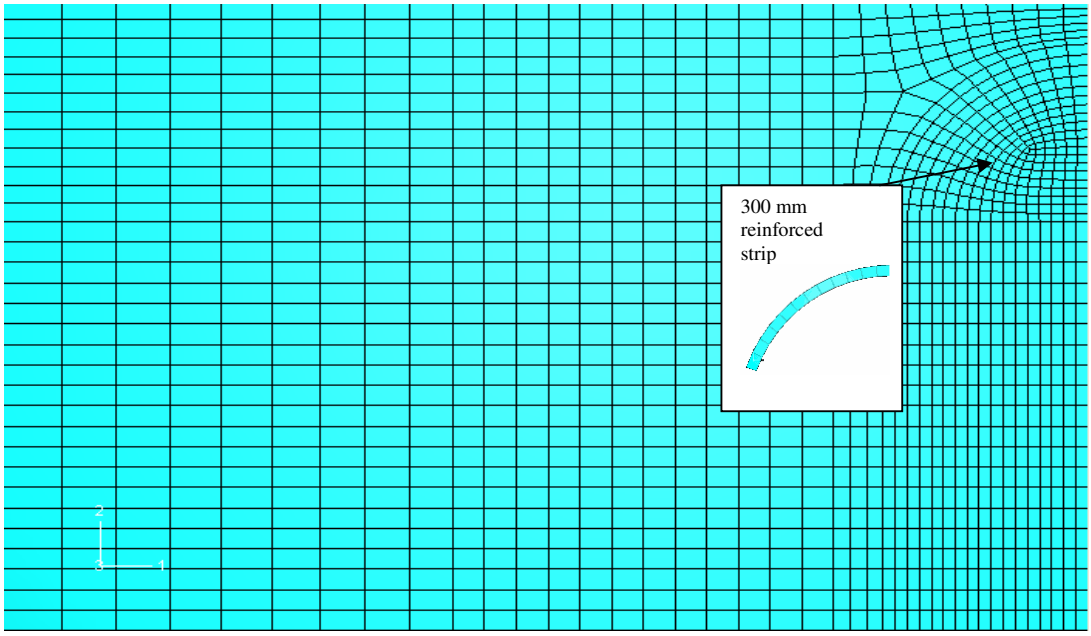

Figure 7-4. Mesh generated for Method 1 - Equivalent Material.

7.1.6.2 Method 2 – Individual Components

In the analyses for the second type of simulation, which relates more to the actual construction of the Umbrella Arch, 21 steel pipes with grout interior are embedded onto the tunnel periphery. Figure 7-5 shows the methodology for Method 2 and the mesh generated for this analysis is shown in Figure 7-6. The steel pipes and grout interiors are modeled using 8-node biquadratic plane strain elements (CPE8).

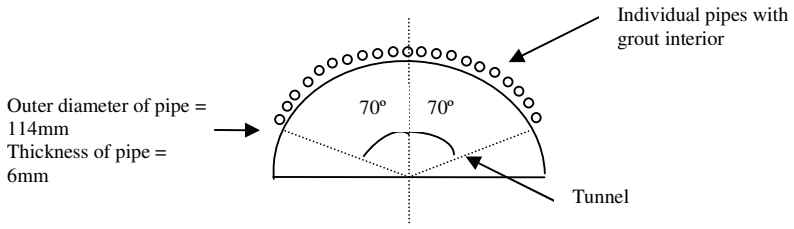

Figure7-5. Methodology used for Method 2 – Individual Components.

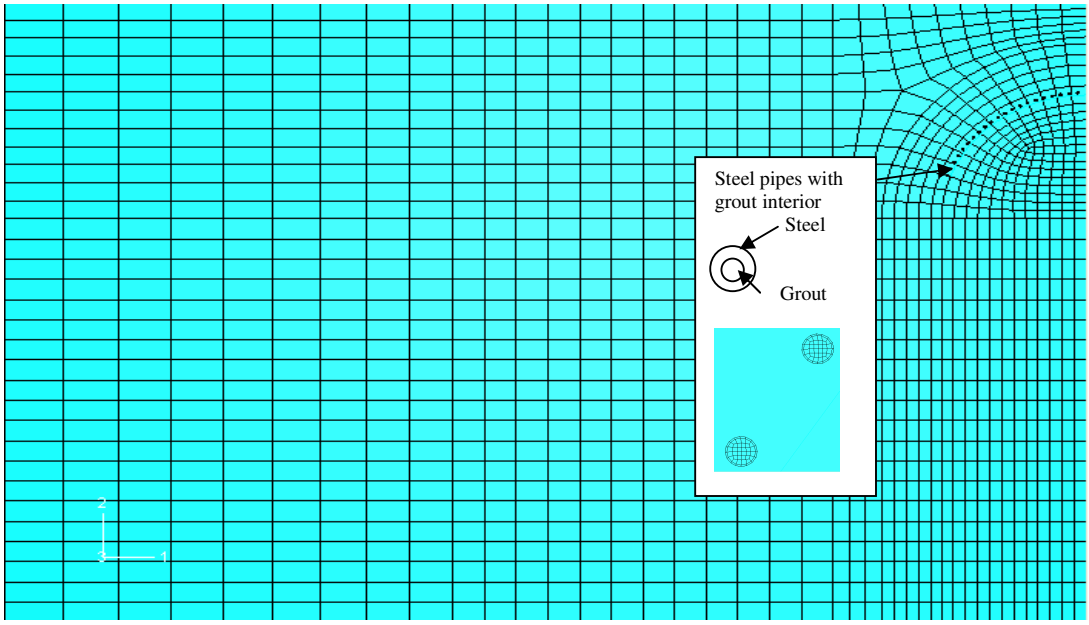

Figure 7-6. Mesh generated for Method 2 – Individual Components.

7.1.6.3 Method 3 – Composite Beam

The third type of simulation is based on the same principle as the first method except that the reinforced strip is replaced by beam elements of 300mm thickness which lined the periphery of the tunnel as shown in Figure 7-7. Figure 7-8 shows the mesh generated using the methodology stated for Method 3. The composite beam is modeled using 3 node quadratic beam (B22) elements.

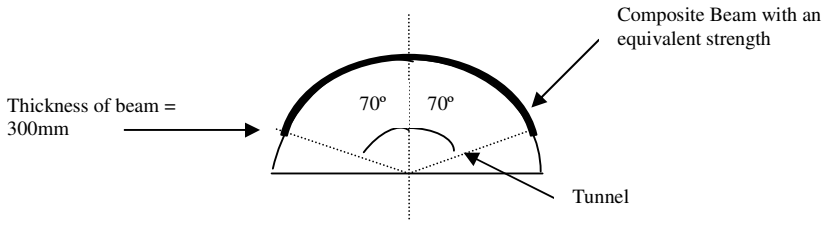

Figure 7-7. Methodology used for Method 3 – Composite Beam.

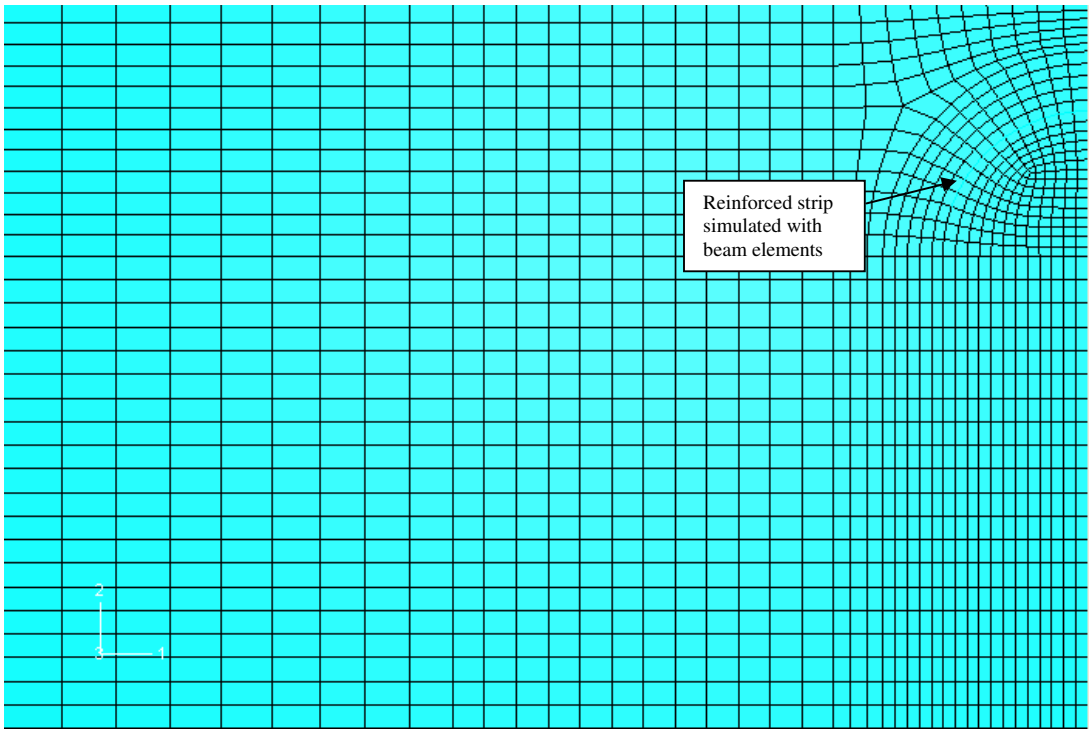

Figure 7-8. Mesh generated for Method 3 – Composite Beam.

7.1.7 **Results for Zone B and Zone A**

The 3 methods described in the previous sections are used for simulating the Pipe Umbrella Arch in Zone B and Zone A of the Maiko Tunnel. The generated vertical ground surface settlements are presented in Figures 7-9 and 7-10 respectively.

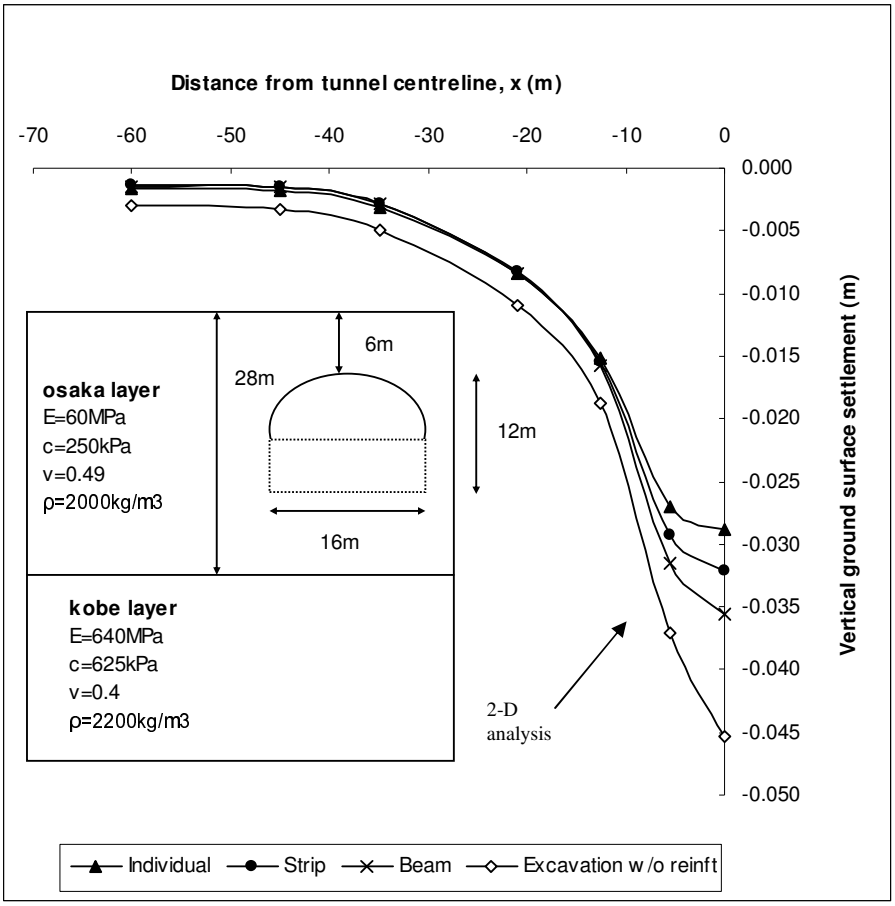

Figure 7-9. Vertical ground surface settlement profile for the 3 methods of simulation (Zone B).

As shown in Figure 7-9, Methods 1, 2 and 3 produced a maximum ground surface settlement of 29mm, 32mm and 35.5mm respectively for Zone B. Method 2 (Individual Components) generated approximately 36% decrease in ground surface settlement as compared to 29% decrease for Method 1 (Equivalent Material) and 21% decrease for Method 3 (Composite Beam). It should be noted that the ground surface settlement from field measurement is 22mm which is lower than the values obtained from the different 2D approximations. This is because the tunnel contained other reinforcement such as concrete tunnel linings, concrete tunnel inverts and steel arches, which were not included in the 2-D analyses.

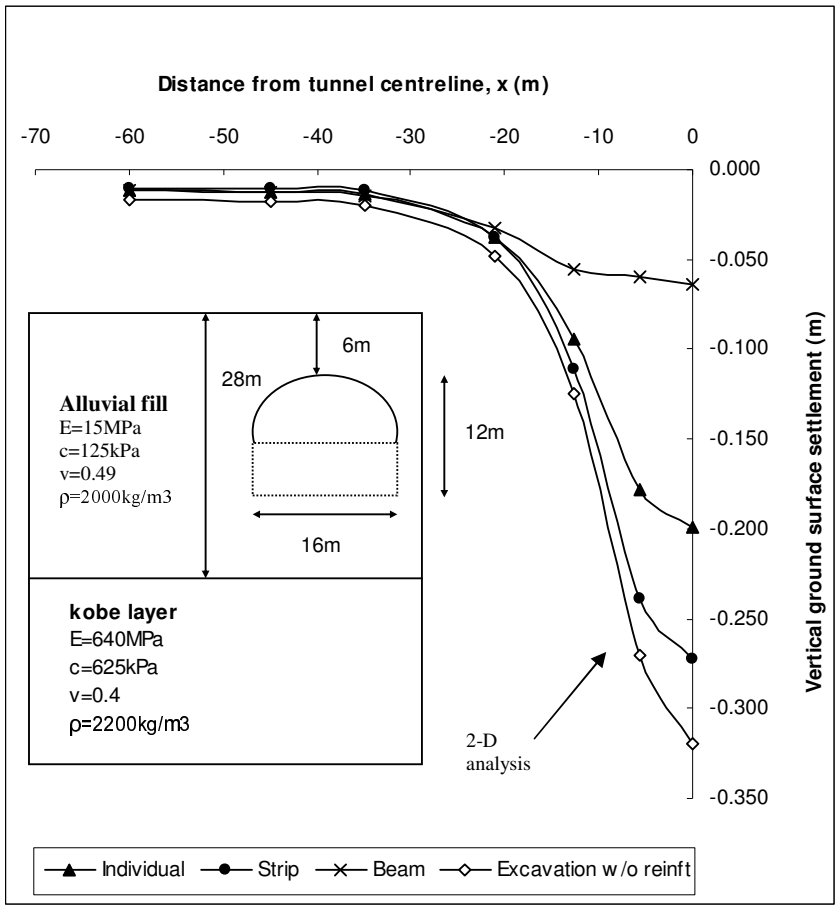

Figure 7-10. Vertical ground surface settlement profile for the 3 methods of simulation (Zone A).

Numerical analyses using Methods 1, 2 and 3 to simulate the Pipe Umbrella Arch in Zone A produced maximum ground surface settlements of 198mm, 270mm and 67.3mm respectively. Method 2 (Individual Components) generated approximately 38% decrease in ground surface settlement as compared to 16% decrease for Method 1 (Equivalent Material) and 79% decrease for Method 3 (Composite Beam). Results for Method 3 seem extremely low and they might not accurately reflect the actual reinforcing effect of the Pipe Umbrella Arch.

7.2 Comparison between 3-D and 2-D analysis results

7.2.1 Zone B

From comparison of the 3-D vertical ground surface settlement for various lap lengths (Zone B) (Figure 7-11) and the generated 2-D ground surface settlement for the three methods of approximations (Zone B) (Figure 7-9), it is observed that there is good agreement between the 3-D ground surface settlement for lap length= 4m and the 2-D ground surface settlement for Method 2 (Individual Components) as shown in Figure 7-12. They produced maximum ground surface settlement of approximately 29mm. Hence, the 2-D model for Method 2 (Individual Components) corresponds to plane strain condition of the 3-D model for the case of lap length = 4m. However, for cases of lap length less than 4m, the 2-D analysis using Method 2 (Individual Components) underestimates the settlement values.

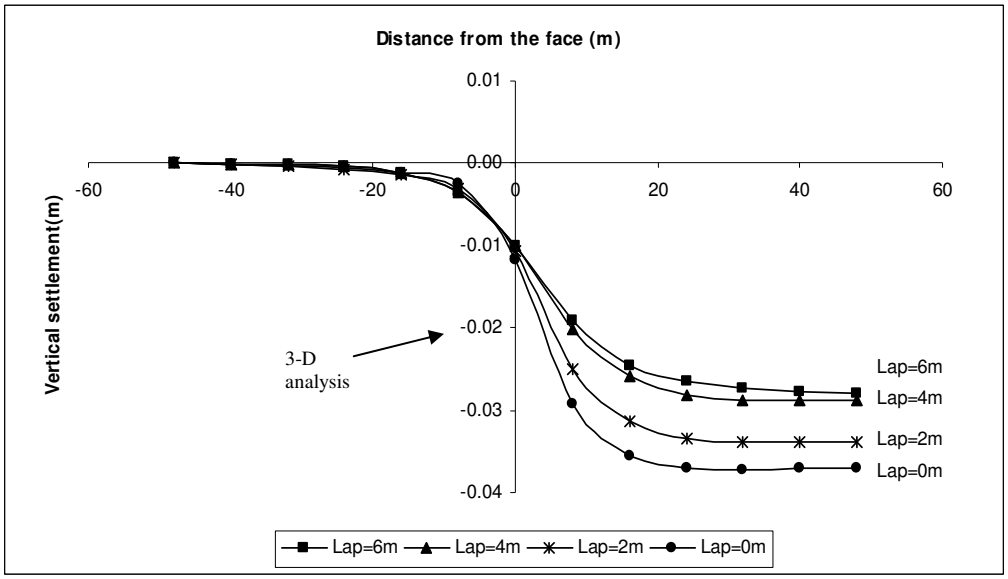

Figure 7-11. Longitudinal ground surface settlement profiles for n=42, OD=114mm and various lap lengths (Zone B).

The 2-D analyses for Method 1 (Equivalent Material) generated a maximum ground surface settlement of 32mm. This method produces a 10% increase in maximum ground surface settlement for lap ratios of 0.33 or greater (lap ratio = l/L, where l is the lap length and L is the length of steel pipe) as compared to using Method 2 (Individual Components) which coincided exactly with maximum ground surface settlement for lap ratio of 0.33 (lap ratio = l/L = 4/12 = 0.33). For cases of lap length less than 4m, the 2-D analysis using Method 1 (Equivalent Material) underestimates the settlement values.

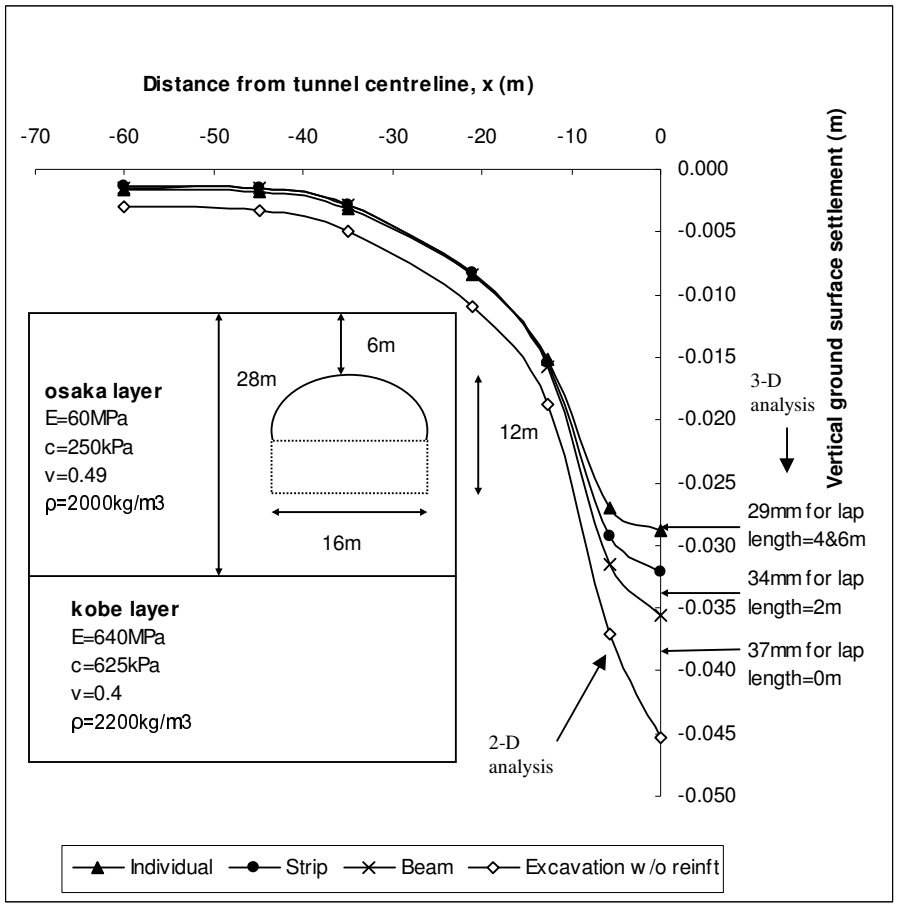

Figure 7-12. Comparison of 3-D vertical ground surface settlement for various lap lengths and the generated 2-D ground surface settlement for the three methods of approximations (Zone B).

7.2.2 Zone A

The 3-D vertical ground surface settlement for various lap lengths (Zone A) and the generated 2-D ground surface settlement for the three methods of approximations (Zone A) are compared in Figure 7-13. It is observed that there is good agreement between the 3-D ground surface settlement for lap length of 4m or greater (192mm) and the 2-D ground surface settlement for Method 2 (Individual Components) (198mm) with only a slight difference of up to 3%. Hence, the 2-D model for Method 2 corresponds to the plane strain condition of 3-D model for the case of lap ratio of 0.33 and greater. The same observations were made for Zone B. The 2-D

analysis using Method 1 (Equivalent Material) produced maximum ground surface settlement of approximately 270mm which is much greater than ground surface settlement generated for all lap ratios by approximately 10%-29%. This observation is different from that made in Zone B, where this method was conservative for lap length ratios of 0.33 and greater but unconservative for lap ratio greater than 0.33. It should be noted that the ground in Zone A (E=15 MPa and c_u = 125 kPa) is relatively weaker than that of Zone B (E=60 MPa and c_u = 250kPa).

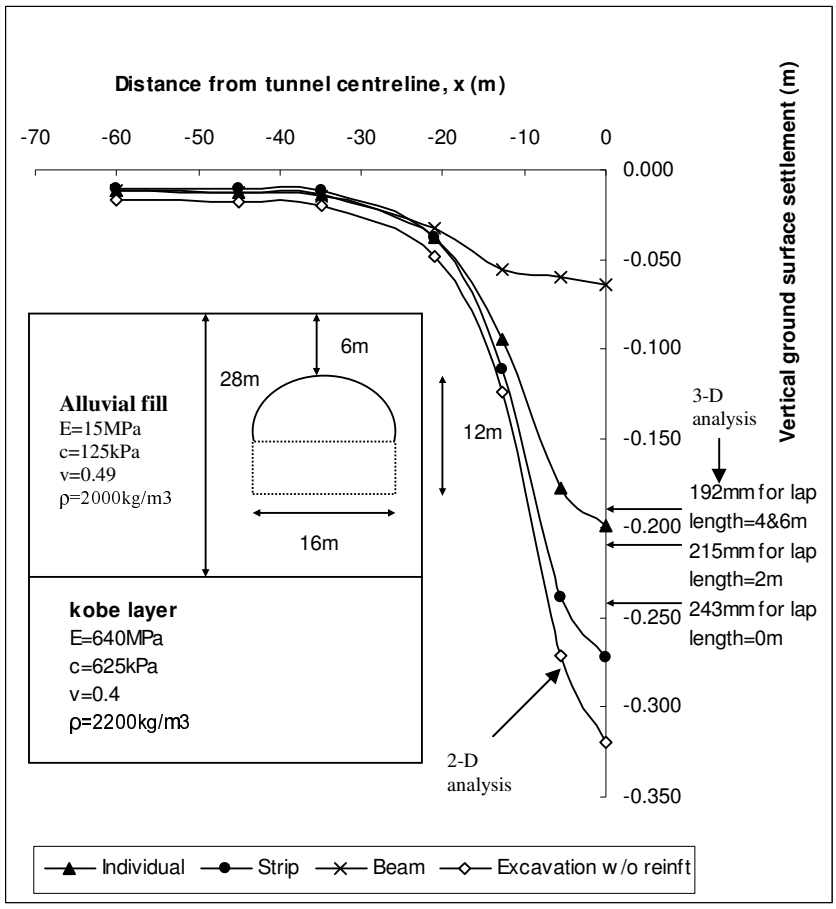

Figure 7-13. Comparison of 3-D vertical ground surface settlement for various lap lengths and the generated 2-D ground surface settlement for the three methods of approximations (Zone A).

7.2.3 Discussion of results for Zones B and A

From the analyses presented in this chapter, the following conclusions are made:

1) For cases of lap ratio of 0.33 or greater, the 2-D analyses using Method 2 (Individual Components) produces ground surface settlement that is in excellent agreement with the 3-D analysis.
2) For cases of lap ratio less than 0.33, the 2-D analysis using Method 2 (Individual Components) underestimates the ground surface settlement obtained for the 3-D analysis.
3) For cases of lap ratio of 0.33 or greater, the 2-D analysis using Method 1 (Equivalent Material) produces ground surface settlement that is conservative, but can become too conservative with weaker soils.
4) For cases of lap ratio of less than 0.33, the 2-D analysis using Method 1 (Equivalent Material) produced ground surface settlement that are conservative for hard soils, but produced unconservative results for relatively weaker soils.

7.3 Proposed Methodology for future research

A methodology to correlate between 2-D and 3-D ground surface settlement generated from tunnel excavations using Pipe Umbrella Arch as pre-support is proposed for future research. Based on using Method 1 (Equivalent Material) to represent the Pipe Umbrella Arch in 2-D analysis, 2-D and 3-D ground surface settlement can be correlated by introducing correction factors to soil strength and deformation parameters of the excavation site. The proposed methodology can be further explored for different soil conditions and tunnel sizes using 2-D and 3-D analyses. An example is illustrated using the case of tunnel excavations in Zone B.

A series of correction factors are applied to the modulus of deformation (E) and cohesion (c) for the case of Zone B. A set of revised values are obtained and tabulated in Table 7-9. The revised equivalent E and c values are applied to the reinforced strip and re-run using the model for Method 1 (Equivalent Material). The generated ground surface settlement for various sets of factored E and c are shown in Figure 7-14.

The correction factors are applied to the respective E and c based on a match to fit basis (i.e. the generated ground surface settlements for all corrected E and c are matched with the 3-D ground surface settlement for various lap lengths and they are fitted to the respective corrected E and c based on agreement of the ground surface settlement.)

Table 7-9. Correction factor and revised values of E and cohesion (Zone B).

Lap length, l (m)	6	4	3	2	0
Lap Ratio, R (l/L)	0.50	0.33	0.25	0.17	0.00
Correction Factor (CF)	1.00	1.00	0.90	0.45	0.30
Modulus of deformation, E_{equiv} (GPa)	6.33	6.33	6.33	6.33	6.33
Revised modulus of deformation, E_{rev} (GPa)	6.33	6.33	5.70	2.85	1.90
Cohesion of strip, C_{equiv} (MPa)	2.7	2.7	2.7	2.7	2.7
Revised equivalent cohesion of the strip, C_{rev} (MPa)	2.7	2.7	2.4	1.2	0.8

For lap ratios less than 0.33, correction factors are modified for the equivalent deformation modulus (E) and cohesion (c) of the strip (Method 1) to obtain maximum ground surface settlement that coincides with respective lap ratios of 0.25, 0.17 and 0 (i.e. l/L = 3/12 = 0.25, l/L = 2/12 = 0.17 and l/L = 0/12 = 0). The calculations and correction factors are described in Table 7-9.

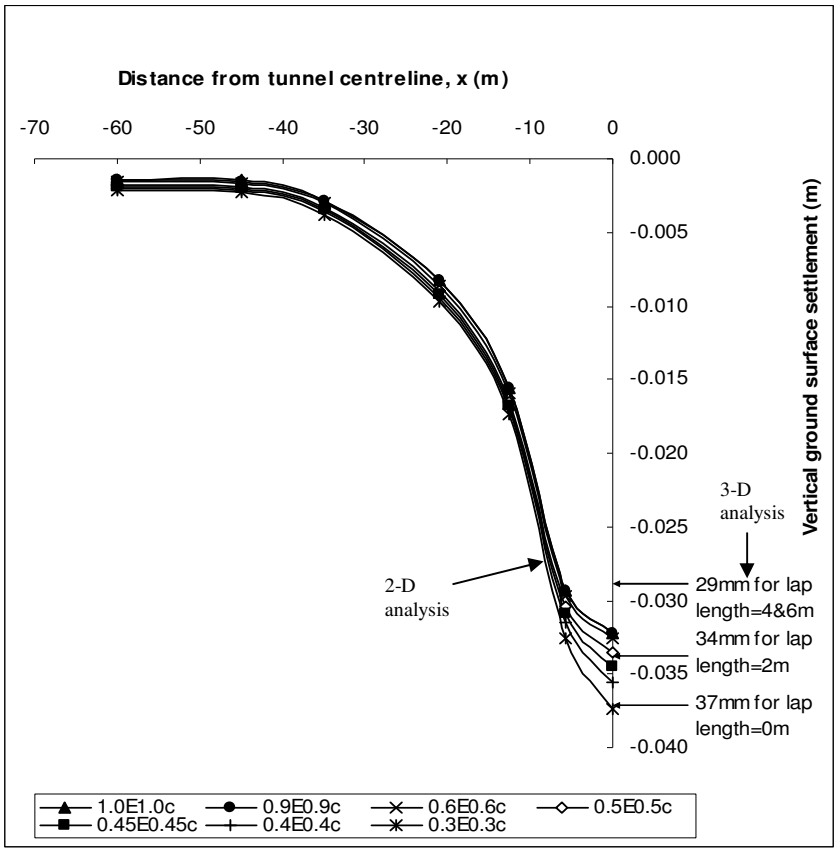

Figure 7-14. Vertical ground surface settlement generated for different factored E and cohesion (Zone B).

The generated 2-D maximum ground surface settlement is compared with the maximum ground surface settlement generated for different lap lengths as shown in Figure 7-14. It can be observed from Figure 7-14 that the maximum ground surface settlement generated for a strip of equivalent material with E and c factored by 0.3 (37.4mm) coincided with the maximum ground surface settlement generated for lap length equal zero (37.1mm). Maximum ground surface settlement generated using a correction factor of 0.45 (34.5mm) is in agreement with the ground surface settlement generated for a lap length of 2m (34mm). By decreasing the correction factors for lap ratio less than 0.33, the generated ground surface settlement results agreed with the respective maximum ground surface settlement generated for different lap lengths. This shows that Method 1 (Equivalent Material) produced

unconservative results for lap ratio less than 0.33. On the other hand, Method 1 (Equivalent Material) produced conservative results for lap ratios of 0.33 or greater.

Hence, it can be seen that by using Method 1 (Equivalent Material) and applying a correction factor to the equivalent soil strength and deformation parameters, ground surface settlement generated are in good agreement with measured ground surface settlement for lap ratios of 0.33 or greater for ground conditions similar to Zone B. In such a way, the 3-D Pipe Umbrella Arch can be modelled as a relatively simpler 2-D problem.

CHAPTER 8 – CONCLUSION & RECOMMENDATION

The use of the Pipe Umbrella Arch method for tunnel face pre-support in weak ground is increasingly becoming more and more popular. The design of the Pipe Umbrella Arch is mainly based on experience and when numerical methods are used, crude approximations are adopted. Most of the approximations are based on the theory of "equivalent material" in which the ground reinforced zone is replaced with a new material of parameters derived from the weighted averages of the properties of the individual components in this zone. These approximations ignore many of the basic characteristics of the Pipe Umbrella Arch especially the overlapping length between consecutive arches in the longitudinal direction.

In this work, 2D and 3D numerical studies are performed to evaluate the differences in the estimated ground displacements when different modelling approximations are used for the Pipe Umbrella Arch, and subsequently parametric studies using 3D finite element method are also performed to investigate the effect of various pipe parameters on the reinforcing capability of the Pipe Umbrella Arch. The studies are based on the analyses of three well-documented case histories in which Pipe Umbrella Arch was used during construction to limit the ground displacement. These three case histories are selected from fifty-six case histories compiled and presented in tabular form in this thesis. One of the case histories is on the use of the Pipe Umbrella Arch in fractured rocks and the other two are for cases of Pipe Umbrella Arch in soils. The following sections summarize the main conclusions drawn from these studies.

A. Analysis of a case history of Pipe Umbrella Arch in fractured rocks

2-D numerical analysis using FLAC software was conducted on a well-documented case history of Pipe Umbrella Arch in fractured rocks, using different methods of approximations. Although the field ground displacement was not reported, the rock material properties, method of construction and parameters of the construction of the Pipe Umbrella Arch are well-documented. Three different approximations for

the Pipe Umbrella Arch were used in the analyses. From the analyses performed, the following conclusions are drawn.

1. Different approximations for the Pipe Umbrella Arch lead to completely different estimated ground surface displacement. The "Equivalent Material" method gives ground displacement that is twice that obtained from the "Individual Components" method.
2. Different approximations for the Pipe Umbrella Arch lead to different estimated tunnel crown displacement. The "Equivalent Material" method gives crown displacement that is greater than twice that obtained from the "Individual Components" method.
3. Different approximations for the Pipe Umbrella Arch lead to different estimated tunnel closure. The horizontal tunnel closure estimated from the "Equivalent Material" method is slightly higher than that estimated from the other methods. However, the vertical closure estimated from the "Equivalent Material" method is 33% higher than that estimated from the "Individual Components" method.

B. Analysis of two case histories of Pipe Umbrella Arch in soil

3-D numerical analyses using ABAQUS software were conducted for 2 well-documented case histories of Pipe Umbrella Arch in soils. The 2 case histories are related to the construction of the Maiko Tunnel in Kobe, Japan. The first case history reported a site along the Maiko Tunnel identified as Zone B and the ground is characterised by Osaka Formation (which is made up of clayey gravel). The second case history reported a second site along the same tunnel identified as Zone A and ground characterised by relatively weaker alluvial fill (which is made up of gravel with clay). Numerical analyses were conducted for a range of documented soil strength and deformation parameters for both zones. The numerical studies generated a range of ground surface displacements for both zones. Reported field measurements were found to lie within the bounds generated. The effects of different tunnel reinforcements on the stability of the tunnel construction were also

studied for the calibrated model of Zone B by varying the application of different types of reinforcement for tunnel excavation. Analyses conducted followed closely the field construction procedures including installation of other reinforcements. From the studies performed, the following conclusions are drawn:

1. The methodology employed to model Pipe Umbrella Arch using 3D numerical analyses for both case histories leads to the identification of calibrated soil strength and deformation parameters for both Zones A and B. The ground surface displacements generated using the calibrated soil parameters are in excellent agreement with the field results both in value and distribution.
2. Studies conducted to investigate the effect of different tunnel reinforcement on induced ground settlement due to tunnel construction showed that Pipe Umbrella Arch controlled soil settlement more efficiently than concrete tunnel lining or steel arches.
3. Based on the calibrated model of Zone B, it was found that Pipe Umbrella Arch reduced ground surface settlement by 40% when they are installed as compared to when the tunnel is unsupported at all.
4. For Zone A, Pipe Umbrella Arch reduced ground surface settlement by approximately 38% when they are installed as compared to when the tunnel is unsupported.

C. Parametric Studies

Parametric studies using 3D finite element analyses were subsequently performed to investigate the effect of various pipe parameters on the reinforcing capability of the Pipe Umbrella Arch using the calibrated 3D numerical models derived from the previous studies. In these studies the effects of number of pipes (n) , pipe diameters (OD) and lap lengths (i.e. overlapping pipe length) (Lap) of the Pipe Umbrella Arch for both Zones A and B on the ground surface settlement were investigated. In order to fully establish and understand the reinforcing effect of the Pipe Umbrella Arch, other structural elements such as the concrete lining and steel arches are omitted

from the parametric studies. Hence, ground displacement results from the parametric studies would represent only the reinforcing effect of the Pipe Umbrella Arch. From the parametric studies performed, the following conclusions are obtained.

1. All the pipe parameters studied (number of pipes, pipe diameters and lap lengths) play an important role in controlling the vertical ground surface settlement during tunnel excavation.
2. For both Zones A and B, the ground surface displacement decreases as the number of pipes increases. The rate of decrease in ground surface displacement as the number of pipes increases.
3. For both Zones A and B, the change in ground displacement become negligible when the number of pipes increases approximately above 42.
4. For studies conducted in Zone B for various numbers of pipes, the 3D vertical ground surface displacement (vertical ground surface displacement at the tunnel face) is within 24-33% of the final ground surface settlement away from the tunnel face.
5. For studies conducted in Zone A for various numbers of pipes, it was also observed that the 3D vertical ground surface displacement (vertical ground surface displacement at the tunnel face) is within 26-29% of the final ground surface settlement away from the tunnel face.
6. The ground surface displacement decreases as the pipe diameter increases for both Zones A and B. The rate of decrease in ground surface displacement decreases as the pipe diameter increases.
7. For both Zones A and B, the change in ground displacement becomes negligible when the pipe diameter increases above 114mm.
8. For studies conducted in Zone B for various pipe diameters, it was also observed that the 3D vertical ground surface displacement (vertical ground surface displacement at the tunnel face) is within the range of 27-37% of the final ground surface settlement away from the tunnel face.
9. For studies conducted in Zone A for various pipe diameters, it was also observed that the 3D vertical ground surface displacement (vertical ground

surface displacement at the tunnel face) is within the range of 25-27% of the final ground surface settlement away from the tunnel face.

10. For both Zones A and B, the ground surface displacement decreases as the lap length of the Pipe Umbrella Arch increases. The rate of decrease in ground surface displacement decreases as the lap length increases.
11. For both Zones A and B, the change in ground displacement becomes negligible when the lap length increases above 4m (one third of the pipe length).
12. For studies conducted in Zones A and B for various lap lengths of Umbrella Arch, it was also observed that the 3D vertical ground surface displacement (vertical ground surface displacement at the tunnel face) is within the range of 25-36% of the final ground surface settlement away from the tunnel face.

D. Study of 3-D Pipe Umbrella Arch as a 2-D problem

A further study was conducted to assess the possibility of analysing the 3D Pipe Umbrella Arch using a simple 2D analysis. Different approximations were used to represent the Pipe Umbrella Arch in 2D using ABAQUS software for both Zones A and B.

For cases of lap ratio of 0.33 or greater, the 2-D analyses using Method 2 (Individual Components) produces ground surface settlement that is in excellent agreement with the 3-D analysis. For cases of lap ratio less than 0.33, the 2-D analysis using Method 2 (Individual Components) underestimates the ground surface settlement obtained for the 3-D analysis.

For cases of lap ratio of 0.33 or greater, the 2-D analysis using Method 1 (Equivalent Material) produces ground surface settlement that is conservative, but can become too conservative with weaker soils. And for cases of lap ratio of less than 0.33, the 2-D analysis using Method 1 (Equivalent Material) produced ground surface settlement that are conservative for hard soils, but becomes unconservative for relatively weaker soils.

E. Recommendations for future studies

1. A methodology to correlate between 2-D and 3-D ground surface settlement generated for tunnel excavations using Pipe Umbrella Arch as pre-support is proposed in this thesis for future research. The modelling techniques and results recommended in this research can provide an excellent assessment of the effect Pipe Umbrella Arch method in shallow and weak grounds.
2. The work presented in this thesis is for the cases of tunnel excavations in hard soils (i.e. Zone A and Zone B of Maiko Tunnel construction). The cases of other type of soil conditions or weak rocks, where Pipe Umbrella Arch method were installed, were not studied in this thesis. It is recommended that these cases are similarly studied to further substantiate the findings in this thesis.
3. In this research, two studies of one particular tunnel shape were conducted. Further research needs to be conducted by accounting for different tunnel shapes, tunnel depths and soil types in order to fully substantiate the drawn conclusions from the numerical analysis
4. Elastic analyses using Mohr-Coulomb model were carried out to detect the tunnel performance and the corresponding ground deformations as a result of the installation of the Pipe Umbrella Arch Method. Soil condition and parameters are generally assumed to be homogenous. Possible disturbance to the soil as a result of initial excavated holes for placement of steel pipes were not modelled. This was due to the limitations of the software. As such, the steel pipes and grout are embedded into the soil. In these numerical analyses, two studies of one particular tunnel shape were conducted. More research needs to be conducted by accounting for different tunnel shapes, tunnel depths and soil types in order to fully substantiate the drawn conclusions from the numerical analysis. Numerical solutions could be further enhanced by correlating to empirical solutions from actual field data of more published case studies.

REFERENCES

Anagnostou, G. and Kovàri, K. (1996a). "Face Stability in Slurry and EPB Shield Tunneling". Proceedings International Symposium Geotechnical Aspects of Underground Construction in Soft Ground, London, 15-17 April 1996, R.J. Mair & R.N. Taylor Eds., pp. 453-458.

Anagnostou, G. and Kovàri, K. (1996b). "Face Stability Conditions with Earth-Pressure-Balanced Shields". Tunnelling and Underground Space Technology, Volume 11, No. 2, pp. 165-173.

Atkinson, J.H. and Potts, D.M.(1977) " Subsidence above shallow circular tunnels in soft ground", Journal of Geotechnical Engineering Division, ASCE, Vol.103, G.T.4, pp.307-325.

Attewell, P.B. and Boden, J.B. (1971) "Development of stability ratios for tunnels driven in clay", Tunnels and Tunnelling, Vol. 3, pp. 195-198.

Attewell, P.B and Woodman, J.P. (1982) "Predicting the dynamics of ground settlement and its derivatives caused by tunnelling in soil", Ground Engineering, Vol.15(8), pp.13-22,36.

Attewell, P.B., Farmer, I.W. and Glossop, N.H. (1978) "Ground deformation caused by tunnelling in a silty alluvial clay", Ground Engineering , Vol.11(8), pp. 32-41.

Attewell, P.B. and Farmer, I.W. (1974) "Ground deformations resulting from shield tunnelling in London clay", Canadian Geotechnical Journal, Vol. 11, pp.380-395.

Attewell, P.B. and Taylor, R.K. (1984) "Ground movements and their effects on structures", Surrey University Press, Chapman and Hall, New York.

Attewell, P.B. and Yeates, J., (1984). "Tunnelling in soil". Chapter 6, Ground Movements in soils and their effect on Structures. P.B. Attewell & R.K. Taylor Eds., pp. 132-215.

Attewell, P.B., Yeates, J. and Selby, A.R. (1986) "Soil movements induced by Tunnelling", Chapman and Hall, New York.

Barisone, G., Pigorini, B. and Pelizza, S. (1982) "Umbrella Arch method for tunneling in difficult conditions- Analysis of Italian cases", Proceedings of the 4th Congress International Association of Engineering Geology, New Delhi, Vol. 4, pp. IV 15- IV 27.

Barisone, G., Campo, F., Corona, G. and Pelizza, S. (1989) "Rapid umbrella-arch axcavation of a tunnel in cohesionless material under an archaeological site", Proc. Int'l Congress Progress and Innovation in Tunnelling, Toronto.

Beltran, A., Soriano, G., Fernandez, J.L. and Rojo, J.L. (1992) "El tunel de 'El Goloso': Cantoblanco-Tres Canotos - UnNuevo metodo de presostenumiento", Towards New Worlds in Tunnelling, Vieitez-Utesa & Montanez-Cartaxo (eds), pp. 881-888.

Bischoff, J.A. and Smart, J.D. (1975) "A method of computing a rock reinforcement system which is structurally equivalent to an internal support system", 16th Symp. On Rock Mechanics, Univ. of Minnesota, pp.179-184.

Borchi, A., Formis, L., Pelizza, S, Ricci, D. and Forlani, E. (1992) "The road tunnels of the SanRemo "corniche' through complex rocks", Towards New Worlds in Tunnelling, Vieitez-Utesa & Montanez-Cartaxo (eds), pp. 889-895.

Bourdeau, Y., Ogunro, V., Lareal, P. and Riondy, G. (1994) "Use of strain gages to predict soil-geotextile interaction in pull out tests", 5th Int'l Conf. on Geotextiles, Geomembranes and Related Products, Singapore, pp.451-455.

Bracegirdle, A., Mair, R.J., Nyren, R.J. and Taylor, R.N. (1996) "A methodology for evaluating potential damage to cast iron pipes induced by tunnelling", Geotechnical Aspects of Underground Construction in Soft Ground, Mair & Taylor (eds), 1996, Balkema, Rotterdam, pp. 659-664.

Broms, B.B. and Bennermark, H. (1967) "Stability of Clay at Vertical Openings", ASCE Journal of Soil Mechanics and Foundation Division 1993, pp. 71-95.

Bulson, P.S. (1985) "Buried Structures: Static and Dynamic Strength", Chapman and Hall, New York.

Burns, J.Q. and Richard, R.M. (1964) "Attenuation of stresses for buried cylinders", Proc. Symp. on Soil-Structure Interaction, Tuscon, Ariz., pp. 378-392.

Carrieri,G., Grasso, P., Mahtab, A. and Pelizza, S. (1991)"Ten years of experience in the use of umbrella arch for tunnelling", Proc. Of Soil and Rock Improvement in Underground Works, Milan, Societa Italiana Gallerie.

Casarin, C., Oureza, A.P.O., Prado, C.M.A. and Tescarolo, L. (1996) "Back Analysis of an Urban Tunnel", Geotechnical Aspects of Underground Construction in Soft Ground, Mair & Taylor (eds), 1996, Balkema, Rotterdam, pp.485-489.

Chambon, P. and Corte, J.F. (1994) "Shallow tunnels in cohesionless soil: Stability of tunnel face", Journal of Geotechnical Engineering, American Society Civil Engineers, Vol. 120, pp. 1148-1165.

Chapman, D.N. (1996) "Ground movements associated with pipejacking operations", Geotechnical Aspects of Underground Construction in Soft Ground, Mair & Taylor (eds), 1996, Balkema, Rotterdam, pp. 665-670.

Chapman, D.N. and C.D.F. Rogers (1991) "Ground movements associated with trenchless pipelaying operations", Proceedings of the Fourth International Conference on Ground Movements and Structures, Cardiff, July 1991, Edited by J.D. Geddes, Pub. Pentech Press, pp.91-107.

Clough, G.W. and Schmidt, B.(1981) " Excavation and Tunnelling", Soft Clay Engineering, Chapter 8, edited by E.W. Brand and R.P. Brenner, Elsevier.

Cording , E.J., Hansmire, W.H., MacPherson, H.H., Lenzini, P.A. and Venderohe, A.D. (1976) " Displacements around tunnels in soil", Final report by University of Illinois on Contract No. DOT FR 30022 to the Office of the Secretary and Federal Railroad Administration, Dept. of Transportation, Washington D.C. 20590, USA.

Cornejo, L. (1989) "Instability at the face: Its repercussions for tunnelling technology", Tunnels and Tunnelling, April 1989, pp. 69-74.

Constantin, B. (1996) "The underground crossing of Toulon", North American Tunnelling '96, Ozdemir (ed.), pp. 113-121.

Davis, E.H., Gunn, M.J., Mair, R.J. and Seneviratne, H.N., (1980). "The stability of shallow tunnels and underground openings in cohesive material". Géotechnique, Volume 30, No. 4, pp. 397-419.

Dias, D., Subrin, D., Wong, H., Dubois, P. and Kastner, R. (1998) "Behaviour of a tunnel face reinforced by bolts: comparison between analytical and numerical models", 2nd Int.l Symposium Geotechnical Engineering, Hard Soils-Soft Rocks, Naples, Italy.

Dias, D., Bourdeau, Y. and Kastner, R. (2001) "Behaviour of a tunnel face reinforced by bolts: Influence of the soil/bolt interface", Modern Tunnelling Science and Technology, Adachi et al (ed.), Swets & Zeitlinger, pp.165-169.

Durand, J.P., Deffayet, M., Jassionnesse, C. and Reith, J.L. (1994) "Surface settlements in urban tunnelling works: Design approach for Toulon underground motorway crossing", Tunnelling and Ground Conditions, Abdel Salam (ed.), 1994, Balkema, Rotterdam, pp. 97-103.

Einstein, H.H. and Schwartz, C.W. (1979) "Simplified Analysis for Tunnel Support", Journal of the Geotechnical Engineering Division, April 1979, pp. 499-518.

Eisenstein, Z. and Ezzeldine, O. (1994) "The role of face pressure for shields with positive ground control", Tunnelling and Ground Conditions, Abdel Salem(ed.), pp.557-571.

Ellstein, A.R. (1986) "Heading failure of lined tunnels in soft soil", Tunnels and Tunnelling, June '86.

Eusebio, A., Grasso, P. and Rabbi, E.(1990) "Geological and geotechnical characterization of the morainic "Amphitheater of Rivoli" in the NW Itlay", Int'l Congress of Geoengineering I.A.E.G., Amsterdam, Vol. 1.

Fasoli, R. and Pastore, R. (1976) "La galleria del Bricco sull'autostrada Torino-Savona', L'industria delle Construzioni.

Gall, V., Zeidler, K, Bohlke, B.M. and Alfredson, L.E. (1998) "Optimization of tunnel pre-support – Softground NATM at Washington D.C. Metro's section F6b", North American Tunnelling, 1998, Balkema, Rotterdam, pp. 229-236.

Gangale, G., Corona, G. and Pelizza, S. (1992) "The Messina-Palermo motorway:Complex rock masses and tunnelling problems", Towards New Worlds in Tunnelling, Vieitez-Utesa & Montanez-Cartaxo (eds), pp. 873-880.

Gentili, G. and Pigorini, B.(1976) "Large motorway tunnels in Liguria, Italy", Proceedings Tunnelling '76, London, pp. 177-198.

Glossop, N.H. (1977) "Soil deformation caused by soft ground tunnelling", Phd thesis, Univ. of Durham.

Grasso, P., Mahtab, M.A., Rabajoli, G. and Pelizza, S. (1993),"Consideration for design of shallow tunnels", International Conference Underground Transportation Infrastructures, Toulon, pp.19-28.

Grasso,P., Mahtab, A. and Pelizza, S. (1989)"Reinforcing a rock zone for stabilising a tunnel in complex formations", Proceedings of the International Congress on Progress and Innovation in Tunnelling, Toronto, pp.663-670.

Guilloux, A., Bretelle, S. and Bienvenue, F. (1996) "Effects of pre-lining methods on the convergence of a tunnel", Geotechnical Aspects of Underground Construction in Soft Ground, Mair & Taylor (eds), 1996, Balkema, Rotterdam, pp. 355-360..

Hara, S. and Igarashi, M. (1996) "Tunnel ground improvement by M.J.S.", North American Tunnelling '96, Ozdemir (eds.), pp. 229-237.

Harazaki, I, Okazawa, T, Masui, N, Nakatani, M and Yoshida, Y (1998) "Design and construction of cut and cover tunnel of six traffic lanes", Tunnels and Metropolises, NegroJr. & Ferreira (eds.), Sao Paulo, Brazil, pp. 727-731.

Haruyama, K., Teramoto, S., Harada, H. and Mori, M. (2001) "Construction of urban expressway tunnel with special large cross section by NATM-Metropolitan Inter-city Highway (ken-O-Do) Ome Tunnel", Modern Tunnelling Science and Technology, Adachi et al. (eds.), pp.693-698.

Haruyama, K., Taira, K., Tanaka, K., Morikawa, S., Namikawa, T., Hibiya, K. and Akutagawa, S. (2001) "Evaluation of a measure taken for controlling subsidence for

a large scale double deck tunnel at shallow depth", Modern Tunnelling Science and Technology, Adachi et al. (eds.), pp.769-774.

Heuer, R.F. (1974) "Important Ground Parameters in Soft Ground Tunnelling", Proceedings of Special Conference on Subsurface exploration for Underground Excavation and Heavy Construction, pp. 41-55, ASCE.

Hefny, A.M., Tan, W.L. Ranjith, P.G., Sharma, J. & Zhao, J. (2004). "Numerical Analysis for Umbrella Arch Method in Shallow Large Scale Excavation in Weak Rocks", Tunnelling and Underground Space Technology Journal, Vol. 19, No.4-5, Paper 500, July-September 2004.

Higo, M., Nagasawa, N., Inoue, K., Maki, H., Furukawa, K. and Nakagawa, K. (1996) "A study on characteristics of material and form of injection for urethane injection forepoling in tunnelling", North American Tunnelling '96, Ozdemir (eds.), pp. 239-248.

Hoek, E. (2000).Numerical Modelling for Shallow Tunnels in Weak Rock. unpublished notes. [Online]. Available: http://www.rocscience.com/library/rocnews/Spring2003/ShallowTunnels.pdf.[2003, March 30]

Hoste, G.R. (1980) "Metro works in Antwerp, Belgium: use of a 6.50m diameter bentonite shield for the tunnels and pipe jacking for the stations", Proceedings of Eurotunnel '80, Basle, pp. 28-32.

Itasca Consulting Group. (1997), "FLAC in 3D User Manual", Minneapolis.

Itasca Consulting Group. (1991), "FLAC User Manual – Version 3.0", Minneapolis.

Itoh, T., Isozaki, T., Iwata, M., Oniki, K. and Fujimoto, K. (2001) "A new urban tunnelling method adopted to the soft ground with high groundwater level", Modern Tunnelling Science and Technology, Adachi et al (eds), Swets & Zeitlinger, pp.745-750.

Jassionesse, C., Dubois, P. and Saitta, A. (1996) "Tunnel face reinforcement by bolting: Soil bolts homogenization, strain approach", Geotechnical Aspects of Underground Construction in Soft Ground, Mair & Taylor (eds), 1996, Balkema, Rotterdam, pp. 373-378.

John, M. and Mattle, B. (2002) "Design of Tube Umbrella", Tunel - ROCNIK, Vol. 3, no. 11, pp. 1-11, Czech Tunneling Committee and Slovak Tunnelling Association.

Korbin, G.E. and Brekke, T.L. (1977) "A Field Study of Spiling Reinforcement in Underground Openings", Technical Report MRD-1-77, Missouri River Division, Corps of Engineers, Omaha, Nebraska.

Kimura, T. and Mair, J.R. (1981) "Centrifugal testing of model tunnels in soft clay", 10th International Conference of Soil Mechanics and Foundation Engineering, Stockholm, Vol. 2, pp. 319-322.

Kitamoto, Y., Date, K., Yamamoto, T., Hibiya, K. and Ohta, H. (2001) "Development of MGF Method based on the Evaluation of Forepiling Supporting Mechanism", Modern Tunnelling Science and Technology, Adachi et al (eds), Swets & Zeitlinger, pp.183-188.

Lang, T.A. and Bischoff, J.A. (1984) "Stability of reinforced structures", ISRM Symposium on design and performance of underground excavations, E.T. Brown and J.A. Hudson (eds.), British Geotech. Society, London, pp. 11-18.

Leach, G. (1985) "Pipeline response to tunnelling", unpublished paper presented to the North of England Gas Association, January 1985.

Leca, E. and Dormieux, L., (1990). "Upper and lower bound solutions for the face stability of shallow circular tunnels in frictional material". Géotechnique, Volume 40, No. 4, pp. 581-606.

Lee, K.M.,Rowe, R.K. and Lo. K.Y. (1992) "Subsidence owing to tunnelling. I: Estimating the gap parameter", Canadian Geotechnical Journal, Ottawa, Canada, Vol. 29, pp. 929-940.

Leto, I and Welburn B. (1999) "Lines 2 and 3 of the Athens Metro", Proceedings of Institution of Civil Engineers, Civ. Engineering, Vol. 132, May/Aug, pp.68-76.

Li Yunfeng (1990) "Pipe Roof supporting method in Karst and Fill section of Nanling Tunnel", Proceedings of the International Congress on Tunnel and Underground Works Today and Future, Chengdu, China, pp.99-106.

Lo, K.Y, Ng, R.M. and Rowe, R.K. (1984) "Predicting settlement due to tunnelling in clays", Proceedings of Tunnelling in Soil and Rocks, ASCE, Vancouver, pp. 48-76.

Loganathan, N. and Flanagan, R.F. (2001) "Predictions of tunnelling-induced ground movements: Assessment and Evaluation", Proc. Of Underground Singapore 2001, pp.102-113.

Loganathan, N.and Poulos, H.G.(1998) " Analytical prediction for tunnelling induced ground movements in clays", Journal of Geotechnical and Geoenvironmental Engineering, ASCE, Vol.124, No.9, pp.846-856.

Lunardi, P., Focaracci, A., Giorgi, P. and Papacella, A. (1992), "Tunnel face reinforcement in soft ground design and controls during excavation", International Congress towards New Worlds in Tunnelling, Acapulco, Vol. 2, pp. 897-908.

Lunardi, P. (2000) "The design and construction of tunnels using the approach based on the analysis of controlled deformation in rocks and soils", Tunnels and Tunnelling International, pp.3-30.

Mair, R.J., (1979). "Centrifugal modelling of tunnelling construction in soft clay". PhD Thesis, University of Cambridge.

Mair, R.J. and Taylor, R.N. (1997). "Bored tunnelling in the urban environment", Theme Lecture, Plenary Session 4, 14th International Conference on Soil Mechanics and Foundation Engineering, Hamburg.

Mair, R.J., Taylor,R.N. and Bracegirdle,A. (1993) "Subsurface settlement profiles above tunnels in clay", Geotechnique, Vol.43, pp.315-320.

Mair, R.J., Taylor,R.N. and Burland, J.B.(1996) "Prediction of ground movements and assessment of the risk of building damage due to bored tunnelling", Geotechnical Aspects of Underground Construction in Soft Ground, Mair & Taylor (eds), 1996, Balkema, Rotterdam, pp. 713-718.

Mair, R.J., Gunn, M.J. and O'Reilly, M.P. (1983) "Ground movements around shallow tunnels in soft clay", 10th International Conference on Soil Mechanics and Foundation Engineering, Stockholm, pp. 323-328.

Matsumoto, Y., Kurose, N., Inoue, T., Kurazono, M. and Nodomi, K. (2001) "New pre support method using pipe roof by semi shield and chemical grouting for shirasu fill", Modern Tunnelling Science and Technology, Adachi et al (eds), Swets & Zeitlinger, pp.751-756.

Matsuo, H., Yamamura, S., Amano, M. and Taira, K. (1996) "New construction method for urban tunnels in uncemented ground under high groundwater pressure", North American Tunnelling '96, Ozdemir (ed.), pp.345-352.

Megaw, T.M. and Bartlett, J.V.(1983) "Tunnels, planning, design, construction",Ellis Horwood International Edition, 1983

Mcfeat-Smith, Ian(1997)"Mechanised tunneling for Asia"Workshop manual, IMS Tunnel Consultancy Ltd.

Mitarashi, Y., Matsuo, T., Okamoto, T., Tsuji, T., Haba, T. and Okabe, T. (2001) "Development of long face reinforcement method with GFRP tubes", Modern Tunnelling Science and Technology, Adachi et al (eds), Swets & Zeitlinger, pp.503-508.

Mitchell, R.J. (1983) "Earth Structures Engineering", Allen andUnwin Inc., Boston.

Miwa, M. and Ogasawara, M. (2001)"Constructing a tunnel through the embankmant of National Road No. 4 using the AGF method", Modern Tunnelling Science and Technology, Adachi et al. (eds.), pp.487-492.

Murata, M, Okazawa, T., Harunaka, K. and Tamai, A.(1996) "Shallow twin tunnel for six lanes beneath densely residential area", North American Tunnelling '96, Ozdemir (ed), pp.371-380.

Muraki, Y. (1997) "Umbrella Method of Tunnelling", Masters Thesis, MIT, USA.

Naito, H. (1992) "Construction of twin road tunnels under special conditions: Miyano Tunnel", Towards New World in Tunnelling, Vieitez-Utesa and Montanez-Cartaxo (eds.), pp. 737-745.

New, B.M. and O'Reilly, M.P. (1991) "Tunnelling induced ground movements: predicting their magnitude and effect", Proceedings of the Fourth International Conference on Ground Movements and Structures, Cardiff, July 1991, Edited by J.D. Geddes, Pub. Pentech Press, pp. 671-697.

Nishimaki, A., Mitarashi, Y. and Uematsu, S. (1995) "Study of the effects of the AGF method", South East Asian Symposium on Tunnelling and Underground Space Development, Bangkok, pp. 125-132.

Norgrove, W.B., Cooper, I. and Attewell, P.B. (1979) "Site investigation procedures adopted for the Northumbrian Water Authority's Tyneside Sewearge Scheme, with special reference to settlement prediction when tunnelling through urban areas", Proc. Tunnelling '79, ed. M.J. Jones, IMM, London, pp.79-104.

O'Reilly, M.P. and New, B.M. (1982) "Settlements above tunnels in the UK- their magnitude and prediction", Tunnelling '82, pp. 173-181.

O'Rourke, T.D. and Trautmann, C.H. (1982) "Buried pipeline response to tunnelling ground movements", Europipe '82 Conference, Basle, Switzerland, pp. 9-15.

Ohtsu, H., Hakoishi, Y., Nago, M. and Taki, H. (1995) "A prediction of ground behaviour due to tunnel excavation under shallow overburden with long length forepilings", South East Asian Symposium on Tunnelling and Underground Space Development, Bangkok, pp. 157-164.

Oteo, C.S. and Sagaseta, C. (1996) "Some Spanish experiences on measurement and evaluation of ground displacements around urban tunnels", Geotechnical Aspects of Underground Construction in Soft Ground, Mair & Taylor (eds), 1996, Balkema, Rotterdam, pp. 731-736.

Pakes, G. (1976) "Edinburgh sewage disposal scheme: tunnelling works", IMM, Tunnelling '76, pp.3-15.

Panet, M. and Guenot, A. (1982)" Analysis of convergence behind the face of a tunnel", Tunnelling'82, IMM, pp.197-204.

Peck, R. B. (1969) "Deep Excavation and Tunnelling in Soft Ground", State of the Art Volume, Seventh International Conference on Soil Mechanics and Foundation Engineering, pp. 225-290, Mexico City.

Peila, D. (1994) "A theoretical study of reinforcement influence on the stability of a tunnel face", Geotechnical and Geological Engineering, Vol. 12, pp. 145-168.

Peila, D., Oreste, P.P., Pelizza, S. and Poma, A. (1996) "Study of the influence of sub horizontal fibre glass pipes on the stability of a tunnel face", North American Tunnelling, 1996, Balkema, Rotterdam, pp. 425-432.

Pelizza, S. and Peila, D. (1992), "Soil and rock reinforcements in tunnelling", First International Symposium on Tunnelling Construction and Underground Structures, Ljubljana, Slovenia.

Piepoli, G. (1976) "La nuova galleria S/ Bernadino della linea Genova-Ventimiglia", Ingegneria Ferroviaria, Vol. 10.

Poma, A., Grassi, F. and Devin, P. (1995) "Finite Difference Analysis of displacement measurements for optimising tunnel construction in swelling soils", 4th Int'l Symp. Field Measurements in Geomechanics, Bergamo, pp.225-236.

Rabcewicz, L. (1973) "Principles of dimensioning the support system for the New Austrian Tunnelling Method", Water Power, Vol. 25, No.3, March, pp.88-93.

Ranken, R.E. and Ghaboussi, J. (1975) "Tunnel Design Considerations: Analysis of stresses and displacement around advancing tunnels", Final report by University of Illinois on Contract No. DOT FR 30022 to the Federal Railroad Administration, Dept. of Transportation, Washington D.C. 20590, USA.

Rhodes, G.W. and Kauschinger, J.L. (1996) "Microtunnelling provides structural support for large tunnels with shallow cover", North American Tunnelling 1996, Balkema, Rotterdam, pp. 443-449.

Rocksoil S.p.A. Full face mechanical precutting and ground improvement of the advance core using glass fibre structural elements,[Online]. Available: http://www.rocksoil.com/ing_tec_costruzione_pretaglio [2003, July 21].

Romo, M.P. and Diaz, C.M. (1981) "Face stability and Ground settlement in Shield Tunnelling", Proc. Of the 10th Int'l Conf. on Soil Mechanics and Foundation Engineering, Vol. 1, Stockholm, pp.357-360.

Rotex OY. Forepoling in Tunnels, [Online]. Available: http://www.rotex.fi/pdf/tunnelling.pdf [2003, August].

Rowe, R.K. and Kack, G.J. (1983) " A theoretical examination of the settlements induced by tunnelling: Four case histories, Canadian Geotechnical Journal, Vol. 20, pp.229-314.

Sagaseta, C. (1987) "Analysis of undrained soil deformation due to ground loss", Geotechnique, Vol.37, pp.301-320.

Sato, J. and Ito, J. (1993) "Numerical analysis of the umbrella method for tunnel excavation", Infrastructures Souterraines de Transports, Reith (ed.), Balkema, Rotterdam, pp.355-360.

Satoh, S., Furuyama, S., Murai, Y. and Endoh, T. (1996), "Construction of a subway tunnel just beneath a conventional railway by means of a large-diameter long pipe-roof method", North American Tunnelling 1996, Balkema, Rotterdam, pp. 473-481.

Sasaki, R., Takayama, T., Tsukada, M., Kimura, M., Torii, S. and Nakagaki, H. (2001) "Excavation monitoring of a large cross section tunnel underpassing an existing railway", Modern Tunnelling Science and Technology, Adachi et al. (eds.), pp.253-258.

Schmidt, B. (1969) "Settlements and ground movements associated with tunnelling in soil", PhD Thesis, University of Illinois.

Schofield, A.N., (1980). "Cambridge Geotechnical Centrifuge Operations". Géotechnique, Volume 30, No.3, pp.227-268.

Sekimoto, H., Kameoka, Y. and Takehara, H. (2001) "Countermeasures for surface settlement in constructing shallow overburden urban tunnels penetrated through active fault", Modern Tunnelling Science and Technology, Adachi et al. (eds.), pp. 711-716.

Shin, H.S., Han, K.C., Sunwoo, C., Choi, S.O. and Choi, Y.K. (1999) "Collapse of a tunnel in weak rock and the optimal design of the support system", Proc. Of the 9th Int'l Congress on Rock Mechanics, Paris, France, ISRM.

Shiraishi, S. (1968) "Recent major shield driven tunnels through soft ground in Japan", Soils and Foundations, Vol. 9, pp. 16-34.

Strack, O.E. and Verruijt, A. (2000) "A complex variable solution for the ovalization of a circular tunnel in an elastic half plane", Proceedings of the International Conference GeoEng 2000, Melbourne, Australia.

Szechy, K. (1970) "Surface settlements due to the shield tunnelling method in cohesionless soils", Proceedings of Conference on Subway Construction, Budapest-Balatonfured, pp.615-624.

Tamez, E. (1984) "Stability of tunnels excavated in soils", Work presented upon joining the Mexican Engineering Academy, Mexico City.

Tan, W.L. and Ranjith, P.G. (2003) "Considerations in Soft Ground Tunnelling", Electronic Journal of Geotechnical Engineering, Volume 8 (D).

Tatar, C., Ertem, M.E., Sen, P. and Kose, H (2002) "NATM for the Karsiyaka Tunnels, Turkey", World Tunnelling, pp. 30.

Terzaghi, K. (1950), "Geologic aspects of soft ground tunneling: In: Applied sedimentation, Chapter 11, Ed. P.D. Trask, John Wiley and Sons.

Van Walsum, E (1992) "The mechanical pre-cutting tunnelling method (MPTM)", Towards New World in Tunnelling, Vieitez-Utesa and Montanez-Cartaxo (eds.), pp. 779-788.

Verruijt, A. (1997) "A complex variable solution for a deforming circular tunnel in an elastic half plane", International Journal for Numerical and Analytical Methods in Geomechanics, Vol. 21, pp. 77-89.

Verruijt, A. and Booker, J.R. (1996) "Surface settlement due to deformation of a tunnel in an elastic half plane, Geotechnique, Vol.46, pp.753-756.

Whittaker, B.N. and Frith, R.C. (1990) "Tunnelling : Design, Stability and Construction", The Institution of Mining and Metallurgy, pp.69-92.

Wood, A.M. Muir (1970) "Soft ground tunnelling", Proceedings TUNCON '79, Johannesburg, Vol. 1 , pp.167-174.

Wong, H., Trompille, V., Subrin, D. and Guilloux, A. (2000) "Tunnel face reinforced by longitudinal bolts: Analytical model and in situ data", Geotechnical Aspects of Underground Construction in Soft Ground, Kusakabe, Fujita & Miyazaki (eds), 2000, Balkema, Rotterdam, pp. 457-462.

Yang, T., Woo, J. and Lee, S. (2001) "Ground reinforcement for a tunnel in weathered soil layer beneath Han riverbed in Korea", Modern Tunnelling Science and Technology, Adachi et al. (eds.), pp.493-496.

Yasuda, T, Tamura, T. and Hashimoto, T (2001) "Development and application of the large-section shallow tunnelling", Modern Tunnelling Science and Technology, Adachi et al. (eds.), pp. 999-1004.

Yoshida, T. and Kusabuka, M. (1994) "Behaviours of ground and adjacent underground piping during shield tunnelling", Tunnelling and Ground Conditions, Abdel Salam (ed.), 1994, Balkema, Rotterdam, pp. 201-206.

Yoo, C.S. and Shin, H.K. (2000) "Behaviour of tunnel face pre-reinforced with sub horizontal pipes", North American Tunnelling 2000, Balkema, Rotterdam, pp. 463-468.

Yoo, C.S. and Yang Ki Ho (2001) "Laboratory investigation of the behaviour of tunnel face reinforced with longitudinal pipes", Modern Tunnelling Science and Technology, Adachi et al (eds), Swets & Zeitlinger, pp.763-768.

Zeccos, D.P. (2002).Begin of Forepoling in the Kakia Skala Tunnel, Greece, [Online].Available:http://www.geoengineer.org/photos/forepol1.jpg.[2003, July 21].